HOLOCENE GLACIER FLUCTUATIONS AND TEPHRA FALL INFERRED FROM LACUSTRINE SEDIMENT, EMERALD LAKE, ALASKA

By Taylor S. LaBrecque

A thesis

Submitted in Partial Fulfillment

of the Requirements for the Degree of

Master of Science

in Geology

Northern Arizona University

August 2014

Darrell Kaufman, Ph.D., Chair

R. Scott Anderson, Ph.D.

Nancy Riggs, Ph.D.

ProQuest LLC.
789 East Eisenhower Parkway
P.O. Box 1346
Ann Arbor, MI 48106 - 1346

ABSTRACT

HOLOCENE GLACIER FLUCTUATIONS AND TEPHRA FALL INFERRED FROM LACUSTRINE SEDIMENT, EMERALD LAKE, ALASKA

TAYLOR S. LABRECQUE

Downcore changes in physical and biological characteristics of lacustrine sediments from Emerald Lake (59°03'N, 151°37'W) were used to reconstruct the Holocene glacier history of Grewingk Glacier, which drains the Grewingk-Yalik Ice Complex on Kenai Peninsula, Alaska. Emerald Lake is a threshold lake, receiving meltwater and clastic sediment when Grewingk Glacier overtops the topographic divide that separates it from Emerald Lake. Glacier meltwater discharge is represented in sediment cores from Emerald Lake by distinct light-gray, stony mud, with high density and low organic-matter content. Sub-bottom acoustical profiles were used to locate two core sites: one with a low sedimentation rate (Core 2; 18 m depth) and one with a high rate (Core 3; 50 m depth) to maximize both the length and resolution of the sedimentary sequence recovered in the ~3-m-long cores. Bulk density, sedimentation rate, stratigraphy, organic-matter content, and chlorophyll were used to record environmental changes since ~12 cal ka, with ^{14}C and ^{210}Pb for geochronology. Ages were assigned to tephra beds in Cores 2 and 3: 18 and 9 beds respectively. A diffuse transition from the basal inorganic mud to organic-rich mud ~11.4 cal ka marks the initial retreat of the Grewingk Glacier below the divide of Emerald Lake. The overlaying organic-rich mud is interrupted by stony mud that records a brief re-advance as ice overtopped the divide again ~10.7 cal ka, followed by the final glacial-interglacial transition ~9.8 cal ka. The glacier did not spill meltwater into the lake again until the Little Ice Age, from around AD 1350-1900, consistent with documented

LIA advances on the Kenai Peninsula. The retreat is estimated from lichen ages on a bouldery moraine on the topographic divide and is consistent with the previously estimated age of the Grewingk Glacier terminal moraine (AD 1858). The retreat of Grewingk Glacier below the divide at 11.4 cal ka took place as temperature and productivity increased across southern Alaska; the subsequent readvance above the divide at 10.7 cal ka corresponds with cooling beginning ~11.0 cal ka in south-central Alaska. Decreased precipitation in southern Alaska from 5.5 to 4.0 cal ka lowered the level of Emerald Lake and sedimentation rate decreased. The initial LIA advance over the divide (AD 1350) and peak meltwater input into Emerald Lake (AD 1660) coincide with documented solar minima, suggesting solar variability influences Grewingk Glacier fluctuations.

ACKNOWLEDGEMENTS

I could never have imagined how much time and effort would be required to produce this Master's thesis; it would not have been possible without my committee and wonderful support group. I owe a great deal of thanks to my advisor, Darrell Kaufman, who saw the potential in this project and guided me towards the finish line in my time at NAU. I would not have been able to produce such a successful project without his enthusiasm and dedication. It was an honor working with one of the leading scientists in the field of paleoclimatology.

I am also very grateful to my thesis committee. Nancy Riggs is an expert in volcanology and helped me make sense of the numerous tephra deposits in my sediment cores. Not only did she share her knowledge of volcanic processes, she proved to be an inspiration as a well-rounded successful woman scientist. Her kind words of motivation helped make my experience at NAU more enjoyable. Scott Anderson was also a source of knowledge for my thesis project. He is an expert in paleoecology and climate history using evidence of past plant communities. He consistently presented me with challenging questions that broadened my understanding of the Alaskan paleoclimatology literature and helped me anticipate future questions. From bonding over our love for my home state of Maine to taking his class in Historical Ecology, Scott is someone I have grown to admire.

I also owe great thanks to the laboratories that assisted with analyses for this thesis project. The Limnological Research Center, Minnesota split my sediment cores and provided down-core anaylsis for each of the cores. Flett Research Ltd, Manitoba, Canada provided me with ^{210}Pb and ^{226}Ra activity and data interpretation. The Keck Carbon Cycle AMS facility at UC Irvine provided me with radiocarbon ages for organic material in both cores. The efficiency from these three labs helped me move forward with my project and eventually graduate in two years.

I would also like to thank the National Science Foundation for funding Darrell, who in turn, funded this project. Having the opportunity to fly to Alaska, see the study site, and extract the sediment cores, was a learning experience I will never forget. I would also like to thank the Geological Society of America for funding portions of the lab analyses to make this project possible.

Lastly, there are a number of individuals I would like to thank. I appreciate the help Brandon Boldt and Jon Griffith put forth in the field and the advice they provided me with in my first year at NAU. Ed Berg, a Homer, AK resident, also contributed useful information about my study site, having seen Grewingk Glacier change first-hand. I am very grateful to Katherine Cooper, who helped me with lab analysis in the NAU sediment lab. Katherine was another smiling face that consistently improved my long days. Finally, I appreciate the support I have received over the past 2 years from my friends and family. My Flagstaff friends have made this small town feel like home; I will never forget the time we have shared together. I could never express the gratitude I feel towards my family back in Maine. I could have written all 64 pages of this thesis about how much I appreciate my parents. They have supported me my entire life, even at age 3 when I

collected every white rock my chubby hands stumbled upon. I am very lucky to have two such loving and inspirational people to call mom and dad.

TABLE OF CONTENTS

LIST OF TABLES

LIST OF FIGURES

PREFACE

This thesis is organized into two chapters. Chapter 1 is an introduction to the literature background, providing more information on topics that are only briefly mentioned in Chapter 2. Chapter 2 is in manuscript form. One compound references-cited list follows Chapters 1 and 2 with Appendixes containing relevant data sets.

CHAPTER 1: INTRODUCTION

PURPOSE

The Holocene glacial history of southern Alaska is a topic of interest for climate scientists because of the abundance of mountain glaciers in Alaska and the sensitivity of glaciers to climate change; however, temporal gaps still remain within the glacial history. Glacier fluctuation records have been used to infer past climate because glaciers fluctuate in response to changes in precipitation and temperature. The majority of the glacier fluctuation reconstructions in Alaska is dominated by geomorphologic evidence through dating and mapping glacial moraines that capture only certain details of a glacier's history (Wiles & Calkin, 1994; Evison et al., 1996; Calkin et al., 2001; Briner & Kaufman, 2008). Moraine ridges mark Holocene ice stabilization positions and can be dated using lichenometry and tree rings (e.g., Wiles & Calkin, 1994; Daigle & Kaufman, 2009; Owen et al., 2009); the use of moraines to document glacier fluctuations is limited by the erosion of evidence of former, less-extensive glacier positions. This is a significant problem considering the most extensive advances during the Holocene in the Northern Hemisphere were relatively recent, during the seventeenth, eighteenth, and nineteenth centuries (Davis et al., 2009). Although moraines can mark maximum Holocene ice extent and other intervals of stabilization, they leave many gaps in the reconstruction, such as when the glacier began to advance.

Lacustrine sediment deposits have helped reveal details of the glacier fluctuation records that were previously unknown from moraine chronologies alone (Levy et al.,

2004; Daigle & Kaufman, 2009). Lake sediments are frequently used to infer past climate variability because they are sensitive to minor changes in the climate regime and typically contain multiple proxies, each of which react to different climate variables. Lakes are so sensitive to changes in climate because the impacts may be widespread, from the organismal to ecosystem scales. Additionally, lake sediment records can provide continuous and independently dated records of changes in climate.

Glacially influenced threshold lakes are particularly effective in filling in the remaining temporal gaps in the record of Holocene glacier history. A threshold lake is a lake separated from a glacier by a topographic divide and only receives meltwater from the glacier when the glacier expands to overtop the divide. Daigle & Kaufman (2009), Bakke et al. (2010), Briner et al. (2010), Maurer et al. (2012) and Osborn et al. (2012) used threshold lake sediments to contribute to the records of glacier fluctuations in the Arctic. Sediments in threshold lakes contain a clear on-off signal of when glaciers enter or exit the catchment of the lake. Recent studies have described the benefit of using threshold lakes to infer Holocene glacier fluctuations (Daigle & Kaufman, 2009; Bakke et al., 2010; Briner et al., 2010; Maurer et al., 2012); for example, threshold lake records are one of few approaches with the potential to reconstruct smaller-than-present ice margin extents (Briner et al., 2010). Sediment records from multiple threshold lakes can help estimate ice extent by determining into which catchments the ice was contributing meltwater. As the ice fluctuated it contributed meltwater into each threshold lake catchment during different intervals of time.

In this study I reconstruct glacial advance and retreat of Grewingk Glacier using sediments from Emerald Lake on the Kenai Peninsula (Figure 1). Emerald Lake is a

threshold lake influenced by Grewingk Glacier when it expands to overtop the topographic divide that currently separates it from Emerald Lake (Figure 2). The on-off signal of meltwater input recognized in the lacustrine sediment signifying glacial advance and retreat will help fill in the remaining temporal gaps of Holocene glacier fluctuation in south-central Alaska, particularly constraining the timing and duration of glacial advances and retreats.

STUDY SITE

Emerald Lake is located in the southern Kenai Peninsula (Figure 1), which has a maritime climate with temperatures moderated by the North Pacific. The western Kenai Peninsula is cooler and drier than the east, with a mean annual temperature and precipitation in Homer (Figure 1; 59° 38'N, 151° 30'W) of 3.1°C and 25 mm yr^{-1}, respectively, compared to 4.3°C and 1746 mm yr^{-1} in Seward (Figure 1; 60° 07'N, 149° 27'W) (Western Regional Climate Center, 2014; based on data from 1932-2012 in Homer and 1949-2012 in Seward). In Homer, precipitation remains high between August and January, with peak precipitation in September and October (Figure 3). Average monthly temperatures in Seward are constantly ~1°C higher than in Homer, with maximum temperatures in July and August (Figure 3).

The Aleutian Low is a semi-permanent, low-pressure system over the North Pacific Ocean (Trenberth & Hurrell, 1994) and the dominant weather pattern on the Kenai Peninsula. Increased precipitation on the Kenai Peninsula is typically associated with a strengthened Aleutian Low that delivers warm air masses from the south

(Trenberth & Hurrell, 1994). The Aleutian Low has two primary decadal modes that determine its strength and position; the Aleutian Low is positive when the system travels eastward towards the Gulf of Alaska (strengthened Aleutian Low) and negative when it moves westward towards the Aleutian Islands (weakened Aleutian Low). In addition to the decadal variability, the Aleutian Low moves east in the winter and west in July, resulting in a strengthened Aleutian Low in winter months and weakened Aleutian Low during summer months (Trenberth & Hurrell, 1994).

In south-central Alaska, land and sea surface temperatures are related to Pacific Decadal Oscillation and North Pacific Index. The Pacific Decadal Oscillation is an index for the mode of the North Pacific sea surface temperatures and the North Pacific Index is an indicator of Aleutian Low intensity (temperature and precipitation). On the Kenai Peninsula, strong Aleutian Low intervals are typically associated with negative North Pacific Index (Rodionov et al. 2007) and Pacific Decadal Oscillation (Mantua et al. 1997).

PREVIOUS WORK IN SOUTH-CENTRAL ALASKA

Late Pleistocene environmental changes

Krinsley (1953) pioneered glacier geological studies on the Kenai Peninsula, mapping drifts and associated marginal ice features in the Kenai Mountains. Krinsley (1953) recognized the Naptowne (last major glaciation) moraines as the most continuous and well-preserved glacial deposits on the Kenai Peninsula. Most of the Kenai Peninsula was inundated by ice during the last major glaciation (Reger et al., 2008). Deglaciation

began ~13 cal ka, inferred from preserved post-glacial sediment sequences in bogs and dated moraines (Karlstrom, 1964).

Daigle and Kaufman (2009), Kaufman et al. (2010), and Jones et al. (2014) proposed the warming associated with this late Pleistocene deglaciation began at different times across Alaska. Daigle and Kaufman (2009) used proxies and stratigraphy in lacustrine sediment extracted from Goat Lake, Kenai Peninsula, to estimate the timing of the retreat of North Goat Glacier from the divide separating the glacier from Goat Lake. Extrapolation of the age model suggests North Goat Glacier dropped below the divide by 9.5 cal ka, indicating the glacial retreat began prior to 9.5 cal ka.

Kaufman et al. (2010) compared their record of pollen, macrofossils, and sedimentologic indicators in lacustrine cores from Discovery Pond, Kenai Lowlands, to a compilation of Younger Dryas records from southern Alaska, which included Arolik Lake (Hu et al., 2006), Hundred Mile Lake (Yu et al., 2008), Greyling Lake (McKay & Kaufman, 2009) and records from the North Pacific Ocean. Fluctuations of organic matter (OM) content, biogenic silica (BSi), and $\delta^{18}O$ coincide between records and reflect an increase in temperature and productivity starting at 12.8 cal ka, peaking ~11 cal ka, followed by decreasing temperature and productivity for ~1 ka. Macrofossil assemblages in the Discovery Pond record suggest an increase in moisture until ~11 cal ka.

Also in south-central Alaska, Yu et al. (2008) conducted a multi-proxy investigation of climate, vegetation, and deglaciation from Hundred Mile Lake, Matanuska Valley. The initiation of the present interglacial is recognized as an increase in OM content (12.8 to 11.1 cal ka), inferred to represent an increase in productivity. OM content decreases upward from 11.1 to 11.0 cal ka, followed by an ~4.5 per mil decrease

in $\delta^{18}O$ around 10.5 cal ka. Both proxies suggest a transition to colder temperatures and less winter precipitation following the Younger Dryas.

Jones et al. (2014) investigated $\delta^{18}O$ values and pollen spores from HT Fen on the Kenai Peninsula (Figure 1). They observed an increase in $\delta^{18}O$ values starting 11.6 cal ka, which they linked to an increase in precipitation related to the Aleutian Low. These oxygen isotope value fluctuations are concurrent with records by Kaufman et al. (2010) and Yu et al. (2008), with a peak in $\delta^{18}O$ ~11 ka, followed by a decrease in values.

Mid-to-late Holocene environmental changes

The onset of the Neoglacial interval (~4 cal ka) coincides with a change in vegetation and isotopic values in peat (Jones et al., 2009, 2010) and a glacial advance (Barclay et al., 2009b) on the Kenai Peninsula. Glaciers first advanced during the early Holocene ~4 cal ka in south-central Alaska (Barclay et al., 2009b), inferred from lacustrine sediment records, and by 3.6 cal ka in the Harding Ice Field (Wiles & Calkin, 1994).

Another glacial advance occurred around AD 600 on the Kenai Peninsula (Barclay et al., 2009b), which included Tebenkof Glacier (AD 710; Barclay et al., 2009a) and Grewingk Glacier (AD 500; Wiles & Calkin, 1994). Wiles and Calkin (1994) noted that this advance at Grewingk Glacier was less extensive than the Little Ice Age (LIA) advances. The AD 600 advance is not apparent in all glaciolacustrine records on the Kenai Peninsula (e.g. Daigle & Kaufman, 2009).

The LIA (from AD 1200-1900) is the most recent cooling phase of the Neoglacial interval during which most glaciers in southern Alaska reached their Holocene maximum

extents (Wiles & Calkin, 1994; Calkin et al., 2001). Glacier fluctuation records suggest the cooling associated with the LIA on the Kenai Peninsula lasted from AD 1350 to 1850 (Wiles & Calkin, 1994; Wiles et al., 2008; Barclay et al., 2009b). The LIA includes three distinct glacial advances: 1) early LIA advance from AD 1180-1320's, 2) middle LIA advance 1540-1710's, and 3) late LIA advance 1810-1880's (Barclay et al., 2009b).

Wolverine Glacier is a frequently monitored benchmark glacier for the USGS on the Kenai Peninsula. Malcomb and Wiles (2013) identified three distinct phases of the LIA at Wolverine Glacier that start and end later than the southern Alaska estimates (Barclay et al., 2009b). Bitz and Battisti (1999) and Malcomb and Wiles (2013) agree that positive mass balance intervals at Wolverine Glacier are associated with increased precipitation, which is likely associated with negative Pacific Decadal Oscillation and strengthened Aleutian Low.

Because the LIA occurred in the last millennium, additional proxies can be used to infer past climate changes, such as tree rings, typically used to infer temperature. Tree ring chronologies can help understand factors that influence glacier fluctuations. For example, Barclay et al. (2003) compiled an 850-year record of the variability in climate and extent of Nellie Juan Glacier in south-central Alaska. Nellie Juan Glacier advanced between AD 1539 and 1610, shortly before the middle-LIA advance of other glaciers in southern Alaska (Barclay et al., 2009b), and was at its maximum extent from AD 1842 to 1893. The tree-ring chronology combined with glacier fluctuation records from western Prince William Sound suggest the 19th century advance was controlled by changes in summer temperature and radiation.

Davi et al. (2003) used the width and density of tree rings to reconstruct summer temperature from the Wrangell Mountain region of Alaska. The July-September record extends from AD 1593 to 1992 and shows two cold intervals, from late 1600s to early 1700s and late 1700s to early 1800s, with warming in the 20th century. The record is consistent with glacier fluctuations from the Wrangell Mountains and several of the coldest reconstructed July-September records coincide with volcanic eruptions.

A more recent 1200-year surface air temperature reconstruction from tree rings in the Gulf of Alaska (Wiles et al., 2014) captures the Medieval Warm Period at AD 950 and the 170- to 220-year cycling consistent with solar variability. Temperature minima occur at AD 969-970 and 1698-1700 and coincide with major volcanic eruptions. The record reflects a negative temperature anomaly from AD 1350 to 1720. Wiles et al. (2014) suggested lunar tidal, solar variability, and internal variability also impact the climate on annual to decadal timescales.

GENERAL REVIEW OF RELEVANT METHODS

Lacustrine sediments are capable of recording subtle environmental changes, including minor advances and retreats of glaciers. Glacially influenced threshold lakes contain useful records of glacier variability that differ from proglacial lakes because the glacier only discharges meltwater directly into the lake when it is thick enough to overtop the topographic divide, reducing glacial and non-glacial sediment mixing, whereas the relative proportion of glacial sediment in non-threshold lakes can be used to infer the relative size of glaciers upvalley. Glacially influenced threshold lakes produce clearly

discernable on/off records of glacial meltwater in the sediment sequence (Daigle & Kaufman, 2009; Briner et al., 2010; Maurer et al., 2012; Osborn et al., 2012). In addition to their potential to reconstruct glacier fluctuations, lake sediments can be analyzed for downcore variation in a number of organic and inorganic glaciolacustrine sediment properties used as proxies to help reconstruct continuous records of past glacier variability (Karlen et al., 1981; Leonard, 1985; Nesje et al., 1991; Leonard, 1997; Doran et al., 1999; Meyers & Lallier-Verges, 1999; Nesje et al., 2001; Dahl et al., 2003; Levy et al., 2004; Bakke at al., 2005a; Bakke et al., 2005b; Daigle & Kaufman, 2009; Osborn et al., 2007; McKay & Kaufman, 2009; Bakke et al., 2010).

Productivity is the measure of the nutrients within a lake produced by both autochthonous and allochthonous sources, limited by nutrient availability and solar radiation (Cohen, 2003). Productivity is an important paleolimnological indicator in climate reconstructions because it provides insight into the factors that control it such as temperature, sunlight, moisture, and nutrient availability (Cohen, 2003). Two techniques used to infer productivity levels in sediments involve the measurement of OM content and plant and algal pigments.

OM content does not differentiate levels of aquatic productivity from terrestrial productivity and for this reason it is typically used as an index of overall productivity within a lake's watershed. Weight loss on ignition (LOI) is a reproducible and comparable method for estimating changes in organic and carbonate content (Heiri et al., 2001). In addition to its use as a proxy for productivity, OM within the sediment can be radiocarbon dated to estimate the timing of deposition.

In addition to the overall watershed productivity, past aquatic productivity can be inferred using algal and plant pigments preserved in lake sediments (Meyers, 2003; Wolfe et al., 2006). Plants and algae use a variety of pigments to absorb visible light energy during photosynthesis (Meyers, 2003); a measure of these pigments in lake sediment can help determine the types of organisms and the amount of photosynthesis that occurred with time. Chlorophyll pigments are the most abundant and can be analyzed in lake sediments using visible and infrared (VIR) reflectance spectroscopy by measuring absorption maxima values between 660- 670 nm (Wolfe et al., 2006).

Inorganic components of the lake sediments also help reveal details about sediment input sources. Magnetic susceptibility (MS) values represent the amount of detrital magnetic minerals in sediments, which is directly related to the amount of in-washed allochthonous inorganic material (Thompson et al., 1975). Igneous rocks and deposits, including ash fall and plutons, can have an abundance of magnetic minerals resulting in high MS values where the ash or plutonic material is present in the sediment core (Collinson, 1986). Increased erosion of plutonic rock associated with glacier activity and tephra beds yield high MS values in sediment records {just said this} (de Fontaine et al., 2007; Daigle & Kaufman, 2009). de Fontaine et al. (2007) demonstrated that MS can effectively highlight tephra beds within lake sediment on Kenai Peninsula.

TEPHROCHRONOLOGY

The Cook Inlet volcanoes have erupted hundreds of times during the present interglacial (e.g., Beget et al., 1994; de Fontaine et al., 2007; Daigle & Kaufman, 2009;

Schiff et al., 2010), but the record of these eruptions remains incomplete. Lake sediments are frequently used to reconstruct local tephra-fall histories because lakes can effectively preserve tephra beds (e.g., de Fontaine et al., 2007), the ages of which can be inferred using radiocarbon ages of organic material in the enclosing lacustrine sediment. Tephra deposits in lakes can be used as time-stratigraphic markers to provide additional ages for sediment records or to support previously estimated ages (Cashman et al., 2000). Tephra beds are typically visible in lake cores as a bed with distinct color and texture with an MS peak compared to the surrounding ambient sediment. The correlation of tephra deposits using tephrochronology can also help determine distributions of volcanic-ash deposits, a crucial component of the eruption record in Alaska, contributing to the hazard assessment.

The Hayes tephra (3720- 4160 cal yr BP; Riehle et al., 1990) is a widely used time-stratigraphic marker in Holocene records in south-central Alaska. The tephra has a distinct mineralogy, containing biotite, amphibole, and pyroxene, that makes it identifiable. Studies have also recognized the Hayes tephra as multiple deposits represented by horizontal pink and white layering (Daigle & Kaufman, 2009; de Fontaine et al., 2007).

Like the Hayes eruption, the Novarupta eruption (AD 1912) left a thick deposit of tephra (up to 100 cm) in southern Alaska and can be used a time-stratigraphic marker. Three explosive episodes over 60 hours deposited around 17 km^2 of fallout (Hildreth & Fierstein, 2012). The Novarupta tephra has been documented on the Kenai Peninsula in deposits 1-3 cm thick.

The Holocene tephrochronology record in south-central Alaska is far from complete. It is impossible to obtain one lake sediment record that documents every Holocene tephra-fall deposit. Sedimentary successions from two nearby lakes can contain different tephra beds (de Fontaine et al., 2007; Schiff et al., 2010), suggesting that the records are complicated by different plume trajectories, including direction and distance (Schiff et al., 2010), and geographic and lake characteristics that influence tephra preservation (Schiff et al., 2008). A complete record of the magnitude and frequency of tephra falls is required to construct an accurate tephra-fall assessment; the lack of correlation between nearby lakes indicates numerous lakes are necessary to make the comprehensive reconstruction.

Schiff et al. (2010) studied two lakes within 25 km of the summit of Redoubt Volcano to construct the tephrostratigraphy from ~11,540 cal yr BP to present. Between 3850 and -55 cal yr BP they documented 31 and 41 tephra beds in the two lakes, and 24 tephra beds with significantly different ages. A tephra deposited 4091 ± 130 cal yr BP falls within the error range of the Hayes tephra (3720- 4160 cal yr BP; Riehle et al., 1990) and contains biotite and amphibole.

de Fontaine et al. (2007) studied tephra-fall deposits from the Cook Inlet volcanoes in two lakes on the Kenai Peninsula. One lake core contain 109 macroscopic tephra beds over 13,200 years and the other lake cores contain nine macroscopic tephra beds and three disseminated tephras over ~9350 years. Six tephra beds correlate between the two lakes from 3660 to 8900 cal yr BP. Multiple tephra layers with biotite, amphibole, and pyroxene were found in both lake sediment cores, one between 3710 and

4140 cal yr BP and the other between 3660 and 3740 cal yr BP, consistent with the timing of the Hayes eruption.

Lacustrine sediment from a Skilak Lake on the Kenai Peninsula captures the last 500 years of tephra-fall (Beget et al., 1994). The sediment contains ash from numerous historical eruptions, including the 500 cal yr BP Mount Augustine eruption, the 350- 450 and 300- 400 cal yr BP Redoubt volcano eruptions, the 250- 350 cal yr BP Crater Peak at Mount Spurr eruption, the AD 1883 Mount Augustine eruption, the AD 1902 Redoubt volcano eruption, and the AD 1912 Novarupta eruption.

CHAPTER 2: GLACIER FLUCTUATIONS INFERRED FROM HOLOCENE LACUSTRINE SEDIMENT AND TEPHRA FALL, EMERALD LAKE, ALASKA

INTRODUCTION

Holocene glacier fluctuations have been used as paleoclimate indicators across Alaska (e.g., Calkin, 1988; Barclay et al., 2009b); glaciers fluctuate in response to changes in temperature during the melt season and precipitation during the accumulation season. Mountain glaciers, in particular, only exist under specific climatic conditions, making it possible for them to record subtle environmental changes that are absent from other proxy records (Owen et al., 2009).

Previous work on Holocene glacier history in southern Alaska has generally focused on mapping and dating glacial moraines (e.g., Wiles & Calkin, 1994; Calkin et al., 2001), but glaciolacustrine deposits have helped fill the temporal gaps in moraine chronologies (Levy et al., 2004; Daigle & Kaufman, 2009). Lacustrine sediments can provide a continuous and independently dated record of glacier fluctuation and proxy records of other environmental changes. Sediments in threshold lakes contain a clear signal of when glaciers are either present or absent within the catchment of a lake (Briner et al., 2010; Maurer et al., 2012; Osborn et al., 2012); however, the sediments from threshold lakes are unable to document fluctuations in glacial extent that occur while the glacier has retreated outside of the lake's catchment. The most complete glacier fluctuation record is one that utilizes both the high-resolution glaciolacustrine records and independently dated glacier landforms (e.g., McKay & Kaufman, 2009).

Emerald Lake (Figure 1) was selected for this study because it provides the opportunity to compare ages from within the sediment record to other records on the Kenai Peninsula. We are able to compare ages from the Emerald Lake glaciolacustrine record to the stabilization age of moraine ridges. Emerald Lake is a threshold lake that receives meltwater from Grewingk Glacier when the glacier expands to overtop the topographic divide that currently separates it from the lake (Figure 2). Another advantage of studying Emerald Lake is its comparability to Goat Lake (Figure 1), a previously studied (Daigle & Kaufman, 2009) threshold lake in the northern Kenai Mountains with morphological similarities to Emerald Lake. Like Emerald Lake, Goat Lake only receives meltwater when North Goat Glacier advances to overtop the topographic divide. Additionally, the Emerald lake study site is its location downwind from the active Cook Inlet volcanoes (Figure 1) including Iliamna (120 km), Redoubt (130 km), and Augustine (135 km), recording eruptions as tephra beds in its stratigraphy. The tephra beds can be used as time stratigraphic markers (Lowe, 2011) to compare Emerald Lake records with other records from the Kenai Peninsula.

Objectives

The aim of this project is to reconstruct the Holocene glacier history of the Grewingk Glacier on the southern Kenai Peninsula (Figure 1) using lacustrine sediment from Emerald Lake, to contribute to understanding the Holocene glacial history of Alaska. My investigation of the glacial history contributes to a larger network of glacier-fluctuation records clarifying the timing, magnitude and duration of Holocene glaciation events in south-central Alaska (e.g., Wiles & Calkin, 1994; Wiles et al., 2008; Yu et al., 2008; Barclay et al., 2009a, 2009b; Daigle et al., 2009; McKay & Kaufman, 2009).

Wiles and Calkin (1994) recognized advances of Grewingk Glacier around 621 AD and between 1400-1800 AD based on radiocarbon ages from the outer rings of a tree stump exhumed by the outwash stream and exposed within the moraines. This moraine chronology likely does not divulge the whole story. From the geomorphic evidence, it is unclear whether Grewingk Glacier retreated during intervals of the LIA, nor is there evidence of Holocene glacier fluctuations prior to 621 AD. Terminal moraines marking the maximum ice positions prior to the LIA are unclear or destroyed by LIA advances, resulting in an incomplete record of glacier fluctuations.

In this thesis, I combined the moraine chronologies with the glacially influenced threshold-lake record to produce a more complete record of glacial activity than moraine evidence alone. Organic material in lake sediment can be radiocarbon dated to estimate the time of deposition throughout the succession. Emerald Lake is well positioned to ascertain the timing of glacial advances, such as the Neoglacial and LIA advances that overtop the elevation of the topographic divide.

I used lichen ages to estimate the stabilization time (Solomina & Calkin, 2003) of the lateral moraine deposited by Grewingk Glacier on the topographic divide. I compared this age to the timing of meltwater input into the Emerald Lake represented by glacial flour in the sediment cores, and to data from previous studies on the southern Kenai Peninsula.

Comparing the sedimentary records of Emerald Lake and Goat Lake (Daigle & Kaufman, 2009), ~100 km north of Emerald Lake (Figure 1), provides an opportunity to verify the timing of climatic events. Synchronous intervals of meltwater input recorded in sediments of the two lakes reinforces the accuracy of the glacier-fluctuation record and

the climate changes they imply. Asynchronous intervals of meltwater input suggests differences in the sensitivity of North Goat Glacier and Grewingk Glacier to changes in climate, or differences in the glacier growth required to reach the elevation of the divides.

As an additional check on the radiocarbon-based ages in the lacustrine sediment from Emerald Lake, I compare the age of the tephra bed inferred to be the Hayes tephra in the sediment to its known time of deposition in southern Alaska, and I tentatively correlate tephra beds in cores from Emerald Lake with those from Goat Lake. The ages of tephra beds from Emerald Lake derived in this study also contribute to documenting the eruption history of Cook Inlet volcanoes. The three independent dating methods (radiocarbon-dated organic material, lichen, tephra beds) create a chronology for past fluctuations of Grewingk Glacier above and below the topographic divide.

Previous studies of glacier history on the Kenai Peninsula

In the lowlands of the Kenai Peninsula, the last major glaciation is known as the Naptowne Glaciation, consisting of four stades (Moosehorn, Killey, Skilak, Elmendorf) (Reger et al., 2008). Kachemak Bay and Cook Inlet (Figure 1) were glaciated during the Moosehorn stade, and to a lesser extend during the Killey and Skilak stades (Reger et al., 2008). Reger et al.'s (2008) glacial-geologic map shows that, during the Elmendorf stade (~15.0 to 11.4 cal ka), Grewingk Glacier nearly expanded to Kachemak Bay and likely covered Emerald Lake.

The knowledge of the climate prior to and during the last glacial-interglacial transition in southern Alaska is growing. Karlstrom (1964) placed the start of the Pleistocene deglaciation of the Northern Kenai Mountains around 13 cal ka and Reger et

al. (2008) suggest the Naptowne glaciation ended ~11 cal ka. Recent records of biogenic silica (BSi) (Kaufman et al., 2010) and isotopes (Jones et al., 2010) from lakes and fens in south-central Alaska suggest temperature was increasing prior to 11 cal ka. Oxygen isotope records from the Kenai Peninsula indicate precipitation also increased around 11 cal ka (Jones et al., 2014). Daigle & Kaufman (2009) and Levy et al. (2004) documented glacial retreat prior to 9 cal ka in southern Alaska. Pollen records from southern Alaska (Anderson et al., 2006) suggest deglaciation began prior to 13 cal ka.

Multiple glacial advances and retreats have been documented on the Kenai Peninsula during the current interglacial interval (e.g., Wiles & Calkin, 1994; Barclay et al., 2009a; Daigle & Kaufman, 2009). The Neoglaciation on the Kenai Peninsula started around 4 cal ka, represented by decreased temperature (Jones et al., 2010) and glacial expansion (Wiles & Calkin, 1994; Barclay et al., 2009b). A subsequent expansion occurred AD 500-600 in many locations around the Gulf of Alaska (Calkin et al., 2001) and on the Kenai Peninsula (Wiles & Calkin, 1994; Barclay et al., 2009b).

The most recent Neoglacial cooling period is the Little Ice Age (LIA), which was the most extensive Holocene expansion in southern Alaska (Barclay et al., 2009b) and lasted from AD 1350-1850 on the Kenai Peninsula (Wiles & Calkin, 1994; Barclay et al., 2009b). The most extensive interval of the LIA advance on the Kenai Peninsula (Figure 1) occurred ~AD 1600 (Wiles & Calkin, 1994; Barclay et al., 2009a). Glaciers in the Harding Ice Field (Figure 1) were retreating from their LIA extent by AD 1900 (Wiles & Calkin, 1994) and have continued to retreat into the 21st century (Hall et al., 2005).

Wiles & Calkin (1994) dated glacial landforms built by multiple glaciers on the Kenai Peninsula, including Grewingk Glacier. They documented an advance ~AD 600 of

Grewingk Glacier based on a radiocarbon-dated stump in the outwash stream. By AD 621, Grewingk Glacier had advanced to within a few kilometers of the LIA limits. Tree-ring cross-dating and radiocarbon ages from logs buried in moraines and exposed along river bluffs suggest that Grewingk Glacier was advancing by AD 1442; lichen and trees on the most distal Holocene moraine suggest a minimum age of retreat of AD 1858.

Cook Inlet tephra-fall history

A few widespread tephra deposits are well documented across south-central Alaska and can be used as time-stratigraphic markers within lake sediments (e.g., de Fontaine et al. 2007). The Hayes tephra, erupted sometime between 3720 and 4160 cal yr BP, is a prominent marker on the Kenai Peninsula, containing a distinctive mineralogy of biotite, amphibole, and pyroxene (Riehle et al., 1990). The AD 1912 eruption of Katmai and Novarupta was the largest historical eruption in Alaska, and is recognized in thick (up to 100 cm) deposits in southern Alaska (Hildreth & Fierstein, 2012). The isopach map of Hildreth & Fierstein (2012) shows that ~1 cm of ash was likely deposited around Emerald Lake.

Study site

Emerald Lake is located in the Kenai Mountains, which separate the Cook Inlet to the west from the Gulf of Alaska to the south (Figure 1). The southern Kenai Mountains support the Harding Ice Field and Grewingk-Yalik Ice Complex (Figure 1), which are drained by 38 outlet glaciers. Grewingk Glacier (72 km^2) is the largest tongue of the

Grewingk-Yalik Ice Complex (Wiles & Calkin, 1994), with a length of 19 km and a pro-glacial lake directly at its terminus (48 m asl).

The local bedrock consists of the Mesozoic McHugh Complex, composed of greenstone, chert, and greywacke beds, with mélanges of the three lithologies (Bradley & Kusky, 1990). The McHugh Complex contains volcanic rocks including a variety of basalts, but apparently lacks ultramafic or mafic plutonic rocks, which have high magnetic susceptibility (Bradley & Kusky, 1990).

At ~445 m asl, Emerald Lake (Figure 2) is about 25 km east of Homer and 5.6 km from Kachemak Bay (Figure 1). Emerald Lake was formed from glacial erosion. The average depth of the 0.5 km^2 lake is approximately 20 m; the greatest depth is in the center (52 m) (Figure 4). Steep rock faces line the edges of Emerald Lake's ~9 km^2 drainage area to the northeast of the lake (Figure 2) with smaller hills to the west The primary inflow to Emerald Lake is from the east (Figure 4), and multiple streams and ponds feed the inflow. The outflow is to the west, where it discharges into the outwash stream from Grewingk Glacier's proglacial lake.

A topographic divide (450 m asl) (Figure 2; Figure 5) currently separates Grewingk Glacier from Emerald Lake. At the divide, Grewingk Glacier is ~2.1 km from Emerald Lake and ~30 m lower than the topographic divide based on topographic data from 2012 satellite images viewed in Google Earth (Figure 5). The divide is 1.6 km from Emerald Lake and 0.5 km from Grewingk Glacier. A prominent ~ 3-km-long right lateral moraine on the divide (Figure 2) is well preserved, composed of gravel with cobbles and scarce boulders, and is covered by little vegetation. Large rock surfaces suitable for lichen growth on the sharp moraine crest are rare. The ridge is discontinuous for ~2 km

down-valley, visible in satellite photos. No inset moraines are visible on or near the divide. A low-relief ridge covered in ~0.5 m of silt and densely rooted grass forms the outermost moraine (Figure 5). The moraine remains undated because it lacks boulders for lichenometry and a test pit did not expose any visible tephra layers.

METHODS

Lake coring

Sediment cores were extracted from Emerald Lake during August 2012 (Table 1) by a research team from Northern Arizona University. The bathymetry of the lake (Figure 4) was mapped prior to coring using a GPS-enabled sonar depth recorder. Cores from three sites were collected using a gravity surface corer and a percussion corer from a stationary floating platform. A Knudsen 320BP acoustic seismic profiler at 12 and 200 khz frequencies was used to image the sediment thickness and stratigraphy. Core sites were chosen based on lake depth and thickness of sediment packages determined using acoustical profiling (Figure 6). Central sites with high sedimentation rates contain a more detailed sequence, whereas distal sites include a longer time span in a compact sequence.

Lithostratigraphy

Density was measured on the whole cores using gamma-ray attenuation at 0.5 cm intervals with a Geotek multi-sensor core logger at the Limnological Research Center at the University of Minnesota. The cores were then split, photographed with digital line-scan imaging, measured for downcore variation in magnetic susceptibility (MS) at 0.5 cm

intervals, and VIS-RS (visible spectrum: 360-740 nm) using a Konica Minolta CM-2600d spectrometer on the split core face. Half of the core was shipped to Northern Arizona University (NAU) for additional analysis and the other (archive half) was stored at the Limnological Research Center. In NAU's Sedimentary Records Laboratory, sedimentary sequences were described by sedimentary structures and textures (bed thickness, sharpness of contacts, color) and major and minor constituents were identified using methods from Schnurrenberger et al. (2003). Colors were described using a Munsell Soil Color Chart.

Tephra descriptions

Tephra beds were located using peaks in MS, color, and texture that contrasted with the surrounding ambient sediment. Internal stratigraphy was noted from exposed core face. Samples of tephra from each bed were extracted and sieved to determine bulk grain size, where < 0.1 mm was designated as fine grained, 0.1 to 0.15 mm as medium grained, 0.15 to 0.25 mm as coarse grained, and > 0.25 mm as very coarse grained using grain-size classification created for this study. Samples were then dried and made into a loose grain mount with a Plexiglas surface to view grains. The relative portion of crystals, ash and glass morphologies, and crystal mineralogy were determined with a binocular scope. Only the relatively pure deposits thicker than 1 mm were analyzed because they are easiest to describe and probably represent the largest tephra-fall events at the study site.

Tephra beds were correlated between Emerald Lake cores and with Goat Lake cores. ^{14}C ages were the primary correlation tool, along with color and thickness. Tephra

beds in Goat Lake were not assigned ages by Daigle & Kaufman (2009) so these were estimated using depths of beds marked on the published stratigraphic column, MS values, and the age-depth relationship in the age model.

Organic content

The organic content of the Emerald Lake sediment was measured using two bulk-sediment indicators that could be measured rapidly at centimeter scale. Visible range scanning reflectance spectroscopic (VIS-RS) data were used to infer the chlorin content within the sediment. Chlorin are molecules from chlorophyll, derived from allochthonous and autochthonous primary productivity (von Gunten et al., 2012). Relative Absorption Band Depth (RABD) is the ratio between the reflectance minimum and the reflectance value for the wavelength, using a linear interpolated reflectance sequence. Sedimentary chlorophyll has absorption peaks between 660-670 nm (Wolf et al., 2006). I used the $RABD_{660;670}$ index (Rein & Sirocko, 2002) to calculate chlorophyll concentrations:

$$[(6*R_{590}+7*R_{730})/13]/R_{min(660;670)}$$

where $R_{min(660;670)}$ = minimum reflectance at 660 or 670 nm, R_{590} = reflectance at 590 nm, and R_{730}= reflectance at 730 nm.

Organic-matter content was also used to infer levels of productivity within and around Emerald Lake. The lacustrine sediment was analyzed for organic matter (OM) content at NAU by loss on ignition (LOI) at 1 cm intervals, using methods from Heiri et al. (2001), where the mass of a sample is measured before and after high-temperature

(550°C for 5 hours) ignition. LOI samples were not contiguous because some samples were shifted to avoid collecting tephra beds. Bulk density was calculated by dividing the mass of wet sample (g) by volume of sample (2 cm^3).

Geochronology – Lichenometry

Lichenometry is based on the premise that the largest individual lichen growing on a surface is the oldest and that lichen size increases systematically with age (Wiles et al., 2010). Regional lichen-growth curves can be used to infer the timing of landform stabilization. Equations have been developed to convert lichen diameter to age for locations on the Kenai Peninsula (Wiles & Calkin, 1994). Multiple lichen-growth curves have been constructed for the Kenai Peninsula (Wiles & Calkin, 1994; Solomina & Calkin, 2003). Solomina & Calkin (2003) developed the most recent lichen-growth curve in Alaska by re-calculating the growth rate using calibrated ^{14}C ages and fitting the mathematical function constructed by Wiles & Calkin (1994). The lichen-growth curves are based on the mean diameter of the five largest *Rhizocarpon* sp. surfaces of known ages, typically from tree-ring counts. Solomina & Calkin (2003) derived the logarithmic curve:

$$t = 43.950 \times 10^{(0.0081712 \times D)}$$

where t = age in years before 2012 and D = lichen diameter (mm).

At Emerald Lake, lichen dimensions from stationary boulders on top of the right lateral moraine on the topographic divide were obtained at two sites of bouldery debris, selected for the abundance of lichens, by measuring the long axis of the largest lichen *Rhizocarpon* sp. with a ruler. Lichen were rejected as irregular if their diameter exceed

the size of the next smallest diameter by 20 % (Calkin & Ellis, 1980). I used the methods and lichen growth curve of Solomina & Calkin (2003) to estimate the timing of moraine stabilization. Accuracy of lichenometric ages using these methods is around ± 15-20% (Calkin & Ellis, 1980).

Geochronology – ^{210}Pb ages

The chronology for the sedimentary sequence from Emerald Lake was based on radiocarbon ages and a ^{210}Pb profile. ^{210}Pb was used to date the last 140 years of sediment at Site 3, the high-sedimentation site. ^{210}Pb in sediments includes both (1) supported ^{210}Pb produced from radioactive decay of ^{226}Ra when both radionuclides have reached equilibrium, and (2) excess ^{210}Pb generated from radioactive decay of ^{222}Rn in the atmosphere and water column. Two samples were analyzed for ^{226}Ra activity at 2.5 cm and 22.5 cm depths. Excess ^{210}Pb was calculated by subtracting the ^{226}Ra activity from the closest sample from the total ^{210}Pb value. Similar ^{210}Pb and ^{226}Ra activities measured in the same section indicates that the background level of supported ^{210}Pb has been reached in the profile. I sampled 2 cm^3 of sediment to obtain 0.5-1.0 g (dry wt) every 1 cm down to 23 cm below lake floor (blf). Samples were sent to Flett Research Ltd, Manitoba, Canada, where analyses of seven ^{210}Pb and two ^{226}Ra samples were determined to provide a sufficiently accurate age model. ^{210}Pb activity was calculated indirectly using alpha-spectrometry measurements of ^{210}Po, which is in secular equilibrium with ^{210}Pb within two years of ^{210}Pb deposition and ^{226}Ra was determined by ^{222}Ra emanation. The error in ^{210}Pb ages was calculated using an exponential equation developed by Vaillencourt et al. (2013) that relates known ages of lake sediment to ^{210}Pb

ages from the same profile, as determined by Binford (1990). Using this approximation, the error increases from ± 2 years at AD 2000 to ± 50 years at AD 1860.

The ^{210}Pb age profile was based on a Constant Rate of Supply model because it can provide valid predictions over the length of the modeled core, even with the sediment accumulation rate changing with time, whereas the linear regression model, also known as the Constant Initial Concentration model, relies on constant concentrations of unsupported ^{210}Pb per unit weight of accumulated sediment (Appleby & Oldfield, 1978). Where ^{210}Pb profiles experience periods of accelerated accumulation rates, the Constant Rate of Supply and Constant Initial Concentration model results diverge. If Constant Rate of Supply model and regression model produce similar results for average sediment accumulation rate during the intervals of constant accumulation rate, the Constant Rate of Supply model is functioning correctly.

Geochronology – ^{14}C ages and age model

Fourteen samples of ~0.3 mg of organic material composed of wood, leaf, or insect macrofossils relatively equally spaced throughout the sedimentary sequence of the Site 2 and 3 cores were analyzed by Keck Carbon Cycle AMS facility, UC Irvine. To prepare samples for radiocarbon dating, approximately 3 cm^3 of sediment was rinsed, sieved at 100 μm, and at least 3 mg collected with tweezers. The organic material was rinsed thoroughly, dried, and weighed. ^{14}C ages were calibrated using CALIB 7.0 (Stuiver and Reimer, 1993) and reported as the median of the calibrated age probability density function. Errors are reported as ± one half of the 1σ calibrated age range. All ages in this thesis are reported in calendar years prior to 1950 (cal yr BP).

An age model was developed using the age-depth modeling software CLAM v2 (Blaauw, 2010) using ^{14}C and ^{210}Pb ages and the age of the sediment-water interface (AD 2012). The model generates Monte Carlo age-depth fits through the age-probability distribution of the ^{14}C calibration to establish the best-fit age-depth curve using 10,000 iterations. Each age model was separated into two segments (upper and lower) because the spline curve fits in CLAM v2.0 were unable to generate a single realistic age model due to abrupt changes in sedimentation rates. The segments were spliced together at the depth where the difference between the ages generated by the two age models was smallest. The thicknesses of tephra beds thicker than 1 mm were removed using the "slump" function in CLAM v2, which accounts for their instantaneous deposition. The gap and cobble in Core 2 were treated as normal sediment accumulation. The ages were fit with a smooth spline (type = 4) with different smoothing values (Core 3 upper = 0.58, lower smooth = 0.22; Core 2 upper = 0.17, lower = 0.15) so that the spline intersected nearly all of the calibrated age ranges. Low smoothing values that generated a curve without age reversals, with a low best-fit value, and with a relatively uniform sedimentation rate throughout a unit of sediment were preferred.

An age model for Goat Lake sediments was also created in CLAM v2 (Blaauw, 2010) using ^{14}C and ^{210}Pb ages in Daigle and Kaufman (2009) to compare to the linear-segmented age model. The model was created using methods applied on Cores 2 and 3 from Emerald Lake. The ages were fit with a smooth spline (type =4) with smoothing value = 0.54.

RESULTS

Seismic profiles

In lacustrine sediment a prominent reflector typically represents a tephra bed surrounded by ambient sediment or the transition from organic-rich to inorganic mud (e.g. Daigle & Kaufman, 2009). The seismic profile across Emerald Lake Site 1 (Figure 6) shows 2 m (17-19 m below water surface) of sediment with reflectors. All 2 m of sediment was captured in the Site 1 cores. The cores from Site 1 were not analyzed so it is difficult to determine whether any tephras or lithological changes correspond to strong reflectors.

The seismic profile across Site 2 is similar to Site 1, with sediment extending ~2 m blf (19- 21 m below water surface), but Site 2 has stronger reflectors in the top 1 m of the profile. The strong reflectors in the top 0.5 m of the profile (50 cm blf; Figure 6) likely represent the peaks in density associated with the inorganic mud and tephra beds from 50 cm blf to the core top (Figure 7B). The bottom 1.5 m (150 cm blf) of the profile lacks strong reflectors and coincides with the inorganic mud from the core bottom to 160 cm blf. The low resolution of the seismic stratigraphy makes it difficult to match reflectors to lithologic changes within the sequence.

The seismic profile from Site 3 (Figure 6) exhibits greater sediment thickness than the other two sites, extending nearly 12 m blf (~51.5 to 64 m below water surface). There are more strong reflectors in the Site 3 profile than sites 1 and 2. The strong reflector at the top of the profile (52 m = 25 cm blf; Figure 6) likely displays the change in density from organic mud (25 cm blf to top) to inorganic mud (80 to 25 cm blf). The strong, thin reflectors (54-53 m = 200-100 cm blf) are likely tephra beds surrounded by the ambient organic-rich mud from 150 to 100 cm blf (Figure 7A). The gap in reflectors (54 m = 200

cm blf) likely corresponds to the gap in tephra beds ~150 to 190 cm blf. The reflectors in all profiles decrease in strength with increasing depth.

Emerald Lake sediment cores

Cores collected from Emerald Lake include three short surface cores (EMD-1C, -2C, -3C), and three longer percussion cores (EMD-1A, -2A, -3A) (Table 1). The cores from sites 2 and 3 were used for laboratory analysis. Site 3 is at the deepest part of the lake where sedimentation rate, and therefore sample resolution, is highest. Site 2 is from the distal end of the lake where sedimentation rate is low and the core extends back ~8 ka further than from Site 3. Site 1 cores were not analyzed because the amount of detail was similar to Site 2 cores but the record did not extend back as far.

Surface core EMD-3C was spliced onto the longer core EMD-3A at 36 and 25 cm tube depth, respectively, using correlations of MS peaks with similar magnitudes and corresponding tephra beds. The total length of the spliced sedimentary sequence from Site 3 is 2.60 m (Figure 7A). The surface core EMD-2C was spliced onto the longer core EMD-2A at 54 and 47 cm, respectively, using the color and texture of one distinct tephra bed to correlate between the two sequences. The total length of the spliced sediment core from Site 2 is 3.03 m.

The sediment from Emerald Lake is dominated by brown organic-rich mud, with contrasting grey inorganic mud at the base and near the top of the sequence (Table 2). Layers of organic-rich mud are massive, lack visible macrofossils, and have high productivity values (chlorophyll and OM) and low MS and density values. Layers of inorganic mud typically are clayey and weakly laminated with angular, lithic granules

(siltstone), and have low productivity values (< 5% OM) and high MS and density values. Units of inorganic mud have higher chlorophyll values and OM content than tephra beds. Tephras are common throughout (Table 3). The two cores contain different tephras, with eight more beds in Core 3 than Core 2. Four tephra beds can be tentatively correlated between the cores (Table 4).

The density values determined by gamma-ray attenuation at the LRC are very similar to the bulk-density values measured at NAU (Appendix A). The broad-scale fluctuations are present in density records of both cores, though the values measured at NAU are typically ~0.2 g/cm^3 higher. The LRC density data are preferred because they were measured at 0.5 cm resolution compared to 1.0 cm intervals at NAU.

Density and chlorophyll values from the LRC are listed in Appendix A and LOI values in Appendix B. Density values range from 1.0 to 2.5 g/cm^3, with averages of 1.1 and 1.3 g/cm^3 for Core 3 and 2, respectively. Chlorophyll has a low baseline (~1.00 to 1.07) with values increasing up to 1.2; OM content hovers around a high baseline of 5-20% and ranges from 0 to 45%. There is no overall trend in OM or chlorophyll in either core.

Density and MS are not correlated ($r = -0.005$; $p = 0.87$) in Cores 2 and 3. Though the parameters fluctuate similarly in beds of organic-rich mud and tephra, the relationship diverges in inorganic mud. Tephra beds have high density because they are composed of fine, well-sorted, and low-OM-content material that results in low porosity.

Chlorophyll and OM content are correlated ($r = 0.45$, $p < 0.01$) in cores 2 and 3, as they are both indicators of productivity (Figure 7). OM is higher in Core 3 (15%) than Core 2 (10%) in the main organic-rich units (Units 3-1 and 2-4). No obvious peaks in

chlorophyll and OM content are visible in Core 3; however, in Core 2, chlorophyll and OM content peak at 32 and 10 cm blf, extending up to 0.22 and 45%, respectively. The high values of chlorophyll content above and below the cobble from 110-100 cm blf in Core 2 are likely from organic-rich debris dislodged by the shifted clast (see below).

Sediment description – Core 3

The Core 3 sequence is composed of three lithostratigraphic units (Figure 7A; Table 2) and all contacts between units are sharp. Unit 3-1 (4.3 cal ka – AD 1381) is brown silty organic-rich mud that extends from the base of the core to 81 cm blf with 16 tephra beds ranging from 1 to 170 mm thick (Table 3) and a diffuse upper contact. Two beds of sandy organic-rich mud are overlain by tephra beds (between 135-145 cm blf; Figure 7A). Unit 3-2 (81-25 cm blf; AD 1380 – 1780) is gray laminated inorganic mud (< 10% OM) interrupted by one thin bed of very dark grayish brown (2.5Y 3/2) to dark brown (7.5YR 3/2) sandy organic-rich mud from 77.0 to 73.5 cm blf with diffuse contacts. The organic-rich mud 77-73.5 cm blf (496- 437 cal ka) corresponds to a 10% increase in OM content and 0.3 increase in chlorophyll. Unit 3-3 (AD 1780 – 2010) is gray silty organic-rich mud and extends from 25 to 0 cm blf, with an ~1-cm-thick light brownish gray (2.5Y 6/2) bed of coarser material. The unit contains 2 tephra beds (2 and 15 mm thick) with sharp contacts.

Sediment description – Core 2

The Core 2 sequence is composed of six distinct lithostratigraphic units (Figure 7B; Table 2) and contacts are generally sharp. Unit 2-1 (303-226 cm blf; prior to 11.4 –

11.4 cal ka) is gray clayey inorganic mud with angular siltstone clasts and no tephra beds. Unit 2-2 (226-206 cm blf; 11.4 – 10.7 cal ka) is brown organic-rich mud with no tephra beds and diffuse contacts. Unit 2-3 (206-164 cm blf; 10.7 – 9.8) is clayey inorganic mud similar to Unit 2-1, and both have high density values (~2 g/cm^3). Unit 2-4 (164 to 11 cm blf; 9.8 cal ka – AD 1580) is dominated by brown organic-rich mud but interrupted by ~5- to 10-cm-thick beds of black (2.5Y 2/0) organic-rich detritus. The unit contains nine tephra beds from 2 to 100 mm thick (Table 3). The thick tephra from 29-19 cm blf has the highest density of the tephra beds (~1.7 g/cm^3). This tephra is disproportionally thick compared to its counterpart in Core 3.

The large (10 cm diameter) clast in Unit 2-4 may have temporarily blocked sediment from entering the core barrel during coring, but realistic and consistent sedimentation rates suggest little offset occurred in sediment surrounding the gap and cobble. The thickness of the cobble is nearly equivalent to the amount of sediment that would have entered the tube. The sediment gap and cobble were entered into the age model using the slump function (alternative model) and as normal sediment (preferred model). The depths with ages generated from the preferred age model have MS peaks that agree with the Goat Lake MS better than the alternative model, suggesting the displacement that occurred during coring captured a sediment thickness similar to what would have entered the tube had the rock not blocked the tube entrance, preventing mud from entering. The gap in sediment (100-90 cm blf) coincides with high-density values. Because density is measured on the whole core, it is likely that the clast was moved as the core was split. LOI samples were not extracted from the interval containing the gap and clast.

Unit 2-5 (11 to 2 cm blf; AD 1580 – 1960) is gray laminated inorganic mud (< 10% OM) with an indistinct lower contact and no tephra beds. The unit is similar to its counterpart in Core 3 (Unit 3-2) in lacking angular clasts that are present in the other inorganic-mud units (2-1 and 2-3). Highest peaks in chlorophyll and OM content correspond to organic-rich detritus layers of Unit 2-5 (Figure 7B). These beds at 85-84.5, 31.5-29, and 18.5-11.5 cm blf are absent from Core 3. Unit 2-6 from 2 to 0 cm (AD 1960 – 2010) blf is organic-rich with an indistinct lower contact and no tephra beds.

Geochronology- Lichenometry

Lichens measured in two locations on the moraine on the topographic divide date the retreat of Grewingk Glacier from the maximum extent during the LIA. The five largest *Rhizocarpon* sp. diameters from lichen sites 1 and 2 were 52 and 42 mm, which imply ages of 1895 and 1915 AD, respectively (Table 5).

Geochronology- Sediment core age models

The ^{210}Pb activity profile (Table 6) in Core 3 shows an exponential decrease with depth (Figure 8A). Sediment-accumulation rates over the past 140 years represented in the ^{210}Pb profile range from ~1.9 to 1.2 mm/yr. These rates are slightly higher than those from Unit 3-3, which average about 1.1 mm/yr based on the ^{14}C age model. The average sedimentation rate in Unit 3-3 fluctuates, suggesting the Constant Rate of Supply model is more suitable for the ^{210}Pb data. The ^{210}Pb Constant Rate of Supply model and linear regression model (average sediment accumulation rate of 1.0 mm/yr) produce similar results, suggesting the Constant Rate of Supply model is functioning correctly.

Fourteen radiocarbon ages (Table 7), ^{210}Pb ages, and the core top (2012) were used to develop age-depth models for cores 2 and 3 (Figure 8). Input values for CLAM are in Appendix C and generated ages for each depth are in Appendix D. One radiocarbon age from Core 2 was rejected because it was significantly younger than the trend defined by the other ages. The 95% confidence (2σ range of the mean of iterations) ranges from ± 5 to 224 years for Core 3 and ± 18 to 557 years for Core 2, with an average of ± 145 and ± 259, respectively.

A composite sedimentary sequence was constructed using Core 2 for the section below a prominent tephra with a distinctive mineralogy (Hayes tephra, 4.0 cal ka) and Core 3 for the section above the prominent tephra. The age model for the younger section of Core 2 is unreliable and not used in this study because it is based on only one ^{14}C age, whereas Core 3 contains a more highly resolved sedimentary sequence.

Sedimentation rate is not constant throughout cores 2 and 3 (Figure 8). Average sediment accumulation rate is much higher in Core 3 (0.75 mm/yr overall) compared to Core 2 (0.28 mm/yr). Sediment is Core 3 represent around one-fifth the time captured in Core 2. In Core 3 the sedimentation rate increases towards the top of the core, with no abrupt changes. The sedimentation rate in Core 2 is low throughout the core, and includes an abrupt decrease in sedimentation rate around 5.5 cal ka.

Tephras

Magnetic susceptibility (MS) in Core 3 has a relatively low and uniform baseline with sharp peaks exceeding 200 (SI x 10^{-5}) (Figure 7A) that coincide with tephra beds.

MS in Core 2 has a low baseline ~20 (SI x 10^{-5}) with sharp peaks extending to ~800 (SI x 10^{-5}) (Figure 7B).

Tephras are generally coarser texture and lighter color compared to the adjacent sediment. Most contacts are sharp. The tephra beds range in thickness from 0.1 to 17 cm, and in color from light gray (2.5Y 7/2) to grayish brown (2.5Y 5/2) (Table 3). Bulk grain size is typically fine to medium grained. Tephras in Core 3 at 198.2 cm blf and Core 2 at 111.5 cm blf are dominated by coarse grains and the tephra in Core 3 at 200.5 cm blf is dominated by very coarse grains.

The tephras are dominated by fine ash particles with rare bubble wall glass shards and angular frothy pumice, and varying concentrations of crystals, including quartz, feldspar, and mafic minerals (Table 3). The crystals are generally too small to identify with confidence under binocular scope. Dark minerals are magnetite, hornblende or biotite. Quartz is the dominant mineral in most tephra beds. The fraction of crystals in the tephra ranges from 0 to 95% (Table 3), though crystal content is generally low. Tephras at 200.5 cm blf (Core 3) and 111.5 cm blf (Core 2) contain at least 70% crystals and are termed crystal-fall deposits.

Core 3 contains 18 distinct tephra deposits and has a tephra-fall frequency of 4.5 tephras per 1000 years. Core 2 contains eight tephra deposits and has a tephra-fall frequency of 0.8 tephras per 1000 years. The lower sedimentation rate at Site 2 resulted in a more compact sequence with missing tephras compared to Site 3.

Four tephra beds show evidence of mixing with the ambient lake sediment. In Core 3 the tephra at 154.6 cm blf contains abundant, ~3 mm, rounded to angular, black chert fragments (Table 4). The tephras in Core 2 at 74.9 and 84.2 cm blf contains

numerous translucent, tubular diatoms. One tephra (187.5 cm blf; Core 3) appears black because of the abundant organic matter, dominated by wood fragments.

The tephra beds with ages of 4017 ± 80 cal yr BP in Core 3 and 3629 ± 140 cal yr BP in Core 2 (Table 3) overlap with the currently accepted eruption date of 3900 ± 250 cal yr BP of the Hayes tephra (de Fontaine et al., 2007). The beds are both thicker than 1 mm and contain biotite, characteristic of the Hayes tephra.

The correlation of tephra beds in Emerald Lake with other lake tephra records is difficult. Ash is typically preserved in only a portion of the deposition sites. Many variables influence whether a tephra is incorporated into a lake's sediment as a distinct layer, including sedimentation rate, underwater currents, and distance from the volcano. A low sedimentation rate may cause multiple distinct tephra deposits to be indistinguishable while currents may cause the tephra to mix with ambient sediment. Eruptions producing thicker tephra-fall deposits are more likely to be incorporated into sediment records. I was able to correlate tephra beds from Emerald Lake with the Hayes tephra recognized in other lake tephra records (Daigle & Kaufman, 2009; de Fontaine et al., 2007) because of the distinct mineralogy and well-known age.

DISCUSSION

Early Holocene glacial retreat and re-advance

Unit 2-1 from Emerald Lake is weakly laminated inorganic mud interpreted as glacial flour with drop stones deposited prior to 11.4 cal ka (Figure 7B) when glacial meltwater flowed into Emerald Lake. The age of the inorganic mud is consistent with the reported ice cover during the Elmendorf stade in southern Alaska (Reger et al., 2008).

The overlying Unit 2-2 is organic-rich mud, which I interpret as representing the cessation of meltwater input into Emerald Lake from 11.4 to 10.7 cal ka, deposited when Grewingk Glacier retreated below the drainage divide. This interpretation is reflected in OM and chlorophyll. The timing of the retreat of Grewingk Glacier below the divide is concurrent with warming across southern Alaska that immediately followed the coldest interval of the Younger Dryas and peaked around 11 cal ka (Figure 9 and references therein).

Sometime after 11.4 cal ka, Grewingk Glacier began to expand again, and by 10.7 cal ka, it had once more overtopped the divide, as indicated by the inorganic mud with drop stones (Unit 2-3). I interpret the inorganic mud as glacial flour, delivered in meltwater from Grewingk Glacier. Grewingk Glacier remained above the divide from 10.7 cal ka until the cessation of meltwater into the lake ~9.8 cal ka, marking the final stage of the last glacial-interglacial transition. The early Holocene re-advance is coincident with several records of temperature fluctuations in southern Alaska (Figure 9) and across Alaska (Viau et al. 2008). Viau et al. (2008) proposed cooling occurred across Alaska from 11 to 9.5 cal ka, inferred from pollen data. The advance may have been influenced by increased moisture as well; Jones et al. (2014) documented increased moisture inferred from oxygen isotopes from HT Fen during intervals of decreased temperature reported in other studies in southern Alaska. Proxy records from Greyling Lake (McKay & Kaufman, 2009), Lone Spruce Pond (Kaufman et al., 2012), Hundred Mile Lake (Yu et al., 2008), Arolik Lake (Hu et al., 2006), and Discovery Pond (Kaufman et al., 2010) document an increase in temperature from 11.8 to 10.8 cal ka, followed by a rapid decrease in temperature from 11.0 to 10.7 cal ka, concurrent with the

retreat and re-advance of Grewingk Glacier below and above the divide (Figure 9). Similarly, Clegg et al. (2011) documented a minimum July temperature around 10.5 cal ka from midge assemblages in Rainbow Lake on the Kenai Peninsula. Lone Spruce and Discovery Pond data suggest a gradual warming and HT Fen suggests decreasing precipitation until 9.8 cal ka, coincident with the retreat of Grewingk Glacier from its position at the time of minimum temperature ~10.7 cal ka.

The early Holocene glacier re-advance has not previously been documented in Alaska, though the advance may be present in Goat Lake but not captured in the sediment cores; however, the re-advance of Grewingk Glacier is concurrent with glacier advances in the Cascade Range (Beget, 1981; Heine et al., 1998). Glaciers near Mt. Rainier advanced from 10.9 to 9.9 cal ka (Heine et al., 1998), synchronous with the Grewingk Glacier advance, suggesting the decreased temperature may have occurred across the coastal northwestern US during the early Holocene.

Post-glacial period

Units 2-4 and 3-1 (Figure 7) are dominated by organic-rich mud deposited while Emerald Lake did not receive meltwater from Grewingk Glacier. The timing of the Grewingk Glacier retreat below the drainage divide of Emerald Lake (9.8 cal ka) is similar to the 9.5 cal ka age for the retreat of North Goat Glacier out of Goat Lake as reported by Daigle and Kaufman (2009). In addition, Ager (2001) established that vegetation was developing on glacial deposits by 9.8 cal ka near Tern Lake on the Kenai Peninsula.

Neoglacial advances (3500- 800 cal yr BP) prior to the LIA have been recognized along margins of the Grewingk-Yalik ice complex (Wiles & Calkin, 1994) but were not recorded in Emerald Lake. The cooler summer temperature that drove early Neoglacial advances (Calkin et al., 2001) is not discernable in OM and chlorophyll data from Emerald Lake. Grewingk Glacier advanced down-valley during the 3 cal ka and AD 621 events documented by Wiles & Calkin (1994), but the lack of inorganic mud at this time suggests Grewingk Glacier did not expand to the divide (Figure 7). This is consistent with the assessment by Wiles and Calkin (1994) who suggested the early to middle Neoglacial advances were less extensive than the LIA.

The shift in sedimentation rate ~5.5 cal ka (Unit 2-4; Figure 7B) might represent a change in climate. This shift could have also been caused by an unconformity, although there are no obvious truncation surfaces in this section of the core. Records from southern Alaska document decreased productivity (McKay & Kaufman, 2009) and decreased amounts of decomposed peat (Jones et al., 2009) beginning ~5.5 cal ka, which may be interpreted as dry conditions at this time. Anderson et al. (2006) attributed an increase in fire event frequencies from 8.5 to 4.6 cal ka to an increase in flammable biomass and warm summers. Finney et al. (2012) found that lake-level lowered from 6 to 4 cal ka at Dune Lake, interior Alaska, suggesting the decreased moisture affected a large portion of Alaska. Clegg et al. (2011) documented peak summer temperatures from midges in Rainbow Lake from 6 to 5.5 cal ka that may be associated with enhanced evaporation. Decreased mineral matter input associated with a lake-level lowering due to dry conditions and/or increased evaporation likely caused the decrease in sedimentation rate ~5.5 cal ka in Emerald Lake. The decreased sedimentation rate is absent from Core 3 (4.2

cal ka to present), which may indicate sedimentation rate increased again at the onset of the Neoglaciation (4 cal ka).

The Little Ice Age

Unit 3-2 is interpreted as glacial flour that was deposited between 596 and 178 cal yr BP (AD 1354-1772) when Grewingk Glacier expanded to overtop the divide and discharged meltwater into Emerald Lake. The absence of drop stones in the inorganic mud suggests Grewingk Glacier was farther from Emerald Lake than during the last glaciation (Unit 2-1), when drop stones were deposited. Grewingk Glacier dropped below the divide briefly from 498 to 440 cal yr BP (AD 1452- 1510), when organic-rich sediment was deposited in Emerald Lake.

The LIA glacier fluctuations recorded in Emerald Lake are synchronous with documented temperature and glacier fluctuations elsewhere in southern Alaska. Tree-ring widths suggest below-average temperatures during the LIA (AD 1200-1850; Figure 9) in southern Alaska (Barclay et al., 2003; Wiles et al., 2014), which overlaps with the period of the meltwater input into Emerald Lake with reasonable lag time (150 years) for Grewingk Glacier to respond to the decreased temperature and to expand over the divide. The age of the Grewingk Glacier LIA advance over the divide (AD 1350) agrees with the widespread advance on the Kenai Peninsula from AD 1400 to 1550, including Tebenkof Glacier (Barclay et al., 2009a), North Goat Glacier (Daigle & Kaufman, 2009), and Bear and Grewingk Glacier (Wiles & Calkin, 1994), and coincides with the Wolf solar minimum (Wiles et al., 2004). The brief input of organic-rich sediment at AD 1452 to 1510 does not coincide with increased temperature from reconstructions inferred from

tree-ring chronologies in south-central Alaska (Barclay et al., 2003), and in the average temperature over the northern hemisphere (Moberg et al., 2005); however, negative Pacific Decadal Oscillation from late 1300s to mid 1400s (MacDonald & Case, 2005) suggests that an interval of increased temperature may have occurred. The minimum OM % in Emerald Lake (AD 1600 and 1660; Figure 7A) coincides with cooling in the late 1600's and early 1700's inferred from tree-ring temperature reconstructions in the Wrangle Mountain region (Davi et al., 2003), phases of reduced tree growth (AD 1500-1700) at Nellie Juan Glacier, south-central Alaska (Barclay et al., 2003), enhanced growth of multiple glaciers in south-central Alaska (Wiles et al., 2004; Barclay et al., 2009b), and the Maunder solar minimum (Wiles et al., 2004).

Recent warming

The introduction of organic-rich mud ~178 cal yr BP (AD 1772) in Unit 3-3 (Figure 7A) marks the most recent Grewingk Glacier retreat below the divide. Davi et al. (2003) documented a warming from AD 1700-1800 which may have caused the retreat of Grewingk Glacier below the divide. The age of the Grewingk Glacier LIA retreat (AD 1772) is older than previous estimates for Grewingk Glacier and other glaciers on the Kenai Peninsula. Wiles and Calkin (1994) used the same lichenometry procedures and growth curve to date Grewingk Glacier's terminal moraine that I used and obtained a stabilization age of AD 1858, consistent with Dall (1896) and Gilbert's (1903) observations that Grewingk Glacier was retreating by the end of the 19th century. Other glacial landforms on the Kenai Peninsula indicate stabilization occurred by the late 1800's (Wiles & Calkin, 1994; Barclay et al., 2009b). Tree-ring widths (Wiles et al., 1998; D`Arrigo & Jacoby, 1999; Davi et al., 2003; Daigle & Kaufman, 2009) from the

Gulf of Alaska suggest warming following the LIA began in the 20th century, 100 years after the cessation of meltwater into Emerald Lake.

Maximum lichen diameters on the moraine that forms the divide above Emerald Lake indicate that it stabilized between AD 1895 and 1915, about 100 years after the cessation of rock flour deposition in the lake. It is possible that Grewingk Glacier began retreating during the warming from AD 1700-1800 reported by Davi et al. (2003), and dropped below the divide at AD 1772 as suggested by the Emerald Lake sediment sequence. Additionally, it is possible Grewingk Glacier did not retreat below the divide at AD 1772 but that the meltwater was directed elsewhere. However, given that Wiles and Calkin (1994) estimated the minimum stabilization age of Grewingk Glacier's outermost moraine as AD 1858, an alternative explanation is that the LIA retreat occurred in the late 1800's, with the moraine on the divide stabilizing ~AD 1900 as the lichenometric ages suggest, indicating the age model for the lake sediment is too old. Compared to the timing of the warming interval following the LIA (AD 1850; Wiles et al., 2014), it is more realistic that the retreat below the divide would occur 50 years after the warming (AD 1900) rather than 80 years before the warming (AD 1772).

Tentative correlations of tephra beds in Unit 3-3 with known eruptions of Cook Inlet volcanoes also suggest that the age of glacier retreat may be younger than the age generated by the age model. The tephra beds at 3.2 (-31 ± 4 cal yr BP = AD 1981) and 23.5 cm blf (159 ± 86.5 cal yr BP = AD 1791) are tentatively correlated with eruptions from Mt. Augustine (Table 4) (Waitt & Beget, 2009). The 1.5 cm thick tephra at 23.5 cm blf in Core 3 overlies the glacial unit by 0.5 cm (Figure 7A) and is tentatively correlated with the 1812 eruption, which is within the uncertainty range of the LIA retreat as

represented in Emerald Lake (AD 1772 ± 98). Alternatively, this tephra may represent the large eruption from Novarupta (AD 1912) previously documented on the Kenai Peninsula (Beget et al., 1994) as deposits of rhyolitic and dacitic ash with 2 geochemically distinct populations of glass shards. The Emerald Lake tephra record is not complete, as other major eruptions of Cook Inlet volcanoes in the past 200 years do not have candidate tephras in the Emerald Lake cores (pure bed > 1 mm thick), potentially including the AD 1912 eruption of Novarupta.

Comparison with Goat Lake

Daigle and Kaufman (2009) analyzed sediment cores from Goat Lake, a threshold lake in geographic position strongly analogous to that of Emerald Lake. The timing of the early Holocene retreat recorded in Emerald Lake (9.8 ± 0.2 cal ka) corresponds to the North Goat Glacier retreat below the divide separating it from Goat Lake (9.5 ± 0.1 cal ka) (Table 8). The brief re-advance from 10.7 to 9.8 cal ka recorded in Emerald Lake was not captured in Goat Lake record, possibly because the record does not extend to 9.8 cal ka.

The transition from gyttja to inorganic mud at AD 1660 marks the advance of North Goat Glacier over the divide, ~300 years after Grewingk Glacier overtopped the divide separating it from Emerald Lake (AD 1350) (Table 8); however, a radiocarbon dated log suggests North Goat Glacier was expanding during the 15th century (Daigle & Kaufman, 2009). The initial burst of meltwater into Goat Lake is overlain by a bryophyte-rich layer dated AD 1660 ± 165 that likely corresponds to the brief Grewingk Glacier retreat below the divide from AD 1452 - 1510 recorded in Emerald Lake. The

Emerald Lake record likely has a more accurate estimate of the brief retreat than the Goat Lake record because the age model is constrained by more ^{14}C ages during this interval. Other potential reasons for the difference in ages of the brief retreat are: (1) the Grewingk Glacier glacier is higher relative to the overtopping point, so Grewingk Glacier contributes meltwater into the lake more readily or (2) Grewingk Glacier responds more rapidly to climate changes than North Goat Glacier. Satellite images from 2012 show that Grewingk Glacier was about 30 m below the topographic divide (Figure 5C), while in 2006 North Goat Glacier was 150 m below its divide with Goat Lake. The dated intervals during which Grewingk Glacier and North Goat Glacier contributed meltwater into Emerald and Goat Lakes, respectively, do not coincide, but the lichenometric ages of the moraine on the divide at Grewingk Glacier are equivalent to those from the divide at Goat Lake (~ AD 1900; Daigle & Kaufman, 2009).

Eight of the 17 tephras > 1 mm thick in Goat Lake can be confidently correlated with tephras in Emerald Lake (Table 4) based on age and bed thickness. Four of the six tephras in Goat Lake are present in Emerald Lake as deposits > 5 mm thick. Three of the seven tephras > 5 mm thick in Core 3 and four of the five tephras > 5 mm thick in EMD-2 have corresponding tephra beds in Goat Lake. The Emerald Lake sediment contains more tephra beds (27 beds) than Goat Lake (13 beds), likely because it is closer to many of the Cook Inlet volcanoes (Figure 1). The agreement of the age of the Hayes tephra inferred from the Emerald and Goat Lake cores and the accepted age of the Hayes tephra reinforces the age model in both studies. See Appendix E for additional tentative correlations with other tephra records from the Kenai Peninsula.

Although ages of tephra beds in Emerald and Goat Lakes overlap, peaks in MS profiles do not coincide and have no systematic offset (Figure 10). The poor correspondence between the Emerald and Goat Lakes tephra and MS records might be associated with the different age modeling procedures used. To evaluate this possibility, tephra ages from Goat Lake were determined using the same modeling routine as used for Emerald Lake (Figure 11). The CLAM-based ages are, however, similar to those in the original Goat Lake age model (Table 4), suggesting that the different age models are not responsible for the discrepancy. I suspect the lack of agreement between the tephra records resulted from the lack of tephra deposition and preservation in both locations. Goat and Emerald Lakes tephra records are underestimates of the number of eruptions and tephra falls partially because both studies only inventoried tephra layers ≥ 1 mm thick.

CONCLUSION

1. Grewingk Glacier began retreating from the final stage of the Naptowne Glaciation prior to 11.4 cal ka. The transition from inorganic to organic-rich mud and increased productivity at 11.4 cal ka indicates the cessation of glacier meltwater input into Emerald Lake. This retreat is concurrent with warming across southern Alaska that immediately followed the peak of the Younger Dryas cold interval ~12.8 cal ka (Kaufman et al., 2010, and references therein).
2. Grewingk Glacier re-advanced above the topographic divide that separates it from Emerald Lake at 10.7 cal ka, reflected in the rapid transition from organic-rich to inorganic mud, which represents the re-introduction of meltwater input

from Grewingk Glacier. This re-advance was likely due to cooling, as it is synchronous with a decrease in temperature ~11 cal ka documented in southern Alaska (Kaufman et al., 2010).

3. Grewingk Glacier retreated out of the Emerald Lake catchment around 9.8 cal ka, as reflected in the transition from inorganic mud back to organic-rich mud. This retreat corresponds to the retreat of North Goat Glacier from its divide around 9.5 cal ka. This Grewingk Glacier retreat marks the start of the post-glacial period in this location.
4. During the Neoglacial advances (~3 cal ka and AD 600) that have been previously documented on the Kenai Peninsula (Wiles & Calkin, 1994; Barclay et al., 2009b), the Grewingk Glacier did not expand to the elevation of the divide near Emerald Lake. Glacial flour is absent from Emerald Lake during most of the Holocene.
5. The Grewingk Glacier once again expanded into the Emerald Lake catchment around AD 1350, as represented by the transition from organic-rich to inorganic mud. The advance occurred during the Wolf solar minimum and is consistent with widespread glacial advance on the Kenai Peninsula (Wiles & Calkin, 1994; Barclay et al., 2009b). The brief retreat below the divide from AD 1450 - 1510 is analogous to an influx of bryophytes into Goat Lake, although it is dated to AD 1660 at Goat Lake (Daigle & Kaufman, 2009).
6. The retreat of Grewingk Glacier from its maximum LIA extent (AD 1900) is estimated with two lichenometric ages from the moraine on the topographic divide and is consistent with the previous age estimates on the Goat Lake lateral

moraine (Daigle & Kaufman, 2009), but is somewhat younger than the Grewingk Glacier terminal moraine (AD 1858) (Wiles & Calkin, 1994). The lichen ages are ~100 years younger than the cessation of meltwater input recorded in the Emerald Lake sediments, suggesting the LIA retreat estimated from the sediment record is too old.

7. Though the records are different, four of the thicker tephra beds (> 5 mm in Emerald Lake) can be correlated between Emerald and Goat Lakes based on thickness and age. In Emerald Lake, Core 2 has a lower tephra-fall frequency than Core 3: 0.8 compared to 4.5 tephra per 1000 years. The Hayes tephra is present ~4 cal ka in the Emerald and Goat Lake cores and the thickest tephra bed ~680 cal yr BP (Core 3) coincides with the thickest deposit in Core 2 and Goat Lake. The presence of the Novarupta (1912) tephra-fall that deposited a 1 cm layer across the southern Kenai Peninsula has not been confirmed from Emerald Lake.

APPENDIX A: GEOTECHNICAL ANALYSIS PERFORMED ON EMERALD LAKE SEDIMENT CORES

Composite Core 3

Depth (blf)	Tube depth (cm)	Age (cal yr BP)	Density (g/cm3)	MS (SI x 10-5)	Chlorophyll
0.5	3C 12.0	-59	0.97	5.3	1.131
1	12.5	-55	1.17	24.8	1.139
1.5	13.0	-49	1.19	29.1	1.120
2	13.5	-46	1.23	55.5	1.068
2.5	14.0	-40	1.24	201.7	1.071
3	14.5	-36	1.20	94.4	1.077
3.5	15.0	-31	1.39	106.1	1.039
4	15.5	-29	1.32	47.9	1.061
4.5	16.0	-23	1.27	49.4	1.049
5	16.5	-19	1.33	53.9	1.049
5.5	17.0	-13	1.28	55.0	1.047
6	17.5	-9	1.33	51.1	1.068
6.5	18.0	-3	1.28	51.2	1.056
7	18.5	2	1.15	66.5	1.062
7.5	19.0	8	1.26	49.3	1.092
8	19.5	13	1.23	29.1	1.074
8.5	20.0	19	1.20	30.8	1.062
9	20.5	24	1.18	22.5	1.067
9.5	21.0	30	1.23	22.4	1.077
10	21.5	35	1.22	24.5	1.078
10.5	22.0	41	1.35	25.6	1.060
11	22.5	46	1.39	29.2	1.047
11.5	23.0	52	1.37	26.4	1.053
12	23.5	57	1.28	31.1	1.082
12.5	24.0	63	1.29	39.3	1.081
13	24.5	67	1.30	43.9	1.083
13.5	25.0	74	1.26	42.0	1.091
14	25.5	78	1.31	42.5	1.097

Composite Core 2

Depth (blf)	Tube depth (cm)	Age (cal yr BP)	Density (g/cm3)	MS (SI x 10-5)	Chlorophyll
0.5	2C 7.5	-68	1.22	95.7	1.080
1	8.0	-56	1.31	67.4	1.085
1.5	8.5	-37	1.30	39.8	1.065
2	9.0	-25	1.30	41.6	1.030
2.5	9.5	-6	1.53	45.0	1.039
3	10.0	7	1.63	50.9	1.036
3.5	10.5	26	1.56	45.1	1.029
4	11.0	40	1.49	36.9	1.034
4.5	11.5	60	1.52	42.9	1.030
5	12.0	74	1.57	43.5	1.027
5.5	12.5	95	1.59	40.9	1.032
6	13.0	110	1.48	39.4	1.029
6.5	13.5	133	1.45	41.0	1.028
7	14.0	149	1.44	46.0	1.032
7.5	14.5	174	1.45	35.2	1.036
8	15.0	191	1.41	37.3	1.034
8.5	15.5	218	1.39	38.5	1.032
9	16.0	237	1.39	37.6	1.038
9.5	16.5	266	1.39	50.9	1.041
10	17.0	286	1.38	49.5	1.040
10.5	17.5	318	1.37	57.2	1.051
11	18.0	340	1.32	59.2	1.039
11.5	18.5	374	1.30	64.4	1.041
12	19.0	398	1.31	51.2	1.073
12.5	19.5	436	1.21	17.1	1.114
13	20.0	463	1.15	9.0	1.110
13.5	20.5	504	1.11	10.3	1.061
14	21.0	533	1.07	9.7	1.041

14.5	26.0	84	1.23	45.8	1.074	14.5	21.5	578	1.08	6.1	1.063
15	26.5	88	1.29	49.4	1.083	15	22.0	609	1.18	6.4	1.235
15.5	27.0	94	1.20	46.6	1.076	15.5	22.5	658	1.15	9.5	1.184
16	27.5	98	1.30	44.5	1.077	16	23.0	692	1.15	8.4	1.082
16.5	28.0	104	1.31	53.7	1.065	16.5	23.5	746	1.14	10.7	1.059
17	28.5	108	1.33	73.4	1.078	17	24.0	783	1.14	12.2	1.100
17.5	29.0	114	1.32	70.0	1.069	17.5	24.5	841	1.23	22.5	1.077
18	29.5	117	1.31	71.4	1.068	18	25.0	881	1.28	32.2	1.091
18.5	30.0	123	1.30	71.5	1.057	18.5	25.5	944	1.33	51.6	1.088
19	30.5	127	1.33	66.8	1.061	19	26.0	987	1.35	64.2	1.045
19.5	31.0	132	1.27	70.0	1.055	19.5	26.5	1055	1.31	55.1	1.046
20	31.5	136	1.34	76.1	1.064	20	27.0	1055	1.30	58.3	1.032
20.5	32.0	141	1.32	78.7	1.051	20.5	27.5	1055	1.32	33.4	0.991
21	32.5	145	1.36	83.9	1.056	21	28.0	1055	1.44	41.3	0.990
21.5	33.0	150	1.42	93.8	1.053	21.5	28.5	1055	1.75	84.7	0.993
22	33.5	153	1.45	116.3	1.044	22	29.0	1055	1.73	85.7	0.994
22.5	34.0	159	1.35	127.9	1.046	22.5	29.5	1055	1.68	91.1	0.993
23	34.5	159	1.32	185.6	1.049	23	30.0	1055	1.72	112.5	0.992
23.5	35.0	159	1.37	197.8	1.044	23.5	30.5	1055	1.84	93.3	1.005
24	35.5	159	1.41	81.2	1.039	24	31.0	1055	1.66	95.5	1.011
24.5	36.0	162	1.38	48.3	1.035	24.5	31.5	1055	1.66	86.6	1.004
25	3A-1 25.0	167	1.48	56.5	1.037	25	32.0	1055	1.85	125.9	0.987
25.5	25.5	170	1.55	42.4	1.032	25.5	32.5	1055	1.89	224.7	1.004
26	26.0	175	1.47	29.0	1.031	26	33.0	1055	1.82	284.1	0.996
26.5	26.5	178	1.42	26.7	1.052	26.5	33.5	1055	1.81	253.5	0.999
27	27.0	183	1.39	17.0	1.039	27	34.0	1055	1.84	272.1	1.010
27.5	27.5	186	1.37	28.6	1.037	27.5	34.5	1055	1.85	279.5	1.001
28	28.0	191	1.40	32.0	1.040	28	35.0	1055	1.79	194.9	0.998
28.5	28.5	194	1.40	31.6	1.035	28.5	35.5	1055	1.54	129.3	1.007
29	29.0	198	1.37	31.4	1.043	29	36.0	1055	1.36	208.6	1.060
29.5	29.5	201	1.36	27.9	1.036	29.5	36.5	1055	1.35	513.8	1.040
30	30.0	205	1.38	33.1	1.036	30	37.0	1103	1.50	863.5	1.029
30.5	30.5	208	1.38	32.3	1.041	30.5	37.5	1176	1.45	849.9	1.110
31	31.0	212	1.33	35.9	1.039	31	38.0	1227	1.29	100.6	1.249
31.5	31.5	215	1.36	37.3	1.040	31.5	38.5	1306	1.13	19.1	1.113
32	32.0	219	1.40	40.5	1.042	32	39.0	1361	1.15	24.2	1.114

32.5	32.5	222	1.37	41.0	1.041	32.5	39.5	1446	1.21	32.4	1.097
33	33.0	226	1.38	34.7	1.040	33	40.0	1505	1.23	51.2	1.086
33.5	33.5	229	1.35	50.6	1.039	33.5	40.5	1597	1.17	55.3	1.090
34	34.0	232	1.40	41.0	1.037	34	41.0	1659	1.22	55.6	1.090
34.5	34.5	235	1.37	37.0	1.042	34.5	41.5	1691	1.31	128.0	1.057
35	35.0	239	1.36	33.4	1.035	35	42.0	1756	1.39	148.6	1.053
35.5	35.5	241	1.40	32.8	1.045	35.5	42.5	1856	1.34	115.7	1.060
36	36.0	245	1.34	35.0	1.040	36	43.0	1925	1.45	187.8	1.048
36.5	36.5	247	1.36	33.0	1.033	36.5	43.5	2029	1.50	129.6	1.057
37	37.0	251	1.33	34.5	1.051	37	44.0	2101	1.33	86.1	1.077
37.5	37.5	253	1.36	41.0	1.038	37.5	44.5	2210	1.36	166.8	1.040
38	38.0	257	1.35	44.6	1.032	38	45.0	2283	1.45	472.2	1.031
38.5	38.5	259	1.40	42.7	1.033	38.5	45.5	2396	1.49	862.8	1.042
39	39.0	262	1.40	45.4	1.041	39	46.0	2472	1.47	593.4	1.048
39.5	39.5	265	1.38	32.8	1.034	39.5	46.5	2587	1.50	473.4	1.058
40	40.0	268	1.39	27.2	1.036	40	47.0	2665	1.49	396.1	1.027
40.5	40.5	270	1.39	28.2	1.039	40.5	47.5	2783	1.33	114.2	1.035
41	41.0	273	1.40	29.3	1.034	41	48.0	2862	1.25	83.7	1.053
41.5	41.5	275	1.39	29.3	1.035	41.5	48.5	2982	1.34	104.8	1.055
42	42.0	278	1.42	33.3	1.034	42	49.0	3062	1.27	122.9	1.038
42.5	42.5	280	1.44	41.0	1.033	42.5	49.5	3183	1.23	145.0	1.035
43	43.0	284	1.47	35.6	1.037	43	50.0	3264	1.42	139.8	1.035
43.5	43.5	285	1.45	30.5	1.031	43.5	50.5	3385	1.24	168.7	1.018
44	44.0	288	1.50	29.4	1.036	44	51.0	3426	1.31	251.0	1.061
44.5	44.5	290	1.47	29.9	1.038	44.5	51.5	3467	1.50	169.1	1.051
45	45.0	293	1.47	27.4	1.040	45	52.0	3548	1.35	207.5	1.056
45.5	45.5	295	1.37	28.8	1.031	45.5	52.5	3589	1.52	339.2	1.046
46	46.0	298	1.43	35.2	1.031	46	53.0	3589	1.68	227.8	1.049
46.5	46.5	300	1.41	36.8	1.036	46.5	53.5	3589	1.68	300.3	1.031
47	47.0	302	1.40	40.2	1.035	47	54.0	3710	1.48	306.7	1.048
47.5	47.5	304	1.42	38.8	1.033	47.5	2A-1 47.0	3791	1.37	155.8	1.049
48	48.0	307	1.44	30.2	1.034	48	47.5	3912	1.29	104.0	1.051
48.5	48.5	309	1.35	26.4	1.036	48.5	48.0	3993	1.27	109.6	1.057
49	49.0	311	1.41	27.5	1.037	49	48.5	4112	1.29	58.5	1.058
49.5	49.5	313	1.37	25.9	1.032	49.5	49.0	4191	1.22	42.6	1.071
50	50.0	315	1.41	30.9	1.034	50	49.5	4309	1.25	43.1	1.076

50.5	50.5	317	1.40	27.2	1.035	50.5	50.0	4387	1.21	40.6	1.067
51	51.0	320	1.41	23.4	1.027	51	50.5	4503	1.22	45.7	1.093
51.5	51.5	321	1.36	28.0	1.039	51.5	51.0	4579	1.33	58.1	1.078
52	52.0	324	1.38	24.2	1.034	52	51.5	4691	1.33	96.1	1.069
52.5	52.5	325	1.39	25.5	1.032	52.5	52.0	4765	1.33	139.4	1.060
53	53.0	327	1.42	27.4	1.034	53	52.5	4838	1.37	350.0	1.068
53.5	53.5	329	1.38	30.3	1.034	53.5	53.0	4909	1.32	541.8	1.069
54	54.0	331	1.39	29.5	1.034	54	53.5	4980	1.32	292.5	1.071
54.5	54.5	333	1.38	33.8	1.036	54.5	54.0	5084	1.32	187.6	1.070
55	55.0	335	1.36	34.8	1.036	55	54.5	5152	1.27	101.9	1.069
55.5	55.5	337	1.37	31.6	1.030	55.5	55.0	5251	1.22	33.5	1.072
56	56.0	339	1.44	33.2	1.031	56	55.5	5315	1.17	22.6	1.068
56.5	56.5	340	1.34	28.0	1.034	56.5	56.0	5409	1.17	27.3	1.082
57	57.0	342	1.35	28.8	1.036	57	56.5	5470	1.17	38.2	1.085
57.5	57.5	344	1.39	31.9	1.035	57.5	57.0	5558	1.17	19.0	1.083
58	58.0	346	1.36	31.1	1.026	58	57.5	5615	1.13	22.7	1.087
58.5	58.5	347	1.38	30.0	1.033	58.5	58.0	5638	1.14	22.0	1.094
59	59.0	349	1.38	30.6	1.040	59	58.5	5660	1.15	20.3	1.100
59.5	59.5	351	1.33	31.1	1.035	59.5	59.0	5695	1.14	36.6	1.101
60	60.0	353	1.34	32.1	1.033	60	59.5	5717	1.22	115.4	1.090
60.5	60.5	354	1.33	32.0	1.033	60.5	60.0	5751	1.19	123.3	1.084
61	61.0	356	1.29	30.9	1.037	61	60.5	5774	1.19	36.2	1.098
61.5	61.5	357	1.30	30.8	1.037	61.5	61.0	5808	1.22	24.9	1.096
62	62.0	359	1.32	29.1	1.039	62	61.5	5830	1.21	31.9	1.109
62.5	62.5	360	1.38	30.9	1.036	62.5	62.0	5864	1.28	21.2	1.111
63	63.0	362	1.37	30.3	1.038	63	62.5	5886	1.25	18.3	1.104
63.5	63.5	364	1.36	32.9	1.030	63.5	63.0	5920	1.25	15.9	1.118
64	64.0	366	1.37	35.1	1.027	64	63.5	5942	1.23	14.9	1.121
64.5	64.5	367	1.33	30.1	1.034	64.5	64.0	5976	1.17	13.5	1.113
65	65.0	369	1.39	32.1	1.042	65	64.5	5998	1.14	15.9	1.122
65.5	65.5	370	1.40	42.8	1.039	65.5	65.0	6031	1.09	17.8	1.115
66	66.0	372	1.32	43.3	1.030	66	65.5	6053	1.16	20.8	1.089
66.5	66.5	373	1.26	34.5	1.036	66.5	66.0	6086	1.18	20.7	1.104
67	67.0	375	1.22	34.3	1.034	67	66.5	6108	1.21	32.3	1.089
67.5	67.5	376	1.21	33.6	1.055	67.5	67.0	6141	1.14	50.6	1.076
68	68.0	378	1.15	27.2	1.037	68	67.5	6163	1.17	59.9	1.078

68.5	68.5	379	1.19	25.5	1.027	68.5	68.0	6195	1.24	50.6	1.082
69	69.0	381	1.27	30.1	1.039	69	68.5	6217	1.21	29.1	1.077
69.5	69.5	382	1.23	33.5	1.036	69.5	69.0	6249	1.20	23.3	1.068
70	70.0	384	1.19	38.4	1.042	70	69.5	6270	1.21	24.2	1.087
70.5	70.5	388	1.35	37.5	1.061	70.5	70.0	6302	1.19	29.2	1.089
71	71.0	396	1.37	35.4	1.053	71	70.5	6323	1.21	28.3	1.075
71.5	71.5	401	1.40	37.3	1.061	71.5	71.0	6355	1.16	32.4	1.086
72	72.0	410	1.32	34.7	1.077	72	71.5	6376	1.19	27.3	1.090
72.5	72.5	416	1.30	44.2	1.062	72.5	72.0	6407	1.18	23.8	1.094
73	73.0	425	1.25	42.5	1.072	73	72.5	6427	1.18	25.5	1.090
73.5	73.5	431	1.23	39.8	1.070	73.5	73.0	6458	1.22	28.4	1.096
74	74.0	440	1.21	43.9	1.064	74	73.5	6479	1.20	37.1	1.091
74.5	74.5	446	1.24	49.6	1.046	74.5	74.0	6509	1.19	47.5	1.089
75	75.0	455	1.20	55.6	1.041	75	74.5	6529	1.28	78.7	1.101
75.5	75.5	462	1.21	67.2	1.040	75.5	75.0	6539	1.23	199.9	1.097
76	76.0	471	1.25	72.3	1.028	76	75.5	6569	1.25	375.0	1.082
76.5	76.5	478	1.17	80.5	1.038	76.5	76.0	6589	1.21	166.1	1.091
77	77.0	488		82.3	1.038	77	76.5	6618	1.17	98.9	1.096
77.5	77.5	495		59.3	1.045	77.5	77.0	6638	1.23	94.2	1.089
78	78.0	505		41.2	1.048	78	77.5	6666	1.25	97.5	1.088
78.5	78.5	512		37.5	1.048	78.5	78.0	6686	1.18	67.3	1.080
79	79.0	522		33.3	1.060	79	78.5	6714	1.14	53.5	1.116
79.5	79.5	529		29.9	1.067	79.5	79.0	6733	1.19	33.0	1.091
80	80.0	540		30.3	1.054	80	79.5	6761	1.21	21.3	1.088
80.5	80.5	547		31.1	1.059	80.5	80.0	6779	1.19	24.8	1.080
81	81.0	558		31.5	1.078	81	80.5	6806	1.19	29.2	1.066
81.5	81.5	565		45.4	1.070	81.5	81.0	6824	1.20	44.6	1.092
82	82.0	577		50.1	1.059	82	81.5	6851	1.19	59.4	1.085
82.5	82.5	584		56.4	1.048	82.5	82.0	6869	1.21	47.2	1.106
83	83.0	596	1.18	46.4	1.023	83	82.5	6895	1.25	39.1	1.114
83.5	83.5	603	1.20	43.3	1.005	83.5	83.0	6912	1.28	34.8	1.077
84	84.0	615	1.18	57.9	0.998	84	83.5	6937	1.20	33.6	1.102
84.5	84.5	623	1.18	58.9	1.002	84.5	84.0	6954	1.24	31.7	1.091
85	85.0	630	1.22	67.2	0.996	85	84.5	6971	1.18	52.5	1.115
85.5	85.5	638	1.18	79.4	0.994	85.5	85.0	6987	1.20	42.6	1.107
86	86.0	650	1.23	64.0	0.992	86	85.5	7011	1.29	78.6	1.094

86.5	86.5	658	1.35	77.9	0.992	86.5	86.0	7027	1.21	167.6	1.115
87	87.0	670	1.46	82.2	1.000	87	86.5	7051	1.23	184.9	1.095
87.5	87.5	679	1.52	114.9	1.020	87.5	87.0	7066	1.22	123.8	1.083
88	88.0	679	1.57	138.4	1.000	88	87.5	7089	1.19	90.6	1.080
88.5	88.5	679	1.63	129.1	1.006	88.5	88.0	7104	1.18	70.6	1.074
89	89.0	679	1.67	128.2	0.992	89	88.5	7126	1.21	62.1	1.085
89.5	89.5	679	1.72	185.1	0.998	89.5	89.0	7141	1.25	56.3	1.049
90	90.0	679	1.72	203.9	0.999	90	89.5	7163	1.33	83.4	1.043
90.5	90.5	679	1.73	82.0	1.018	90.5	90.0	7177	1.99	92.3	1.014
91	91.0	679	1.73	79.0	1.014	91	90.5	7198	2.11	76.8	1.011
91.5	91.5	679	1.73	147.3	1.009	91.5	91.0	7212	2.17	61.8	1.012
92	92.0	679	1.65	155.9	1.004	92	91.5	7232	2.26	58.1	1.010
92.5	92.5	679	1.61	157.4	1.020	92.5	92.0	7246	2.31	71.6	1.008
93	93.0	679	1.63	173.5	1.030	93	92.5	7266	2.30	80.7	1.003
93.5	93.5	679	1.60	152.4	1.024	93.5	93.0	7279	2.34	58.4	1.002
94	94.0	679	1.60	113.3	1.053	94	93.5	7299	2.32	50.8	1.000
94.5	94.5	679	1.61	125.4	1.021	94.5	94.0	7312	2.24	37.3	1.009
95	95.0	679	1.63	178.5	1.021	95	94.5	7331	2.27	33.3	1.020
95.5	95.5	679	1.66	229.9	1.074	95.5	95.0	7343	2.21	32.2	1.009
96	96.0	679	1.66	197.0	0.997	96	95.5	7362	2.18	27.8	1.024
96.5	96.5	679	1.68	111.2	0.996	96.5	96.0	7375	2.21	34.1	1.040
97	97.0	679	1.70	78.3	0.995	97	96.5	7393	2.23	32.4	1.010
97.5	97.5	679	1.65	76.8	1.004	97.5	97.0	7405	2.16	31.9	1.083
98	98.0	679	1.65	72.5	1.043	99	97.5	7423	2.12	28.6	1.094
98.5	98.5	679	1.63	52.9	1.042	99.5	98.0	7465	2.02	35.3	1.176
99	99.0	679	1.67	32.3	1.029	100	98.5	7482	1.93	20.2	1.071
99.5	99.5	679	1.66	49.7	1.010	100.5	99.0	7494	1.75	19.2	1.038
100	100.0	679	1.66	91.3	0.996	101	99.5	7511	1.34	41.8	1.027
100.5	100.5	679	1.66	113.2	1.047	101.5	100.0	7523	1.37	45.0	1.000
101	101.0	679	1.70	111.6	1.000	102	100.5	7540	1.32	114.2	1.000
101.5	101.5	679	1.67	55.8	1.012	102.5	101.0	7551	1.28	88.9	0.999
102	102.0	679	1.69	40.1	1.012	103	101.5	7569	1.24	62.6	1.000
102.5	102.5	679	1.53	40.3	1.026	103.5	102.0	7580	1.28	18.9	0.999
103	103.0	679	1.33	52.2	1.060	104	102.5	7597	1.19	5.2	1.001
103.5	103.5	679	1.22	104.9	1.061	104.5	103.0	7608	1.23	4.6	1.012
104	104.0	679	1.19	132.9	1.033	105	103.5	7625	1.22	5.3	1.028

104.5	104.5	679	1.18	108.7	1.068	105.5	104.0	7636	1.19	6.7	1.041
105	105.0	691	1.20	109.3	1.063	106	104.5	7653	1.17	5.5	1.088
105.5	105.5	699	1.23	72.1	1.073	106.5	105.0	7664	1.21	4.4	1.136
106	106.0	712	1.28	65.7	1.075	107	105.5	7681	1.35	3.7	1.173
106.5	106.5	720	1.26	98.9	1.081	107.5	106.0	7693	1.48	3.3	1.093
107	107.0	733	1.21	318.0	1.079	108	106.5	7710	1.28	2.7	0.997
107.5	107.5	733	1.19	232.7	1.081	108.5	107.0	7721	1.29	2.4	1.003
108	108.0	741	1.20	58.5	1.073	109	107.5	7738	1.27	2.5	1.009
108.5	108.5	750	1.19	29.9	1.086	109.5	108.0	7749	1.19	2.9	1.009
109	109.0	763	1.15	28.2	1.077	110	108.5	7766	1.16	5.3	1.046
109.5	109.5	771	1.19	24.8	1.088	110.5	109.0	7778	1.12	10.7	1.038
110	110.0	784	1.13	23.9	1.084	111	109.5	7795	1.20	14.0	1.056
110.5	110.5	793	1.17	26.5	1.083	111.5	110.0	7801	1.16	23.2	1.075
111	111.0	806	1.17	30.5	1.086	112	110.5	7807	1.19	96.4	1.069
111.5	111.5	815	1.14	29.1	1.071	112.5	111.0	7818	1.17	465.7	1.089
112	112.0	828	1.20	24.6	1.079	113	111.5	7836	1.17	780.4	1.093
112.5	112.5	837	1.17	22.7	1.106	113.5	112.0	7848	1.24	185.7	1.102
113	113.0	850	1.13	23.5	1.106	114	112.5	7866	1.22	31.7	1.120
113.5	113.5	859	1.09	20.4	1.104	114.5	113.0	7878	1.18	19.2	1.110
114	114.0	873	1.13	21.8	1.108	115	113.5	7896	1.19	13.1	1.094
114.5	114.5	882	1.15	18.7	1.088	115.5	114.0	7908	1.19	11.0	1.101
115	115.0	896	1.12	17.7	1.088	116	114.5	7926	1.21	11.3	1.099
115.5	115.5	905	1.15	18.0	1.097	116.5	115.0	7939	1.21	10.8	1.087
116	116.0	919	1.12	16.0	1.082	117	115.5	7958	1.20	10.4	1.098
116.5	116.5	928	1.15	16.3	1.092	117.5	116.0	7970	1.22	11.0	1.117
117	117.0	942	1.15	16.3	1.059	118	116.5	7990	1.22	16.6	1.086
117.5	117.5	951	1.17	18.1	1.066	118.5	117.0	8003	1.20	15.9	1.096
118	118.0	965	1.20	22.6	1.099	119	117.5	8022	1.23	15.3	1.107
118.5	118.5	974	1.21	35.3	1.046	119.5	118.0	8035	1.24	13.9	1.097
119	119.0	988	1.22	53.8	1.057	120	118.5	8055	1.24	18.1	1.089
119.5	119.5	997	1.16	50.3	1.061	120.5	119.0	8069	1.30	27.6	1.086
120	120.0	1011	1.13	35.4	1.066	121	119.5	8090	1.23	47.4	1.090
120.5	120.5	1021	1.20	27.4	1.089	121.5	120.0	8104	1.23	79.4	1.090
121	121.0	1035	1.44	34.9	1.087	122	120.5	8125	1.20	78.8	1.074
121.5	121.5	1044	1.22	78.2	1.056	122.5	121.0	8139	1.22	24.5	1.083
122	122.0	1059	1.16	238.1	1.073	123	121.5	8161	1.21	14.8	1.098

122.5	122.5	1068	1.09	190.2	1.084	123.5	122.0	8175	1.19	20.7	1.085
123	123.0	1078	1.13	45.7	1.097	124	122.5	8197	1.18	16.2	1.081
123.5	123.5	1082	1.14	25.3	1.095	124.5	123.0	8212	1.21	19.8	1.099
124	124.0	1097	1.13	20.1	1.102	125	123.5	8235	1.21	17.3	1.095
124.5	124.5	1106	1.11	22.4	1.088	125.5	124.0	8250	1.19	15.3	1.089
125	125.0	1120	1.14	22.5	1.089	126	124.5	8273	1.27	14.0	1.075
125.5	125.5	1130	1.10	20.5	1.087	126.5	125.0	8289	1.22	20.7	1.066
126	126.0	1144	1.16	20.8	1.100	127	125.5	8312	1.16	24.2	1.066
126.5	126.5	1154	1.14	20.1	1.077	127.5	126.0	8328	1.23	21.6	1.074
127	127.0	1168	1.13	28.2	1.066	128	126.5	8352	1.21	29.6	1.089
127.5	127.5	1178	1.09	22.7	1.065	128.5	127.0	8368	1.19	54.4	1.076
128	128.0	1192	1.10	20.6	1.094	129	127.5	8392	1.28	61.9	1.085
128.5	128.5	1202	1.17	20.7	1.106	129.5	128.0	8409	1.23	24.0	1.081
129	129.0	1216	1.15	25.3	1.121	130	128.5	8433	1.22	22.4	1.073
129.5	129.5	1226	1.24	33.3	1.096	130.5	129.0	8450	1.22	18.1	1.081
130	130.0	1240	1.20	25.6	1.094	131	129.5	8475	1.18	24.8	1.075
130.5	130.5	1250	1.19	24.1	1.092	131.5	130.0	8491	1.19	24.6	1.092
131	131.0	1264	1.20	34.6	1.078	132	130.5	8516	1.30	31.3	1.068
131.5	131.5	1264	1.21	46.5	1.078	132.5	131.0	8533	1.28	40.8	1.079
132	132.0	1274	1.19	57.7	1.063	133	131.5	8559	1.21	95.8	1.071
132.5	132.5	1288	1.19	64.4	1.077	133.5	132.0	8576	1.24	33.6	1.071
133	133.0	1298	1.19	56.2	1.075	134	132.5	8601	1.27	17.7	1.062
133.5	133.5	1312	1.04	46.6	1.094	134.5	133.0	8618	1.42	21.1	1.062
134	134.0	1321	1.17	42.9	1.086	135	133.5	8644	1.38	36.0	1.028
134.5	134.5	1336	1.15	35.2	1.063	135.5	134.0	8661	1.28	68.6	1.057
135	135.0	1345	1.12	24.8	1.048	136	134.5	8679	1.21	128.1	1.063
135.5	135.5	1360	1.13	25.8	1.065	136.5	135.0	8679	1.25	107.2	1.067
136	136.0	1369	1.14	17.8	1.075	137	135.5	8696	1.21	325.4	1.046
136.5	136.5	1383	1.17	17.9	1.064	137.5	136.0	8722	1.22	143.3	1.055
137	137.0	1393	1.20	24.4	1.085	138	136.5	8739	1.25	22.3	1.056
137.5	137.5	1407	1.20	37.2	1.082	138.5	137.0	8765	1.25	11.4	1.066
138	138.0	1416	1.23	27.2	1.071	139	137.5	8783	1.26	12.0	1.076
138.5	138.5	1431	1.19	35.8	1.076	139.5	138.0	8809	1.19	15.6	1.073
139	139.0	1435	1.23	45.5	1.072	140	138.5	8827	1.20	17.1	1.083
139.5	139.5	1435	1.19	65.7	1.073	140.5	139.0	8853	1.19	15.0	1.086
140	140.0	1449	1.14	50.8	1.086	141	139.5	8870	1.13	16.0	1.090

140.5	140.5	1459	1.01	54.5	1.093	141.5	140.0	8897	1.11	13.6	1.080
141	141.0	1473	0.97	61.4	1.072	142	140.5	8914	1.13	13.1	1.096
141.5	141.5	1482	1.06	54.4	1.065	142.5	141.0	8940	1.14	15.9	1.109
142	142.0	1496	1.19	30.7	1.079	143	141.5	8958	1.19	12.7	1.096
142.5	142.5	1505	1.17	26.3	1.087	143.5	142.0	8984	1.18	11.5	1.101
143	143.0	1519	1.16	23.3	1.075	144	142.5	9002	1.13	8.7	1.085
143.5	143.5	1528	1.19	28.9	1.099	144.5	143.0	9028	1.12	10.7	1.089
144	144.0	1542	1.17	39.7	1.097	145	143.5	9045	1.14	8.5	1.090
144.5	144.5	1551	1.12	29.3	1.087	145.5	144.0	9071	1.13	11.5	1.062
145	145.0	1565	1.09	15.8	1.080	146	144.5	9089	1.10	9.8	1.084
145.5	145.5	1574	1.12	15.2	1.078	146.5	145.0	9114	1.13	10.0	1.075
146	146.0	1587	1.14	17.5	1.073	147	145.5	9132	1.14	10.2	1.073
146.5	146.5	1596	1.15	19.3	1.081	147.5	146.0	9157	1.13	10.3	1.072
147	147.0	1610	1.15	20.5	1.066	148	146.5	9175	1.17	9.8	1.089
147.5	147.5	1619	1.21	19.6	1.036	148.5	147.0	9200	1.18	11.7	1.086
148	148.0	1632	1.13	22.2	1.006	149	147.5	9217	1.14	12.3	1.074
148.5	148.5	1641	1.12	24.6	1.014	149.5	148.0	9242	1.17	14.8	1.098
149	149.0	1654	1.11	21.7	1.075	150	148.5	9259	1.15	14.4	1.089
149.5	149.5	1663	1.18	23.9	1.093	150.5	149.0	9284	1.12	27.5	1.072
150	150.0	1676	1.19	22.8	1.085	151	149.5	9301	1.13	56.2	1.073
150.5	150.5	1685	0.95	18.3	1.087	151.5	150.0	9326	1.12	15.9	1.058
151	151.0	1698		16.9	1.042	152	150.5	9342	1.11	9.6	1.075
151.5	3A-2 1.0	1707	0.95	5.3	1.075	152.5	151.0	9367	1.13	10.6	1.012
152	1.5	1720	1.12	6.7	1.056	153	151.5	9383	1.16	12.3	1.010
152.5	2.0	1729	1.15	19.0	1.072	153.5	152.0	9407	1.16	2.8	1.044
153	2.5	1742	1.06	18.6	1.056	154	152.5	9423	1.07	4.1	1.013
153.5	3.0	1750	1.10	17.7	1.073	154.5	153.0	9447	1.30	2.2	1.115
154	3.5	1763	1.09	18.9	1.082	155	2A-2 2.0	9463	1.28	10.4	1.094
154.5	4.0	1772	1.25	33.4	1.093	155.5	2.5	9486	1.29	14.8	1.078
155	4.5	1776	1.20	24.8	1.072	156	3.0	9502	1.28	13.9	1.116
155.5	5.0	1785	1.11	27.3	1.066	156.5	3.5	9525	1.26	13.9	1.101
156	5.5	1797	1.12	28.3	1.047	157	4.0	9540	1.26	19.2	1.068
156.5	6.0	1806	1.19	27.3	1.076	157.5	4.5	9563	1.23	17.6	1.063
157	6.5	1819	1.14	25.1	1.076	158	5.0	9578	1.22	24.5	1.058
157.5	7.0	1827	1.17	29.3	1.073	158.5	5.5	9600	1.25	17.6	1.096
158	7.5	1840	1.18	31.6	1.077	159	6.0	9614	1.27	17.5	1.081

158.5	8.0	1849	1.11	34.6	1.097	159.5	6.5	9636	1.28	23.0	1.092
159	8.5	1861	1.18	31.8	1.092	160	7.0	9650	1.27	30.2	1.072
159.5	9.0	1870	1.11	32.2	1.106	160.5	7.5	9671	1.27	24.1	1.063
160	9.5	1883	1.15	26.6	1.108	161	8.0	9685	1.32	21.0	1.017
160.5	10.0	1891	1.12	25.0	1.120	161.5	8.5	9705	1.44	19.2	1.010
161	10.5	1904	1.17	30.0	1.120	162	9.0	9719	1.43		1.008
161.5	11.0	1912	1.06	27.4	1.110	162.5	9.5	9739	1.43	30.3	1.014
162	11.5	1925	1.09	40.5	1.104	163	10.0	9752	1.46	86.7	1.014
162.5	12.0	1933	1.21	34.3	1.105	163.5	10.5	9771	1.45	173.6	1.016
163	12.5	1946	1.12	38.5	1.106	164	11.0	9784	1.60	145.9	1.021
163.5	13.0	1954	1.20	19.9	1.097	164.5	11.5	9802	1.73	44.5	1.035
164	13.5	1967	1.10	32.7	1.090	165	12.0	9815	1.77	33.3	1.029
164.5	14.0	1975	1.14	40.8	1.107	165.5	12.5	9833	1.94	36.8	1.022
165	14.5	1988	1.05	17.4	1.112	166	13.0	9844	1.95	29.8	1.020
165.5	15.0	1996	1.11	21.9	1.110	166.5	13.5	9862	1.80	29.1	1.019
166	15.5	2009	1.11	18.8	1.099	167	14.0	9873	1.64	25.3	1.021
166.5	16.0	2017	1.09	16.6	1.128	167.5	14.5	9890	1.76	33.5	1.030
167	16.5	2030	1.08	16.9	1.115	168	15.0	9901	1.79	52.1	1.029
167.5	17.0	2039	1.09	20.6	1.089	168.5	15.5	9917	1.82	38.0	1.037
168	17.5	2051	1.11	18.3	1.050	169	16.0	9928	1.80	36.6	1.043
168.5	18.0	2060	1.11	17.0	1.078	169.5	16.5	9943	1.77	42.6	1.044
169	18.5	2072	1.09	14.8	1.084	170	17.0	9953	1.73	38.3	1.050
169.5	19.0	2081	1.14	18.2	1.115	170.5	17.5	9968	1.76	34.9	1.035
170	19.5	2094	1.12	16.7	1.120	171	18.0	9978	1.78	36.8	1.037
170.5	20.0	2102	1.06	15.1	1.094	171.5	18.5	9993	1.76	36.1	1.040
171	20.5	2115	1.07	17.5	1.070	172	19.0	10002	1.79	36.7	1.047
171.5	21.0	2123	1.04	17.4	1.040	172.5	19.5	10017	1.80	35.7	1.055
172	21.5	2136	1.08	17.7	1.022	173	20.0	10026	1.75	37.7	1.041
172.5	22.0	2145	1.13	18.3	1.012	173.5	20.5	10040	1.80	39.9	1.048
173	22.5	2157	1.11	16.9	1.026	174	21.0	10049	1.78	40.4	1.048
173.5	23.0	2166	1.10	16.9	1.032	174.5	21.5	10062	1.80	33.9	1.067
174	23.5	2179	1.04	19.3	1.043	175	22.0	10071	1.80	30.8	1.060
174.5	24.0	2187	1.09	18.4	1.081	175.5	22.5	10084	1.85	28.6	1.051
175	24.5	2200	1.06	20.8	1.041	176	23.0	10092	1.79	28.7	1.047
175.5	25.0	2209	1.11	31.0	1.032	176.5	23.5	10105	1.80	24.7	1.046
176	25.5	2222	1.07	38.9	1.043	177	24.0	10113	1.82	20.6	1.053

176.5	26.0	2230	1.08	39.9	1.089	177.5	24.5	10125	1.82	27.8	1.048
177	26.5	2243	1.07	30.3	1.108	178	25.0	10133	1.83	35.7	1.061
177.5	27.0	2252	1.12	19.1	1.097	178.5	25.5	10145	1.85	37.8	1.049
178	27.5	2265	1.13	18.4	1.030	179	26.0	10153	1.94	34.5	1.035
178.5	28.0	2274	1.14	16.1	1.013	179.5	26.5	10165	1.96	30.1	1.038
179	28.5	2287	1.14	15.3	1.036	180	27.0	10173	1.86	31.7	1.043
179.5	29.0	2296	1.07	17.9	1.077	180.5	27.5	10184	1.82	30.8	1.040
180	29.5	2309	1.13	16.3	1.060	181	28.0	10192	1.84	30.5	1.038
180.5	30.0	2318	1.10	12.8	1.096	181.5	28.5	10203	1.88	27.2	1.037
181	30.5	2331	1.11	16.3	1.097	182	29.0	10211	1.91	33.6	1.036
181.5	31.0	2340	1.12	20.9	1.112	182.5	29.5	10222	1.88	25.2	1.029
182	31.5	2353	1.09	19.0	1.085	183	30.0	10229	1.89	16.3	1.058
182.5	32.0	2362	1.09	18.1	1.023	183.5	30.5	10240	1.98	18.9	1.034
183	32.5	2376	1.07	22.2	1.036	184	31.0	10247	2.00	21.6	1.032
183.5	33.0	2385	1.08	21.7	1.068	184.5	31.5	10258	2.06	14.5	1.055
184	33.5	2398	1.11	29.4	1.013	185	32.0	10266	2.07	7.0	1.004
184.5	34.0	2408	1.15	28.8	1.024	185.5	32.5	10276	1.89	3.4	1.013
185	34.5	2421	1.11	36.5	1.018	186	33.0	10284	1.85	3.7	1.007
185.5	35.0	2430	1.20	69.8	1.014	186.5	33.5	10295	1.89	7.8	1.005
186	35.5	2430	1.15	90.6	1.019	187	34.0	10302	1.89	9.5	1.014
186.5	36.0	2430	1.23	69.7	1.014	187.5	34.5	10312	1.92	8.5	1.013
187	36.5	2430	1.03	72.3	1.018	188	35.0	10320	1.88	8.7	1.005
187.5	37.0	2430	1.24	44.1	1.013	188.5	35.5	10330	1.86	12.8	1.002
188	37.5	2430	1.21	19.0	1.012	189	36.0	10338	1.84	18.9	1.010
188.5	38.0	2444	1.05	14.0	1.016	189.5	36.5	10349	1.82	26.3	1.038
189	38.5	2453	1.07	12.7	1.016	190	37.0	10356	1.84	34.0	1.037
189.5	39.0	2453	1.11	20.9	1.044	190.5	37.5	10367	1.87	31.9	1.047
190	39.5	2453	1.16	42.2	1.024	191	38.0	10374	1.85	29.4	1.040
190.5	40.0	2453	1.15	44.7	1.060	191.5	38.5	10385	1.90	28.3	1.046
191	40.5	2453	1.14	41.7	1.041	192	39.0	10392	2.03	33.4	1.037
191.5	41.0	2453	1.17	34.9	1.032	192.5	39.5	10404	1.93	30.5	1.037
192	41.5	2453	1.18	38.3	1.022	193	40.0	10411	1.99	28.7	1.032
192.5	42.0	2453	1.08	19.8	1.020	193.5	40.5	10422	1.86	34.3	1.037
193	42.5	2458	1.03	14.3	1.024	194	41.0	10430	1.83	35.5	1.049
193.5	43.0	2472	1.07	16.7	1.041	194.5	41.5	10442	1.81	32.3	1.032
194	43.5	2481	1.13	19.5	1.048	195	42.0	10449	1.78	36.7	1.043

194.5	44.0	2495	1.11	19.0	1.047	195.5	42.5	10461	1.82	40.4	1.037
195	44.5	2505	1.11	17.2	1.018	196	43.0	10469	1.75	39.5	1.045
195.5	45.0	2519	1.10	17.8	1.016	196.5	43.5	10481	1.76	43.0	1.046
196	45.5	2528	1.16	19.4	1.015	197	44.0	10489	1.79	42.4	1.045
196.5	46.0	2543	1.12	24.1	1.023	197.5	44.5	10501	1.86	40.4	1.045
197	46.5	2552	1.13	51.2	1.058	198	45.0	10509	1.80	48.0	1.046
197.5	47.0	2567	1.09	237.4	1.072	198.5	45.5	10522	1.86	51.2	1.041
198	47.5	2576	1.28	195.3	1.059	199	46.0	10531	1.94	45.5	1.048
198.5	48.0	2581	1.26	34.4	1.017	199.5	46.5	10543	1.90	54.5	1.052
199	48.5	2591	1.18	30.9	1.021	200	47.0	10552	1.87	61.4	1.041
199.5	49.0	2605	1.24	171.7	1.023	200.5	47.5	10565	1.85	37.1	1.042
200	49.5	2615	1.16		1.021	201	48.0	10574	1.83	45.3	1.043
200.5	50.0	2630	1.30	184.7	1.012	201.5	48.5	10588	1.88	47.7	1.044
201	50.5	2635	1.14	34.3	1.014	202	49.0	10597	1.83	43.2	1.040
201.5	51.0	2645	1.13	17.1	1.018	202.5	49.5	10612	1.69	33.4	1.032
202	51.5	2660	1.14	13.1	1.011	203	50.0	10621	1.66	24.1	1.038
202.5	52.0	2670	1.07	14.3	1.011	203.5	50.5	10636	1.85	24.3	1.040
203	52.5	2685	1.16	17.0	1.016	204	51.0	10646	1.67	59.2	1.046
203.5	53.0	2695	1.15	26.9	1.017	204.5	51.5	10661	1.51	116.0	1.043
204	53.5	2710	1.20	27.4	1.033	205	52.0	10671	1.34	84.8	1.039
204.5	54.0	2721	1.20	16.3	1.055	205.5	52.5	10686	1.35	101.1	1.042
205	54.5	2736	1.14	22.3	1.070	206	53.0	10697	1.37	38.4	1.046
205.5	55.0	2746	1.15	31.6	1.028	206.5	53.5	10713	1.42	25.9	1.050
206	55.5	2762	1.09	25.7	1.024	207	54.0	10724	1.39	14.1	1.049
206.5	56.0	2772	1.13	15.2	1.021	207.5	54.5	10741	1.33	14.6	1.088
207	56.5	2788	1.13	12.8	1.022	208	55.0	10752	1.30	13.2	1.087
207.5	57.0	2799	1.12	14.4	1.018	208.5	55.5	10769	1.36	14.8	1.071
208	57.5	2814	1.11	24.4	1.036	209	56.0	10781	1.33	14.4	1.060
208.5	58.0	2825	1.15	19.0	1.016	209.5	56.5	10799	1.28	13.1	1.057
209	58.5	2841	1.16	21.0	1.100	210	57.0	10811	1.22	13.5	1.059
209.5	59.0	2851	1.19	24.1	1.072	210.5	57.5	10830	1.31	13.2	1.055
210	59.5	2868	1.19	25.3	1.084	211	58.0	10843	1.32	13.8	1.077
210.5	60.0	2878	1.16	27.9	1.050	211.5	58.5	10862	1.32	16.3	1.064
211	60.5	2894	1.13	15.9	1.073	212	59.0	10875	1.35	13.4	1.053
211.5	61.0	2905	1.05	15.8	1.048	212.5	59.5	10895	1.30	13.6	1.066
212	61.5	2922	1.10	20.6	1.022	213	60.0	10909	1.30	13.1	1.067

212.5	62.0	2933	1.02	54.4	1.081	213.5	60.5	10929	1.29	11.3	1.066
213	62.5	2949	1.15	130.2	1.072	214	61.0	10944	1.34	9.1	1.079
213.5	63.0	2960	1.13	28.5	1.085	214.5	61.5	10965	1.31	7.2	1.061
214	63.5	2971	1.09	23.8	1.117	215	62.0	10980	1.40	9.5	1.055
214.5	64.0	2987	1.15	37.3	1.105	215.5	62.5	11002	1.37	10.7	1.053
215	64.5	2999	1.15	55.7	1.091	216	63.0	11017	1.36	12.9	1.058
215.5	65.0	3015	1.12	21.6	1.106	216.5	63.5	11040	1.25	18.5	1.043
216	65.5	3026	1.11	14.8	1.075	217	64.0	11056	1.33	17.3	1.055
216.5	66.0	3043	1.12	12.6	1.108	217.5	64.5	11080	1.30	10.4	1.056
217	66.5	3054	1.13	16.4	1.116	218	65.0	11096	1.27	9.9	1.062
217.5	67.0	3071	1.16	29.2	1.079	218.5	65.5	11120	1.42	11.5	1.053
218	67.5	3083	1.15	39.6	1.122	219	66.0	11136	1.36	12.4	1.052
218.5	68.0	3100	1.17	54.6	1.086	219.5	66.5	11160	1.36	14.9	1.057
219	68.5	3111	1.20	30.0	1.110	220	67.0	11177	1.32	16.3	1.056
219.5	69.0	3128	1.14	31.6	1.116	220.5	67.5	11201	1.38	16.2	1.056
220	69.5	3139	1.19	25.5	1.120	221	68.0	11217	1.39	15.7	1.050
220.5	70.0	3157	1.17	26.9	1.091	221.5	68.5	11242	1.36	16.6	1.053
221	70.5	3168	1.17	29.0	1.129	222	69.0	11258	1.36	16.3	1.055
221.5	71.0	3185	1.18	23.6	1.146	222.5	69.5	11283	1.40	17.2	1.055
222	71.5	3197	1.14	33.1	1.109	223	70.0	11299	1.32	18.9	1.056
222.5	72.0	3208	1.13	21.9	1.099	223.5	70.5	11323	1.41	22.4	1.052
223	72.5	3226	1.16	27.4	1.134	224	71.0	11340	1.41	18.1	1.054
223.5	73.0	3237	1.20	47.7	1.093	224.5	71.5	11364	1.44	18.6	1.047
224	73.5	3255	1.14	346.5	1.102	225	72.0	11381	1.45	29.1	1.048
224.5	74.0	3267	1.24	90.9	1.111	225.5	72.5	11405	1.48	26.8	1.044
225	74.5	3284	1.19	26.7	1.050	226	73.0	11421	1.51	29.4	1.038
225.5	75.0	3296	1.15	23.0	1.028	226.5	73.5	11446	1.55	23.6	1.035
226	75.5	3313	1.14	19.5	1.144	227	74.0		1.54	22.9	1.036
226.5	76.0	3325	1.12	17.9	1.112	227.5	74.5		1.57	24.3	1.035
227	76.5	3343	1.10	24.1	1.110	228	75.0		1.58	23.1	1.037
227.5	77.0	3355	1.13	20.1	1.092	228.5	75.5		1.55	21.8	1.045
228	77.5	3372	1.08	18.6	1.142	229	76.0		1.60	19.1	1.038
228.5	78.0	3384	1.14	17.6	1.111	229.5	76.5		1.67	16.9	1.034
229	78.5	3396	1.23	15.8	1.111	230	77.0		1.63	17.5	1.032
229.5	79.0	3414	1.11	38.4	1.094	230.5	77.5		1.70	19.6	1.028
230	79.5	3426	1.14	34.3	1.102	231	78.0		1.67	21.8	1.028

230.5	80.0	3444	1.14	22.3	1.113	231.5	78.5	1.66	31.3	1.029
231	80.5	3456	1.13	22.7	1.150	232	79.0	1.63	47.4	1.036
231.5	81.0	3474	1.12	18.9	1.118	232.5	79.5	1.70	33.7	1.033
232	81.5	3486	1.14	20.3	1.101	233	80.0	1.70	32.5	1.039
232.5	82.0	3504	1.16	30.5	1.122	233.5	80.5	1.66	24.1	1.035
233	82.5	3516	1.15	30.1	1.093	234	81.0	1.81	20.4	1.035
233.5	83.0	3534	1.15	61.3	1.093	234.5	81.5	1.81	21.0	1.037
234	83.5	3546	1.15	65.9	1.094	235	82.0	1.75	8.4	1.029
234.5	84.0	3564	1.15	30.7	1.066	235.5	82.5	2.09	2.3	1.054
235	84.5	3576	1.13	24.1	1.091	236	83.0	2.04	3.2	1.047
235.5	85.0	3594	1.17	29.7	1.091	236.5	83.5	1.78	11.2	1.019
236	85.5	3607	1.14	30.6	1.058	237	84.0	1.79	13.3	1.040
236.5	86.0	3625	1.15	41.3	1.095	237.5	84.5	1.87	9.2	1.040
237	86.5	3637	1.17	47.2	1.083	238	85.0	1.80	9.3	1.040
237.5	87.0	3655	1.18	40.2	1.082	238.5	85.5	1.71	14.1	1.043
238	87.5	3667	1.15	60.6	1.074	239	86.0	1.62	22.7	1.044
238.5	88.0	3686	1.19	52.6	1.086	239.5	86.5	1.67	31.4	1.035
239	88.5	3698	1.16	47.3	1.083	240	87.0	1.68	30.9	1.037
239.5	89.0	3716	1.18	41.3	1.103	240.5	87.5	1.70	31.3	1.040
240	89.5	3728	1.12	44.9	1.114	241	88.0	1.73	32.3	1.032
240.5	90.0	3747	1.18	45.9	1.108	241.5	88.5	1.77	34.9	1.036
241	90.5	3759	1.13	41.1	1.107	242	89.0	1.75	36.1	1.034
241.5	91.0	3777	1.15	43.7	1.112	242.5	89.5	1.73	35.8	1.040
242	91.5	3790	1.13	48.2	1.098	243	90.0	1.86	34.0	1.035
242.5	92.0	3808	1.09	46.9	1.108	243.5	90.5	1.82	35.5	1.040
243	92.5	3820	1.13	44.0	1.081	244	91.0	1.81	33.1	1.037
243.5	93.0	3839	1.16	41.0	1.098	244.5	91.5	1.81	31.8	1.041
244	93.5	3851	1.20	41.5	1.082	245	92.0	1.90	32.7	1.037
244.5	94.0	3870	1.19	41.1	1.080	245.5	92.5	1.83	31.9	1.053
245	94.5	3882	1.18	43.0	1.095	246	93.0	1.81	37.9	1.054
245.5	95.0	3900	1.20	47.3	1.039	246.5	93.5	1.72	34.7	1.045
246	95.5	3913	1.21	43.7	1.059	247	94.0	1.73	33.0	1.046
246.5	96.0	3931	1.16	92.7	1.058	247.5	94.5	1.80	41.0	1.047
247	96.5	3943	1.14	179.4	1.062	248	95.0	1.81	62.0	1.035
247.5	97.0	3956	1.20	57.1	1.044	248.5	95.5	1.81	53.1	1.040
248	97.5	3968	1.14	54.4	1.044	249	96.0	1.85	44.8	1.040

248.5	98.0	3986	1.16	72.2	1.059	249.5	96.5	1.83	41.2	1.033
249	98.5	3999	1.17	80.2	1.085	250	97.0	1.77	29.4	1.039
249.5	99.0	4011	1.26	115.5	1.091	250.5	97.5	1.77	39.2	1.036
250	99.5	4011	1.41	69.0	1.105	251	98.0	1.77	43.3	1.041
250.5	100.0	4011	1.36	70.0	1.127	251.5	98.5	1.75	36.4	1.038
251	100.5	4011	1.34	75.8	1.123	252	99.0	1.75	35.8	1.039
251.5	101.0	4011	1.31	108.9	1.114	252.5	99.5	1.76	43.2	1.052
252	101.5	4017	1.31	161.5	1.104	253	100.0	1.72	37.3	1.043
252.5	102.0	4036	1.33	101.8	1.098	253.5	100.5	1.80	36.4	1.036
253	102.5	4048	1.50	59.1	1.120	254	101.0	1.84	30.0	1.049
253.5	103.0	4067	1.22	29.2	1.102	254.5	101.5	1.77	30.2	1.044
254	103.5	4079	1.26	14.3	1.092	255	102.0	1.85	25.8	1.042
254.5	104.0	4097	1.27	5.7	1.065	255.5	102.5	1.89	34.1	1.038
255	104.5	4110	1.60	13.2	1.098	256	103.0	1.81	38.9	1.039
255.5	105.0	4128	1.26	34.8	1.106	256.5	103.5	1.79	29.5	1.043
256	105.5	4141	1.16	51.1	1.100	257	104.0	1.81	23.0	1.042
256.5	106.0	4159	1.16	40.1	257.000	257.5	104.5	1.79	26.5	1.039
257	106.5		1.19	18.2		258	105.0	1.81	28.6	1.046
257.5	107.0		1.20	17.1		258.5	105.5	1.79	22.1	1.050
258	107.5		1.14	23.2		259	106.0	1.84	22.7	1.052
258.5	108.0		1.12	27.7		259.5	106.5	1.90	29.5	1.060
259	108.5		1.09	35.5		260	107.0	1.86	31.5	1.040
259.5	109.0		1.15	37.4		260.5	107.5	1.95	34.1	1.041
260	109.5		1.16	23.1		261	108.0	1.92	32.2	1.050
260.5	110.0		1.11	15.5		261.5	108.5	1.90	34.2	1.038
						262	109.0	1.85	40.1	1.037
						262.5	109.5	2.00	39.8	1.034
						263	110.0	2.01	35.9	1.034
						263.5	110.5	2.09	28.1	1.047
						264	111.0	2.04	33.3	1.046
						264.5	111.5	2.04	31.9	1.037
						265	112.0	2.04	32.9	1.036
						265.5	112.5	2.09	31.1	1.049
						266	113.0	2.10	20.7	1.032
						266.5	113.5	2.09	13.1	1.039
						267	114.0	2.04	22.2	1.034

267.5	114.5	2.08	27.5	1.035
268	115.0	2.04	24.4	1.043
268.5	115.5	2.06	19.6	1.048
269	116.0	2.12	25.7	1.044
269.5	116.5	2.12	25.3	1.039
270	117.0	2.05	25.0	1.043
270.5	117.5	2.08	23.4	1.035
271	118.0	2.12	21.8	1.043
271.5	118.5	2.22	19.6	1.030
272	119.0	2.15	10.9	1.017
272.5	119.5	2.01	7.0	1.037
273	120.0	1.97	8.4	1.027
273.5	120.5	2.07	8.6	1.038
274	121.0	1.94	16.0	1.016
274.5	121.5	1.82	21.0	1.034
275	122.0	1.96	24.7	1.050
275.5	122.5	1.89	25.2	1.042
276	123.0	1.96	16.0	1.033
276.5	123.5	1.86	14.4	1.048
277	124.0	1.85	22.6	1.037
277.5	124.5	1.82	26.9	1.041
278	125.0	1.91	24.1	1.043
278.5	125.5	1.89	26.4	1.049
279	126.0	1.77	28.3	1.047
279.5	126.5	1.76	30.3	1.044
280	127.0	1.84	26.9	1.042
280.5	127.5	1.83	33.4	1.046
281	128.0	1.83	34.4	1.046
281.5	128.5	1.74	30.3	1.046
282	129.0	1.80	33.3	1.048
282.5	129.5	1.71	37.7	1.043
283	130.0	1.77	30.2	1.043
283.5	130.5	1.96	36.3	1.036
284	131.0	2.04	34.3	1.042
284.5	131.5	1.84	33.8	1.055
285	132.0	1.70	24.8	1.039

285.5	132.5	1.68	24.6	1.046
286	133.0	1.73	29.4	1.049
286.5	133.5	1.82	32.0	1.041
287	134.0	1.78	32.7	1.040
287.5	134.5	1.80	31.4	1.048
288	135.0	1.79	35.0	1.045
288.5	135.5	1.74	32.7	1.045
289	136.0	1.73	36.1	1.046
289.5	136.5	1.94	35.3	1.043
290	137.0	1.85	31.6	1.039
290.5	137.5	1.75	32.7	1.042
291	138.0	1.75	34.5	1.050
291.5	138.5	1.81	35.7	1.043
292	139.0	1.72	34.0	1.045
292.5	139.5	1.79	40.6	1.045
293	140.0	1.83	37.3	1.037
293.5	140.5	1.70	31.5	1.038
294	141.0	1.78	31.9	1.051
294.5	141.5	1.70	34.8	1.047
295	142.0	1.74	32.8	1.039
295.5	142.5	1.90	31.3	1.042
296	143.0	1.75	28.5	1.042
296.5	143.5	1.68	39.2	1.052
297	144.0	1.70	34.5	1.046
297.5	144.5	1.70	29.2	1.046
298	145.0	1.73	34.6	1.044
298.5	145.5	1.86	29.9	1.047
299	146.0	1.75	32.6	1.039
299.5	146.5	1.72	29.4	1.038
300	147.0	1.74	30.9	1.042
300.5	147.5	1.71	43.2	1.047
301	148.0	1.82	61.9	1.047
301.5	148.5	1.83	39.6	1.040
302	149.0	1.95	31.5	1.056
302.5	149.5	1.88	32.1	1.048
303	150.0	1.84	38.0	1.051

303.5	150.5		1.81	43.4	1.047
304	151.0		1.72	39.8	

APPENDIX B: EMERALD LAKE LOSS ON IGNITION (LOI) ANALYSIS

Composite Core 3

Sample	Depth midpoint (cm blf)	Wet weight (g)	Dry weight (g)	Bulk density (g/cm^3)[b]	LOI (%)
3C-12	0.5	2.1	0.6	1.0	19.9
3C-13	1	2.1	0.7	1.1	13.8
3C-14	2	1.9	0.7	1.0	13.1
3C-15	3	1.8	0.9	0.9	11.4
3C-16	4	2.0	1.0	1.0	12.0
3C-17	5	2.0	0.9	1.0	12.9
3C-18	6	2.3	1.0	1.2	11.9
3C-19	7	2.1	0.7	1.0	16.8
3C-20	8	2.0	0.7	1.0	17.2
3C-21	9	2.2	0.7	1.1	17.6
3C-22	10	1.7	0.8	0.9	16.1
3C-23	11	2.0	1.1	1.0	12.8
3C-24	12	1.6	0.7	0.8	19.2
3C-25	13	2.1	0.9	1.0	21.2
3C-26	14	1.7	0.8	0.8	20.5
3C-27	15	2.2	1.0	1.1	20.8
3C-28	16	2.1	1.0	1.1	17.4
3C-29	17	2.3	1.1	1.1	17.0
3C-30	18	2.3	1.1	1.1	17.1
3C-31	19	2.0	0.9	1.0	16.2
3C-32	20	2.3	1.1	1.1	15.5
3C-33	21	2.0	1.0	1.0	16.6
3C-34	22	2.4	1.4	1.2	11.2
3C-35	23	2.6	1.2	1.3	13.4
3C-36	24	2.7	1.4	1.3	7.9
3A-25	25	1.8	0.8	0.9	17.1
3A-26	26	2.6	1.4	1.3	12.3

Composite Core 2

Sample	Depth midpoint (cm blf)	Wet weight (g)	Dry weight (g)	Bulk density (g/cm^3)[b]	LOI (%)
2C-08	1	2.3	0.8	1.1	14.4
2C-09	2	2.3	0.8	1.1	17.2
2C-10	3	2.5	1.5	1.3	6.7
2C-11	4	2.7	1.5	1.3	7.5
2C-12	5	2.5	1.5	1.3	6.8
2C-13	6	2.5	1.4	1.3	7.3
2C-14	7	3.1	1.5	1.5	8.3
2C-15	8	2.6	1.2	1.3	9.5
2C-16	9	2.4	1.0	1.2	10.6
2C-17	10	2.6	1.2	1.3	11.3
2C-18	11	2.4	1.0	1.2	16.5
2C-19	12	2.2	0.7	1.1	23.9
2C-20	13	1.9	0.4	1.0	49.0
2C-21	14	2.0	0.5	1.0	45.8
2C-22	15	1.9	0.5	1.0	44.2
2C-23	16	2.1	0.7	1.1	30.0
2C-24	17	2.1	0.7	1.1	30.9
2C-25	18	1.9	0.8	0.9	23.5
2C-26	19	2.6	1.2	1.3	13.6
2C-27	20	2.7	1.1	1.3	10.1
2C-28	21	3.1	1.9	1.5	2.4
2C-29	22	3.2	1.9	1.6	1.1
2C-30	23	3.0	2.0	1.5	0.7
2C-31	24	2.9	1.8	1.4	0.7
2C-32	25	3.2	2.2	1.6	0.7
2C-33	26	2.8	2.0	1.4	0.5
2C-34	27	3.0	2.1	1.5	0.4

3A-27	27	1.9	1.0	1.0	12.8	2C-35	28	2.8	1.9	1.4	0.4
3A-28	28	2.1	1.0	1.1	12.7	2C-36	29	2.6	1.3	1.3	7.3
3A-29	29	2.3	1.1	1.2	9.0	2C-37	30	2.5	1.4	1.3	4.5
3A-30	30	2.7	1.3	1.3	8.5	2C-38	31	1.8	0.6	0.9	25.2
3A-31	31	3.0	1.5	1.5	7.9	2C-39	32	1.8	0.3	0.9	45.6
3A-32	32	2.2	1.2	1.1	7.4	2C-40	33	2.6	0.7	1.3	17.2
3A-33	33	2.6	1.3	1.3	9.0	2C-41	34	2.4	0.7	1.2	15.1
3A-34	34	2.8	1.4	1.4	8.3	2C-42	35	3.1	1.4	1.5	7.1
3A-35	35	2.7	1.4	1.4	10.3	2C-43	36	2.7	1.3	1.3	8.2
3A-36	36	2.7	1.5	1.4	6.7	2C-44	37	2.7	1.0	1.3	10.8
3A-37	37	2.9	1.6	1.5	7.2	2C-45	38	2.7	1.2	1.3	8.3
3A-38	38	3.3	1.8	1.6	7.1	2C-46	39	2.9	1.7	1.5	4.8
3A-39	39	2.8	1.6	1.4	6.5	2C-47	40	3.0	1.6	1.5	5.9
3A-40	40	2.5	1.6	1.2	5.4	2C-48	41	2.4	0.8	1.2	8.3
3A-41	41	2.4	1.3	1.2	6.4	2C-49	42	2.7	1.0	1.4	9.2
3A-42	42	2.5	1.3	1.3	7.5	2C-50	43	2.5	1.0	1.3	7.0
3A-43	43	2.6	1.3	1.3	7.7	2C-51	44	2.9	1.3	1.5	5.8
3A-44	44	2.4	1.3	1.2	8.0	2C-52	45	2.8	1.5	1.4	5.8
3A-45	45	2.4	1.2	1.2	11.5	2C-53	46	2.9	2.0	1.4	2.3
3A-46	46	2.4	1.3	1.2	9.8	2C-54	47	2.7	1.4	1.4	5.7
3A-47	47	2.5	1.3	1.3	7.4	2A1-47	48	2.5	1.1	1.2	8.0
3A-48	48	3.1	1.7	1.5	7.4	2A1-48	49	2.8	1.2	1.4	8.0
3A-49	49	3.4	1.8	1.7	8.5	2A1-49	50	2.4	0.9	1.2	9.5
3A-50	50	2.5	1.4	1.3	8.1	2A1-50	51	2.2	0.8	1.1	11.5
3A-51	51	3.4	1.7	1.7	7.7	2A1-51	52	2.4	0.8	1.2	11.7
3A-52	52	3.5	2.0	1.8	7.6	2A1-52	53	2.4	1.0	1.2	10.5
3A-53	53	2.6	1.4	1.3	7.3	2A1-53	54	2.5	1.1	1.2	7.5
3A-54	54	3.1	1.7	1.6	6.8	2A1-54	55	2.0	0.8	1.0	14.8
3A-55	55	3.2	1.9	1.6	6.4	2A1-55	56	2.4	0.9	1.2	11.0
3A-56	56	3.3	2.1	1.7	5.6	2A1-56	57	1.8	0.7	0.9	11.4
3A-57	57	3.3	1.9	1.6	6.4	2A1-57	58	1.9	0.6	1.0	11.3
3A-58	58	3.0	1.6	1.5	7.4	2A1-58	59	2.2	0.7	1.1	13.2
3A-59	59	3.4	1.8	1.7	7.9	2A1-59	60	1.8	0.6	0.9	12.0
3A-60	60	3.3	1.8	1.7	8.0	2A1-60	61	2.2	0.7	1.1	12.2
3A-61	61	3.4	1.8	1.7	8.5	2A1-61	62	2.4	0.7	1.2	12.3
3A-62	62	3.1	1.7	1.6	8.6	2A1-62	63	2.1	0.7	1.1	12.2

3A-63	63	4.1	2.2	2.0	8.8	2A1-63	64	2.5	0.8	1.3	12.8
3A-64	64	3.0	1.6	1.5	9.1	2A1-64	65	2.5	0.7	1.2	12.8
3A-65	65	3.1	1.7	1.5	9.8	2A1-65	66	2.5	0.8	1.3	12.7
3A-66	66	3.5	1.9	1.8	9.6	2A1-66	67	2.2	0.7	1.1	13.2
3A-67	67	3.3	1.7	1.7	10.7	2A1-67	68	2.3	0.8	1.2	10.9
3A-68	68	4.0	2.0	2.0	10.7	2A1-68	69	2.6	0.9	1.3	11.7
3A-69	69	3.2	1.8	1.6	9.0	2A1-69	70	2.2	0.8	1.1	11.1
3A-70	70	3.4	1.9	1.7	9.1	2A1-70	71	2.5	0.9	1.2	11.4
3A-71	71	3.2	1.7	1.6	9.4	2A1-71	72	2.2	0.8	1.1	11.3
3A-72	72	3.1	1.7	1.6	9.8	2A1-72	73	2.5	0.9	1.3	11.6
3A-73	73	2.6	1.2	1.3	15.4	2A1-73	74	2.2	0.7	1.1	10.7
3A-74	74	2.9	1.3	1.5	18.8	2A1-74	75	1.9	0.8	1.0	8.7
3A-75	75	3.4	1.4	1.7	18.9	2A1-75	76	2.4	0.9	1.2	11.4
3A-76	76	2.1	0.9	1.0	14.4	2A1-76	77	2.1	0.8	1.1	9.3
3A-77	77	3.1	1.7	1.5	9.9	2A1-77	78	2.0	0.7	1.0	10.1
3A-78	78	2.8	1.5	1.4	9.6	2A1-78	79	2.4	0.9	1.2	9.8
3A-79	79	4.0	1.8	2.0	10.8	2A1-79	80	2.0	0.7	1.0	9.1
3A-80	80	2.2	1.1	1.1	11.1	2A1-80	81	2.4	0.8	1.2	10.7
3A-81	81	2.5	1.2	1.2	12.0	2A1-81	82	2.4	0.9	1.2	9.6
3A-82	82	2.2	1.0	1.1	12.1	2A1-82	83	2.2	0.7	1.1	10.3
3A-83	83	2.0	1.0	1.0	11.2	2A1-83	84	2.1	0.8	1.1	10.2
3A-84	84	2.6	1.2	1.3	11.1	2A1-84	85	2.3	1.0	1.2	8.2
3A-85	85	2.5	1.1	1.2	10.1	2A1-85	86	2.3	0.8	1.1	13.7
3A-86	86	2.7	1.2	1.3	9.2	2A1-86	87	2.5	1.0	1.2	8.8
3A-87	87	2.6	1.5	1.3	4.4	2A1-87	88	2.4	0.8	1.2	9.6
3A-88	88	2.5	1.8	1.3	1.4	2A1-88	89	2.3	0.9	1.2	11.1
3A-89	89	2.7	2.0	1.3	0.8	2A1-89	90	2.4	0.9	1.2	10.0
3A-90	90	2.7	2.0	1.4	0.9	2A1-90	111	2.3	0.9	1.1	9.5
3A-91	91	2.7	1.9	1.3	0.9	2A1-111	112	2.5	1.3	1.3	5.1
3A-92	92	2.8	2.0	1.4	0.9	2A1-112	113	2.2	1.2	1.1	5.0
3A-93	93	2.8	1.9	1.4	1.3	2A1-113	114	2.2	0.7	1.1	11.6
3A-94	94	2.6	1.8	1.3	2.5	2A1-114	115	2.1	0.7	1.0	9.6
3A-95	95	3.0	2.0	1.5	1.9	2A1-115	116	2.2	0.7	1.1	8.8
3A-96	96	2.8	2.0	1.4	0.8	2A1-116	117	2.0	0.7	1.0	9.3
3A-97	97	3.4	2.5	1.7	0.6	2A1-117	118	2.4	0.8	1.2	9.3
3A-98	98	2.8	2.1	1.4	1.6	2A1-118	119	2.2	0.7	1.1	10.2

3A-99	99	3.1	2.3	1.6	0.9	2A1-119	120	2.6	0.9	1.3	9.9
3A-100	100	2.7	1.9	1.4	1.3	2A1-120	121	2.6	1.0	1.3	9.4
3A-101	101	2.6	1.9	1.3	0.8	2A1-121	122	2.4	0.9	1.2	8.8
3A-102	102	3.4	2.4	1.7	1.3	2A1-122	123	2.6	0.9	1.3	9.7
3A-103	103	2.7	1.9	1.4	1.2	2A1-123	124	2.7	1.1	1.3	9.5
3A-104	104	3.0	2.0	1.5	2.3	2A1-124	125	2.2	0.8	1.1	9.8
3A-105	105	2.6	0.9	1.3	12.1	2A1-125	126	2.2	0.8	1.1	9.9
3A-106	106	2.5	1.2	1.3	6.7	2A1-126	127	2.3	0.7	1.2	11.5
3A-107	107	2.9	1.4	1.4	7.9	2A1-127	128	2.4	0.9	1.2	8.3
3A-108	108	3.0	1.2	1.5	14.0	2A1-128	129	2.4	0.9	1.2	10.1
3A-109	109	3.0	1.0	1.5	18.2	2A1-129	130	2.3	0.8	1.2	10.0
3A-110	110	3.1	0.9	1.5	17.9	2A1-130	131	2.3	0.8	1.1	9.1
3A-111	111	2.8	0.8	1.4	17.5	2A1-131	132	2.6	1.0	1.3	7.9
3A-112	112	2.5	0.7	1.2	18.0	2A1-132	133	3.0	1.1	1.5	9.5
3A-113	113	1.7	0.5	0.9	17.9	2A1-133	134	2.7	1.0	1.3	8.9
3A-114	114	1.8	0.5	0.9	18.2	2A1-134	135	2.5	1.1	1.3	6.9
3A-115	115	2.5	0.7	1.3	18.7	2A1-135	136	2.8	1.4	1.4	5.1
3A-116	116	2.1	0.6	1.1	18.6	2A1-136	137	2.3	0.9	1.2	9.1
3A-117	117	2.1	0.6	1.0	18.9	2A1-137	138	2.1	0.7	1.1	10.4
3A-118	118	2.3	0.8	1.2	15.9	2A1-138	139	2.6	1.0	1.3	9.4
3A-119	119	2.4	0.8	1.2	15.0	2A1-139	140	2.2	0.9	1.1	8.6
3A-120	120	2.3	0.8	1.2	17.0	2A1-140	141	2.2	0.7	1.1	10.5
3A-121	121	2.5	0.9	1.2	12.3	2A1-141	142	2.1	0.7	1.0	11.1
3A-122	122	2.2	0.9	1.1	9.5	2A1-142	143	2.5	0.8	1.3	11.0
3A-123	123	2.8	0.8	1.4	16.8	2A1-143	144	2.6	0.8	1.3	11.3
3A-124	124	2.5	0.7	1.2	18.7	2A1-144	145	2.3	0.7	1.2	10.8
3A-125	125	2.4	0.7	1.2	17.7	2A1-145	146	2.5	0.8	1.3	11.5
3A-126	126	1.9	0.5	0.9	18.9	2A1-146	147	2.5	0.7	1.3	11.3
3A-127	127	2.3	0.7	1.1	17.6	2A1-147	148	2.4	0.9	1.2	9.6
3A-128	128	2.5	0.8	1.2	17.4	2A1-148	149	2.2	0.8	1.1	9.7
3A-129	129	1.9	0.6	1.0	18.2	2A1-149	150	2.3	0.8	1.2	10.8
3A-130	130	2.3	0.9	1.1	19.9	2A1-150	151	2.4	0.8	1.2	14.9
3A-131	131	2.3	0.9	1.2	22.6	2A2-2	154	2.5	0.8	1.3	11.5
3A-132	132	2.1	0.8	1.0	21.8	2A2-3	155	2.3	0.7	1.1	10.8
3A-133	133	1.9	0.7	1.0	23.3	2A2-4	156	2.2	0.7	1.1	10.2
3A-134	134	2.4	0.8	1.2	20.5	2A2-5	157	2.1	0.7	1.1	9.4

3A-135	135	1.9	0.6	1.0	18.6	2A2-6	158	2.3	0.8	1.1	9.7
3A-136	136	2.5	0.7	1.3	18.4	2A2-7	159	2.4	0.8	1.2	9.4
3A-137	137	2.3	0.9	1.2	18.5	2A2-8	160	2.5	0.9	1.3	9.4
3A-138	138	2.1	0.8	1.0	20.1	2A2-9	161	2.4	0.9	1.2	9.2
3A-139	139	2.0	0.8	1.0	20.7	2A2-10	162	2.4	1.0	1.2	7.5
3A-140	140	2.5	1.0	1.2	18.9	2A2-11	163	3.0	1.6	1.5	5.1
3A-141	141	2.1	0.8	1.1	18.5	2A2-12	164	3.1	1.7	1.5	5.1
3A-142	142	2.2	0.7	1.1	19.4	2A2-13	165	3.6	1.8	1.8	5.2
3A-143	143	1.8	0.6	0.9	21.3	2A2-14	166	2.9	1.3	1.4	6.2
3A-144	144	1.9	0.6	1.0	18.7	2A2-15	167	2.8	1.5	1.4	6.0
3A-145	145	2.2	0.7	1.1	18.5	2A2-16	168	3.0	1.7	1.5	5.3
3A-146	146	2.1	0.7	1.1	17.6	2A2-17	169	3.2	2.5	1.6	3.6
3A-147	147	1.8	0.6	0.9	17.7	2A2-18	170	2.8	1.7	1.4	4.9
3A-148	148	2.0	0.7	1.0	18.1	2A2-19	171	3.0	2.2	1.5	3.5
3A-149	149	2.0	0.7	1.0	17.5	2A2-20	172	3.3	2.2	1.6	4.4
3A2-1	150	1.9	0.7	0.9	18.3	2A2-21	173	2.7	2.0	1.4	4.0
3A2-2	151	2.2	0.7	1.1	18.1	2A2-22	174	3.3	2.4	1.6	3.6
3A2-3	152	1.7	0.8	0.8	11.0	2A2-23	175	2.7	2.0	1.4	4.0
3A2-4	153	1.9	0.7	1.0	14.5	2A2-24	176	3.5	2.5	1.7	3.8
3A2-5	154	2.1	0.8	1.1	14.5	2A2-25	177	3.2	2.3	1.6	3.7
3A2-6	155	2.4	0.9	1.2	13.9	2A2-26	178	3.0	2.1	1.5	3.8
3A2-7	156	2.3	0.8	1.1	14.3	2A2-27	179	3.4	2.6	1.7	3.5
3A2-8	157	2.3	0.8	1.1	15.1	2A2-28	180	2.6	1.9	1.3	4.0
3A2-9	158	2.0	0.7	1.0	14.7	2A2-29	181	3.2	2.3	1.6	3.8
3A2-10	159	2.0	0.7	1.0	16.4	2A2-30	182	3.5	2.8	1.7	3.3
3A2-11	160	2.3	0.8	1.2	14.7	2A2-31	183	2.7	2.1	1.4	3.2
3A2-12	161	2.1	0.7	1.0	15.5	2A2-32	184	3.1	2.2	1.5	3.7
3A2-13	162	1.8	0.5	0.9	19.3	2A2-33	185	3.0	2.2	1.5	3.8
3A2-14	163	2.2	0.7	1.1	18.6	2A2-34	186	3.0	2.2	1.5	3.6
3A2-15	164	2.1	0.6	1.0	19.5	2A2-35	187	2.8	1.9	1.4	3.8
3A2-16	165	2.0	0.7	1.0	18.0	2A2-36	188	3.0	2.1	1.5	3.7
3A2-17	166	2.1	0.6	1.0	19.2	2A2-37	189	3.2	2.3	1.6	3.7
3A2-18	167	1.8	0.6	0.9	18.4	2A2-38	190	3.6	2.9	1.8	2.7
3A2-19	168	1.9	0.6	1.0	18.9	2A2-39	191	3.3	2.4	1.6	3.7
3A2-20	169	1.9	0.6	0.9	18.7	2A2-40	192	4.0	3.1	2.0	3.4
3A2-21	170	2.3	0.8	1.1	17.7	2A2-41	193	2.9	2.1	1.4	3.8

3A2-22	171	2.2	0.7	1.1	19.1	2A2-42	194	3.1	2.3	1.6	3.9
3A2-23	172	2.0	0.7	1.0	17.9	2A2-43	195	3.0	2.2	1.5	3.7
3A2-24	173	2.2	0.8	1.1	21.4	2A2-44	196	3.2	2.4	1.6	3.8
3A2-25	174	2.1	0.8	1.1	19.5	2A2-45	197	3.7	2.8	1.8	3.8
3A2-26	175	1.9	0.7	1.0	17.9	2A2-46	198	3.8	2.7	1.9	4.0
3A2-27	176	2.1	0.7	1.0	17.6	2A2-47	199	3.5	2.5	1.7	4.2
3A2-28	177	2.2	0.7	1.1	18.2	2A2-48	200	3.3	2.4	1.6	3.8
3A2-29	178	2.2	0.7	1.1	19.2	2A2-49	201	2.5	1.9	1.3	3.6
3A2-30	179	2.1	0.7	1.1	18.3	2A2-50	202	3.2	2.5	1.6	3.5
3A2-31	180	2.2	0.7	1.1	19.0	2A2-51	203	3.3	2.4	1.6	3.9
3A2-32	181	2.2	0.7	1.1	18.8	2A2-52	204	3.3	2.5	1.7	3.9
3A2-33	182	2.0	0.7	1.0	20.4	2A2-53	205	3.5	2.5	1.8	3.9
3A2-34	183	2.2	0.9	1.1	22.4	2A2-54	206	2.4	1.0	1.2	6.7
3A2-35	184	2.1	0.9	1.0	16.3	2A2-55	207	2.4	0.9	1.2	7.2
3A2-36	185	2.2	0.9	1.1	16.1	2A2-56	208	2.6	1.0	1.3	7.2
3A2-37	186	1.9	0.6	0.9	17.6	2A2-57	209	3.2	1.3	1.6	6.4
3A2-38	187	1.8	0.6	0.9	13.5	2A2-58	210	2.5	1.0	1.3	6.6
3A2-39	188	2.1	0.8	1.0	11.8	2A2-59	211	3.2	1.1	1.6	7.3
3A2-40	189	2.3	0.8	1.1	12.7	2A2-60	212	2.6	1.1	1.3	7.0
3A2-41	190	2.2	0.7	1.1	16.2	2A2-61	213	2.5	1.0	1.2	10.1
3A2-42	191	2.0	0.6	1.0	16.9	2A2-62	214	2.4	0.9	1.2	8.0
3A2-43	192	2.4	0.8	1.2	16.5	2A2-63	215	2.6	1.1	1.3	6.9
3A2-44	193	2.2	0.7	1.1	16.9	2A2-64	216	2.6	1.2	1.3	6.6
3A2-45	194	2.2	0.7	1.1	15.1	2A2-65	217	2.8	1.2	1.4	7.0
3A2-46	195	2.6	1.3	1.3	6.9	2A2-66	218	2.5	1.1	1.3	6.8
3A2-47	196	2.0	0.7	1.0	14.9	2A2-67	219	3.2	1.6	1.6	5.7
3A2-48	197	2.1	0.9	1.0	11.3	2A2-68	220	2.5	1.1	1.3	6.3
3A2-49	198	1.9	0.6	1.0	15.5	2A2-69	221	2.9	1.3	1.5	5.9
3A2-50	199	2.0	0.6	1.0	16.8	2A2-70	222	2.7	1.2	1.3	6.0
3A2-51	200	2.2	0.7	1.1	16.2	2A2-71	223	2.6	1.2	1.3	5.2
3A2-52	201	2.3	0.9	1.2	19.0	2A2-72	224	2.8	1.4	1.4	5.1
3A2-53	202	2.0	0.7	1.0	17.1	2A2-73	225	3.1	1.6	1.5	4.9
3A2-54	203	2.0	0.7	1.0	12.9	2A2-74	226	3.2	1.8	1.6	4.6
3A2-55	204	1.9	0.6	0.9	16.5	2A2-75	227	2.9	1.8	1.5	4.3
3A2-56	205	2.2	0.7	1.1	15.6	2A2-76	228	3.2	1.9	1.6	4.1
3A2-57	206	2.2	0.8	1.1	15.6	2A2-77	229	2.6	1.5	1.3	4.3

3A2-58	207	2.2	0.8	1.1	16.0	2A2-78	230	3.6	2.3	1.8	3.7
3A2-59	208	2.2	0.7	1.1	16.3	2A2-79	231	3.7	2.4	1.9	3.6
3A2-60	209	1.6	0.5	0.8	15.2	2A2-80	232	3.4	2.2	1.7	3.7
3A2-61	210	1.8	0.6	0.9	15.0	2A2-81	233	3.5	2.3	1.8	3.7
3A2-62	211	1.9	0.7	0.9	16.5	2A2-82	234	4.0	3.0	2.0	3.1
3A2-63	212	1.7	0.6	0.8	14.7	2A2-83	235	3.6	2.6	1.8	3.1
3A2-64	213	1.7	0.5	0.9	16.5	2A2-84	236	3.7	2.7	1.9	3.5
3A2-65	214	2.1	0.6	1.1	17.4	2A2-85	237	3.4	2.4	1.7	3.4
3A2-66	215	1.9	0.6	0.9	16.5	2A2-86	238	3.1	2.1	1.5	3.6
3A2-67	216	1.8	0.6	0.9	14.3	2A2-87	239	3.6	2.4	1.8	3.9
3A2-68	217	2.3	0.8	1.1	17.1	2A2-88	240	2.9	1.8	1.4	4.0
3A2-69	218	2.0	0.7	1.0	21.1	2A2-89	241	3.4	2.3	1.7	3.9
3A2-70	219	1.8	0.6	0.9	16.9	2A2-90	242	3.9	2.7	2.0	3.5
3A2-71	220	1.9	0.6	1.0	16.1	2A2-91	243	3.7	2.6	1.9	3.6
3A2-72	221	1.9	0.6	0.9	16.0	2A2-92	244	3.3	2.4	1.6	3.4
3A2-73	222	2.0	0.7	1.0	15.7	2A2-93	245	3.9	3.0	1.9	3.3
3A2-74	223	2.0	0.6	1.0	18.5	2A2-94	246	3.5	2.5	1.8	4.0
3A2-75	224	1.9	0.6	0.9	17.0	2A2-95	247	3.9	2.7	1.9	4.0
3A2-76	225	1.6	0.5	0.8	16.4	2A2-96	248	3.5	2.5	1.8	3.9
3A2-77	226	2.2	0.8	1.1	14.3	2A2-97	249	4.2	3.1	2.1	3.7
3A2-78	227	1.8	0.6	0.9	17.6	2A2-98	250	3.0	2.1	1.5	3.9
3A2-79	228	2.3	0.7	1.1	18.0	2A2-99	251	4.4	3.2	2.2	4.3
3A2-80	229	2.2	0.7	1.1	16.2	2A2-100	252	3.5	2.5	1.8	3.7
3A2-81	230	1.9	0.6	0.9	16.9	2A2-101	253	3.7	2.6	1.9	3.7
3A2-82	231	2.3	0.8	1.1	15.4	2A2-102	254	3.5	2.5	1.7	3.8
3A2-83	232	2.0	0.6	1.0	16.0	2A2-103	255	3.7	3.0	1.9	3.3
3A2-84	233	2.3	0.8	1.1	15.6	2A2-104	256	3.2	2.2	1.6	3.6
3A2-85	234	2.1	0.8	1.1	14.6	2A2-105	257	3.7	2.6	1.8	3.5
3A2-86	235	2.3	0.8	1.1	15.9	2A2-106	258	3.7	2.8	1.9	3.4
3A2-87	236	2.3	0.8	1.1	13.8	2A2-107	259	3.6	2.7	1.8	3.3
3A2-88	237	2.5	0.8	1.2	14.0	2A2-108	260	3.9	2.8	1.9	3.6
3A2-89	238	2.0	0.6	1.0	15.1	2A2-109	261	4.1	3.0	2.0	3.7
3A2-90	239	2.2	0.7	1.1	15.2	2A2-110	262	4.0	2.9	2.0	4.0
3A2-91	240	2.3	0.8	1.1	14.8	2A2-111	263	3.9	2.9	2.0	3.6
3A2-92	241	2.3	0.8	1.1	14.3	2A2-112	264	3.5	2.5	1.7	3.8
3A2-93	242	2.1	0.7	1.0	14.8	2A2-113	265	3.6	2.6	1.8	3.6

3A2-94	243	2.2	0.8	1.1	16.9	2A2-114	266	3.7	2.9	1.9	3.5
3A2-95	244	1.8	0.6	0.9	14.2	2A2-115	267	3.9	2.8	2.0	3.6
3A2-96	245	1.8	0.6	0.9	13.6	2A2-116	268	3.3	2.4	1.7	3.6
3A2-97	246	1.8	0.7	0.9	13.6	2A2-117	269	3.4	2.5	1.7	3.6
3A2-98	247	2.1	1.2	1.1	6.1	2A2-118	270	3.5	2.6	1.7	3.8
3A2-99	248	1.8	0.9	0.9	7.3	2A2-119	271	3.9	2.9	2.0	3.9
3A2-100	249	1.6	0.8	0.8	7.2	2A2-120	272	3.4	2.4	1.7	4.4
3A2-101	250	2.3	1.3	1.2	5.6	2A2-121	273	3.9	2.8	1.9	3.8
3A2-102	251	1.9	0.8	0.9	12.0	2A2-122	274	3.6	2.6	1.8	3.8
3A2-103	252	1.9	0.7	1.0	16.7	2A2-123	275	3.7	2.7	1.8	3.6
3A2-104	253	1.7	0.6	0.9	17.1	2A2-124	276	3.6	2.7	1.8	3.4
3A2-105	254	1.7	0.7	0.8	18.8	2A2-125	277	3.6	2.6	1.8	3.7
3A2-106	255	1.8	0.7	0.9	17.2	2A2-126	278	4.3	3.4	2.2	3.4
3A2-107	256	2.0	0.7	1.0	15.8	2A2-127	279	3.5	2.5	1.8	4.0
3A2-108	257	2.0	0.8	1.0	15.3	2A2-128	280	3.9	2.8	2.0	3.9
						2A2-129	281	4.1	2.9	2.0	3.9
a Sample identifier is core ID followed by tube depth (cm)						2A2-130	282	3.9	2.8	2.0	4.3
b Sample size was 2 cm^3						2A2-131	283	3.2	2.1	1.6	4.4
						2A2-132	284	3.7	2.6	1.9	3.9
						2A2-133	285	3.4	2.3	1.7	4.2
						2A2-134	286	3.8	2.8	1.9	3.7
						2A2-135	287	3.6	2.7	1.8	3.7
						2A2-136	288	3.5	2.3	1.7	4.5
						2A2-137	289	3.8	2.8	1.9	3.7
						2A2-138	290	3.8	2.6	1.9	4.2
						2A2-139	291	3.2	2.3	1.6	4.1
						2A2-140	292	3.6	2.7	1.8	3.7

2A2-141	293	4.1	2.8	2.1	4.1
2A2-142	294	3.5	2.4	1.8	4.4
2A2-143	295	4.0	2.9	2.0	3.9
2A2-144	296	4.2	2.7	2.1	4.5
2A2-145	297	3.9	2.8	1.9	4.2
2A2-146	298	3.5	2.5	1.8	4.0
2A2-147	299	3.6	2.4	1.8	4.4
2A2-148	300	4.1	3.0	2.1	4.3
2A2-149	301	3.5	2.6	1.8	4.1
2A2-150	302	3.5	2.5	1.8	4.6

APPENDIX C: EMERALD LAKE INPUT VALUES FOR SEDIMENT CORE AGE MODELS

ID	^{14}C age	Age (cal yr BP)	Error	Reservoir	Depth (cm)
Part 1, Composite Core 3					
surface		-62	2		0
GR0001		-50	2		0.5
GR0002		-34.1	2		2.5
GR0003		-18.5	4		5.5
GR0004		46.2	18		8.5
GR0005		78.5	39		12.5
GR0006	180		20		21.5
GR0007	320		15		72.5
Part 2, Composite Core 3					
GR0001	180		20		21.5
GR0002	320		15		72.5
GR0003	590		110		82
GR0004	1665		15		144
GR0005	2515		15		200
GR0006	3685		20		252.5
Part 1, Composite Core 2					
Surface		-62	2		0
EMD001	1455		25		32
EMD002	4785		15		56
EMD003	6145		20		86
Part 2, Composite Core 2					
EMD002	4785		15		56
EMD003	6145		20		86
EMD004	7255		20		121
EMD005	7160		35		151.5
EMD006	8815		20		164
EMD007	9525		20		214.5
EMD008	9835		30		220

Note: Age model generated in CLAM (Blaauw, 2010)

APPENDIX D: OUTPUT VALUES FOR EMERALD LAKE AGE MODELS

Core 3

Depth (cm blf)	min95%	max95%	Best
0.0	-62	-55	-59
0.2	-60	-54	-57
0.4	-58	-52	-55
0.6	-56	-50	-53
0.8	-54	-49	-51
1.0	-52	-47	-49
1.2	-50	-45	-48
1.4	-48	-43	-46
1.6	-46	-41	-44
1.8	-45	-39	-42
2.0	-43	-37	-40
2.2	-41	-35	-38
2.4	-39	-33	-36
2.6	-37	-30	-34
2.8	-36	-28	-32
3.0	-34	-26	-31
3.4	-32	-24	-29
3.6	-30	-21	-27
3.8	-29	-19	-25
4.0	-27	-17	-23
4.2	-25	-14	-21
4.4	-24	-12	-19
4.6	-22	-9	-17
4.8	-21	-7	-15
5.0	-19	-5	-13
5.2	-17	-2	-11
5.4	-16	0	-9
5.6	-14	3	-7
5.8	-13	5	-5
6.0	-11	8	-3
6.2	-10	10	0
6.4	-8	13	2
6.6	-7	15	4
6.8	-5	18	6
7.0	-4	21	8
7.2	-2	23	10
7.4	-1	26	13
7.6	0	28	15
7.8	2	31	17
8.0	3	33	19
8.2	4	36	22
8.4	5	39	24
8.6	6	41	26
8.8	8	44	28
9.0	9	47	30
9.2	10	49	33

Core 2

Depth (cm blf)	min95%	max95%	best
0.0	-84	-62	-68
0.2	-78	-55	-62
0.4	-72	-48	-56
0.6	-66	-40	-49
0.8	-60	-33	-43
1.0	-54	-25	-37
1.2	-48	-18	-31
1.4	-42	-10	-25
1.6	-36	-3	-18
1.8	-29	5	-12
2.0	-23	12	-6
2.2	-17	20	1
2.4	-11	28	7
2.6	-4	35	13
2.8	2	43	20
3.0	8	51	26
3.2	15	59	33
3.4	22	67	40
3.6	28	75	46
3.8	35	83	53
4.0	42	91	60
4.2	48	99	67
4.4	55	108	74
4.6	62	116	81
4.8	69	124	88
5.0	76	133	95
5.2	83	141	103
5.4	90	150	110
5.6	97	159	118
5.8	105	168	126
6.0	112	177	133
6.2	119	186	141
6.4	127	195	149
6.6	135	205	157
6.8	142	214	166
7.0	150	224	174
7.2	158	233	182
7.4	166	243	191
7.6	175	253	200
7.8	183	263	209
8.0	192	273	218
8.2	201	284	227
8.4	209	294	237
8.6	219	305	246
8.8	228	315	256
9.0	237	326	266

9.4	11	52	35	9.2	247	337	276
9.6	12	54	37	9.4	257	349	286
9.8	13	57	39	9.6	267	360	296
10.0	14	59	41	9.8	277	372	307
10.2	15	62	44	10.0	287	383	318
10.4	16	65	46	10.2	298	395	329
10.6	17	67	48	10.4	309	406	340
10.8	17	70	50	10.6	320	418	351
11.0	18	72	52	10.8	331	431	363
11.2	19	75	55	11.0	342	443	374
11.4	20	77	57	11.2	354	456	386
11.6	21	80	59	11.4	366	469	398
11.8	21	83	61	11.6	378	482	411
12.0	22	85	63	11.8	390	495	423
12.2	22	88	65	12.0	403	509	436
12.4	23	91	67	12.2	415	523	449
12.6	24	93	69	12.4	428	537	463
12.8	24	96	72	12.6	441	551	476
13.0	25	99	74	12.8	455	565	490
13.2	25	101	76	13.0	469	580	504
13.4	26	104	78	13.2	483	595	518
13.6	26	106	80	13.4	497	610	533
13.8	26	109	82	13.6	512	625	547
14.0	27	111	84	13.8	526	641	562
14.2	27	114	86	14.0	541	657	578
14.4	27	116	88	14.2	557	673	593
14.6	28	119	90	14.4	572	688	609
14.8	28	121	92	14.6	588	705	625
15.0	28	124	94	14.8	604	722	641
15.2	29	126	96	15.0	621	739	658
15.4	29	129	98	15.2	637	756	675
15.6	29	131	100	15.4	655	773	692
15.8	29	134	102	15.6	672	791	710
16.0	29	136	104	15.8	690	809	727
16.2	29	139	106	16.0	708	828	746
16.4	29	141	108	16.2	726	846	764
16.6	30	144	110	16.4	745	866	783
16.8	30	146	112	16.6	763	884	802
17.0	30	149	114	16.8	783	904	821
17.2	30	151	116	17.0	802	925	841
17.4	30	154	117	17.2	822	944	861
17.6	30	156	119	17.4	842	964	881
17.8	30	159	121	17.6	863	985	901
18.0	31	161	123	17.8	884	1005	922
18.2	31	163	125	18.0	905	1026	944
18.4	31	166	127	18.2	927	1048	965
18.6	31	168	129	18.4	949	1069	987
18.8	31	171	130	18.6	971	1091	1010
19.0	31	173	132	18.8	994	1115	1032
19.2	31	175	134	19.0	1017	1138	1055
19.4	32	177	136	29.2	1041	1162	1079
19.6	32	180	138	29.4	1064	1186	1103
19.8	32	182	139	29.6	1088	1211	1127
20.0	32	184	141	29.8	1113	1236	1151

20.2	32	187	143	30.0	1138	1261	1176
20.4	32	189	145	30.2	1163	1287	1201
20.6	32	191	147	30.4	1188	1313	1227
20.8	32	194	148	30.6	1214	1339	1253
21.0	32	196	150	30.8	1239	1366	1279
21.2	32	198	152	31.0	1265	1393	1306
21.4	33	200	153	31.2	1292	1421	1333
21.6	33	203	155	31.4	1318	1449	1361
21.8	33	205	157	31.6	1345	1478	1389
22.0	34	207	159	31.8	1373	1507	1417
23.7	34	209	160	32.0	1401	1536	1446
23.9	34	211	162	32.2	1429	1566	1476
24.1	34	214	164	32.4	1458	1596	1505
24.3	35	216	165	32.6	1486	1626	1535
24.5	35	218	167	32.8	1516	1657	1566
24.7	35	220	169	33.0	1545	1688	1597
24.9	36	222	170	33.2	1575	1720	1628
25.1	36	224	172	33.4	1605	1752	1659
25.3	36	227	173	33.6	1635	1784	1691
25.5	37	229	175	34.2	1666	1817	1724
25.7	37	231	177	34.4	1696	1849	1756
25.9	38	233	178	34.6	1728	1883	1789
26.1	38	235	180	34.8	1759	1916	1823
26.3	38	237	181	35.0	1791	1950	1856
26.5	39	239	183	35.2	1823	1984	1890
26.7	39	241	184	35.4	1855	2019	1925
26.9	40	243	186	35.6	1888	2053	1959
27.1	40	244	187	35.8	1921	2089	1994
27.3	41	246	189	36.0	1954	2124	2029
27.5	41	248	191	36.2	1987	2160	2065
27.7	42	250	192	36.4	2021	2196	2101
27.9	42	252	194	36.6	2054	2232	2137
28.1	43	254	195	36.8	2088	2269	2173
28.3	44	256	197	37.0	2122	2305	2210
28.5	44	258	198	37.2	2156	2342	2246
28.7	45	259	199	37.4	2191	2380	2283
28.9	46	261	201	37.6	2226	2417	2321
29.1	46	263	202	37.8	2261	2455	2358
29.3	47	265	204	38.0	2296	2493	2396
29.5	48	267	205	38.2	2331	2531	2434
29.7	48	268	207	38.4	2367	2570	2472
29.9	49	270	208	38.6	2403	2608	2510
30.1	50	272	210	38.8	2439	2647	2548
30.3	50	274	211	39.0	2475	2686	2587
30.5	51	275	212	39.2	2512	2725	2626
30.7	52	277	214	39.4	2547	2764	2665
30.9	53	279	215	39.6	2584	2803	2704
31.1	54	281	216	39.8	2620	2842	2743
31.3	54	282	218	40.0	2657	2882	2783
31.5	55	284	219	40.2	2694	2921	2822
31.7	56	286	221	40.4	2731	2961	2862
31.9	57	287	222	40.6	2769	3001	2902
32.1	58	289	223	40.8	2806	3041	2942
32.3	58	290	225	41.0	2844	3081	2982

32.5	59	292	226	41.2	2882	3121	3022
32.7	60	294	227	41.4	2919	3161	3062
32.9	61	295	229	41.6	2957	3202	3102
33.1	62	297	230	41.8	2994	3242	3142
33.3	63	298	231	42.0	3032	3282	3183
33.5	64	300	232	42.2	3070	3323	3223
33.7	65	301	234	42.4	3107	3364	3264
33.9	66	303	235	42.6	3145	3404	3304
34.1	67	304	236	42.8	3183	3445	3345
34.3	67	306	237	43.0	3221	3485	3385
34.5	68	307	239	43.2	3259	3525	3426
34.7	69	309	240	44.0	3297	3566	3467
34.9	70	310	241	44.2	3335	3606	3507
35.1	71	312	242	44.4	3373	3647	3548
35.3	72	313	244	44.6	3411	3688	3589
35.5	73	314	245	46.1	3450	3729	3629
35.7	74	316	246	46.3	3488	3769	3670
35.9	75	317	247	46.5	3526	3810	3710
36.1	76	318	248	46.7	3565	3850	3751
36.3	77	320	250	46.9	3603	3890	3791
36.5	78	321	251	47.1	3641	3930	3832
36.7	79	322	252	47.3	3679	3971	3872
36.9	80	324	253	47.5	3717	4011	3912
37.1	81	325	254	47.7	3755	4051	3952
37.3	83	326	256	47.9	3792	4091	3993
37.5	84	328	257	48.1	3830	4131	4033
37.7	85	329	258	48.3	3868	4171	4072
37.9	86	330	259	48.5	3905	4210	4112
38.1	87	332	260	48.7	3942	4250	4152
38.3	88	333	261	48.9	3979	4290	4191
38.5	90	334	262	49.1	4016	4329	4231
38.7	91	335	263	49.3	4053	4368	4270
38.9	92	336	265	49.5	4090	4407	4309
39.1	93	338	266	49.7	4127	4446	4348
39.3	94	339	267	49.9	4163	4485	4387
39.5	95	340	268	50.1	4200	4523	4426
39.7	97	341	269	50.3	4236	4562	4464
39.9	98	342	270	50.5	4272	4600	4503
40.1	99	344	271	50.7	4308	4638	4541
40.3	100	345	272	50.9	4343	4676	4579
40.5	101	346	273	51.1	4379	4714	4616
40.7	103	347	274	51.3	4414	4752	4654
40.9	104	348	275	51.5	4449	4789	4691
41.1	105	349	276	51.7	4484	4826	4728
41.3	106	350	277	51.9	4519	4863	4765
41.5	107	351	278	52.1	4553	4899	4801
41.7	109	352	279	52.3	4588	4936	4838
41.9	110	353	280	52.8	4622	4972	4874
42.1	111	355	281	53.0	4656	5007	4909
42.3	112	356	283	53.2	4689	5042	4945
42.5	113	357	284	53.4	4723	5077	4980
42.7	115	358	285	53.6	4756	5112	5015
42.9	116	359	285	53.8	4790	5147	5050
43.1	118	360	286	54.0	4823	5181	5084

43.3	119	361	287	54.2	4855	5215	5118
43.5	120	362	288	54.4	4887	5248	5152
43.7	122	363	289	54.6	4919	5282	5185
43.9	123	364	290	54.8	4951	5315	5218
44.1	124	365	291	55.0	4982	5347	5251
44.3	126	366	292	55.2	5013	5379	5283
44.5	127	367	293	55.4	5044	5411	5315
44.7	129	368	294	55.6	5075	5443	5347
44.9	130	368	295	55.8	5105	5474	5378
45.1	131	369	296	56.0	5134	5505	5409
45.3	132	370	297	56.2	5163	5535	5440
45.5	134	371	298	56.4	5192	5565	5470
45.7	135	372	299	56.6	5221	5594	5499
45.9	136	373	300	56.8	5249	5624	5529
46.1	138	374	301	57.0	5277	5653	5558
46.3	139	375	302	57.2	5305	5681	5586
46.5	141	376	302	57.4	5333	5710	5615
46.7	142	377	303	58.0	5599	5708	5638
46.9	144	377	304	58.2	5610	5719	5649
47.1	145	378	305	58.4	5621	5730	5660
47.3	147	379	306	58.6	5632	5742	5672
47.5	148	380	307	58.8	5643	5753	5683
47.7	149	381	308	59.0	5653	5765	5695
47.9	151	382	309	59.2	5664	5776	5706
48.1	152	382	310	59.4	5675	5788	5717
48.3	154	383	310	59.6	5686	5799	5729
48.5	155	384	311	59.8	5696	5811	5740
48.7	156	385	312	60.0	5707	5822	5751
48.9	158	385	313	60.2	5718	5834	5762
49.1	159	386	314	60.4	5728	5845	5774
49.3	161	387	315	60.6	5739	5857	5785
49.5	162	387	315	60.8	5750	5868	5796
49.7	164	388	316	61.0	5761	5880	5808
49.9	165	389	317	61.2	5771	5891	5819
50.1	167	390	318	61.4	5782	5903	5830
50.3	168	391	319	61.6	5792	5914	5841
50.5	170	391	320	61.8	5803	5926	5853
50.7	171	392	320	62.0	5813	5937	5864
50.9	173	393	321	62.2	5824	5949	5875
51.1	174	394	322	62.4	5835	5960	5886
51.3	176	394	323	62.6	5845	5971	5897
51.5	177	395	324	62.8	5856	5983	5909
51.7	178	396	324	63.0	5866	5994	5920
51.9	180	396	325	63.2	5877	6006	5931
52.1	182	397	326	63.4	5887	6017	5942
52.3	183	397	327	63.6	5897	6028	5953
52.5	184	398	327	63.8	5908	6040	5964
52.7	186	399	328	64.0	5918	6051	5976
52.9	187	399	329	64.2	5928	6063	5987
53.1	189	400	330	64.4	5939	6074	5998
53.3	190	401	331	64.6	5949	6085	6009
53.5	192	401	331	64.8	5959	6096	6020
53.7	193	402	332	65.0	5970	6108	6031
53.9	194	402	333	65.2	5980	6119	6042

54.1	196	403	334	65.4	5990	6130	6053
54.3	198	404	334	65.6	6001	6142	6064
54.5	199	404	335	65.8	6011	6153	6075
54.7	201	405	336	66.0	6021	6164	6086
54.9	202	405	337	66.2	6031	6175	6097
55.1	204	406	337	66.4	6042	6186	6108
55.3	205	407	338	66.6	6052	6197	6119
55.5	206	407	339	66.8	6062	6208	6130
55.7	208	408	339	67.0	6072	6220	6141
55.9	210	408	340	67.2	6082	6231	6152
56.1	211	409	341	67.4	6092	6242	6163
56.3	212	409	342	67.6	6102	6253	6173
56.5	214	410	342	67.8	6112	6264	6184
56.7	215	411	343	68.0	6122	6275	6195
56.9	217	411	344	68.2	6132	6286	6206
57.1	219	412	344	68.4	6142	6297	6217
57.3	220	412	345	68.6	6152	6308	6227
57.5	221	413	346	68.8	6162	6318	6238
57.7	223	413	346	69.0	6172	6329	6249
57.9	224	414	347	69.2	6182	6340	6259
58.1	225	415	348	69.4	6192	6351	6270
58.3	227	415	349	69.6	6202	6362	6281
58.5	228	416	349	69.8	6212	6373	6291
58.7	230	416	350	70.0	6222	6383	6302
58.9	231	417	351	70.2	6232	6394	6313
59.1	233	418	351	70.4	6242	6405	6323
59.3	234	418	352	70.6	6252	6416	6334
59.5	236	419	353	70.8	6262	6426	6344
59.7	237	420	353	71.0	6271	6437	6355
59.9	239	420	354	71.2	6281	6448	6365
60.1	240	421	355	71.4	6291	6458	6376
60.3	241	421	355	71.6	6301	6469	6386
60.5	243	422	356	71.8	6310	6480	6396
60.7	245	422	357	72.0	6320	6490	6407
60.9	246	423	357	72.2	6330	6500	6417
61.1	247	423	358	72.4	6339	6511	6427
61.3	249	424	358	72.6	6349	6521	6438
61.5	250	425	359	72.8	6358	6532	6448
61.7	252	425	360	73.0	6368	6542	6458
61.9	253	426	360	73.2	6378	6553	6468
62.1	254	427	361	73.4	6387	6563	6479
62.3	256	427	362	73.6	6397	6573	6489
62.5	257	428	362	73.8	6406	6583	6499
62.7	259	428	363	74.0	6416	6594	6509
62.9	260	429	364	74.2	6425	6604	6519
63.1	261	429	364	74.4	6434	6614	6529
63.3	263	430	365	74.6	6444	6624	6539
63.5	264	430	366	75.1	6453	6634	6549
63.7	265	431	366	75.3	6463	6644	6559
63.9	267	431	367	75.5	6472	6654	6569
64.1	268	432	367	75.7	6481	6664	6579
64.3	270	433	368	75.9	6491	6674	6589
64.5	271	433	369	76.1	6500	6684	6599
64.7	272	434	369	76.3	6509	6694	6608

64.9	274	434	370	76.5	6518	6704	6618
65.1	275	435	370	76.7	6528	6714	6628
65.3	276	435	371	76.9	6537	6724	6638
65.5	278	436	372	77.1	6546	6733	6647
65.7	279	436	372	77.3	6555	6743	6657
65.9	280	437	373	77.5	6564	6753	6666
66.1	282	438	374	77.7	6574	6763	6676
66.3	283	438	374	77.9	6583	6772	6686
66.5	284	439	375	78.1	6592	6782	6695
66.7	286	439	375	78.3	6601	6792	6705
66.9	287	440	376	78.5	6610	6801	6714
67.1	288	440	377	78.7	6619	6811	6723
67.3	290	441	377	78.9	6628	6820	6733
67.5	291	441	378	79.1	6637	6829	6742
67.7	292	442	378	79.3	6645	6839	6751
67.9	294	443	379	79.5	6654	6848	6761
68.1	295	443	380	79.7	6663	6857	6770
68.3	296	444	380	79.9	6672	6867	6779
68.5	298	444	381	80.1	6681	6876	6788
68.7	299	445	381	80.3	6690	6885	6797
68.9	300	445	382	80.5	6698	6894	6806
69.1	302	446	383	80.7	6707	6904	6815
69.3	303	447	383	80.9	6716	6913	6824
69.5	304	447	384	81.1	6725	6922	6833
69.7	310	460	385	81.3	6733	6931	6842
69.9	313	462	388	81.5	6742	6940	6851
70.1	316	465	390	81.7	6750	6949	6860
70.3	319	467	393	81.9	6759	6958	6869
70.5	323	470	396	82.1	6767	6967	6877
70.7	326	472	399	82.3	6776	6975	6886
70.9	329	475	401	82.5	6784	6984	6895
71.1	332	478	404	82.7	6793	6993	6903
71.3	336	480	407	82.9	6801	7002	6912
71.5	339	483	410	83.1	6809	7010	6920
71.7	342	486	413	83.3	6817	7019	6929
71.9	346	489	416	83.5	6826	7028	6937
72.1	349	491	419	83.7	6834	7036	6946
72.3	353	494	422	83.9	6842	7045	6954
72.5	356	497	425	84.3	6850	7053	6962
72.7	359	500	428	84.5	6858	7062	6971
72.9	363	502	431	84.7	6866	7070	6979
73.1	366	505	434	84.9	6874	7078	6987
73.3	370	508	437	85.1	6883	7087	6995
73.5	374	511	440	85.3	6891	7095	7003
73.7	377	514	443	85.5	6899	7103	7011
73.9	381	516	446	85.7	6907	7111	7019
74.1	384	519	449	85.9	6914	7119	7027
74.3	388	522	452	86.1	6922	7127	7035
74.5	391	525	455	86.3	6930	7135	7043
74.7	395	528	458	86.5	6938	7143	7051
74.9	398	531	462	86.7	6945	7151	7059
75.1	402	534	465	86.9	6953	7159	7066
75.3	406	537	468	87.1	6961	7167	7074
75.5	409	540	471	87.3	6968	7175	7082

75.7	413	543	475	87.5	6976	7182	7089
75.9	416	546	478	87.7	6984	7190	7097
76.1	420	549	481	87.9	6991	7197	7104
76.3	424	553	484	88.1	6998	7205	7112
76.5	428	556	488	88.3	7006	7212	7119
76.7	431	559	491	88.5	7013	7220	7126
76.9	435	562	495	88.7	7021	7227	7134
77.1	439	565	498	88.9	7028	7235	7141
77.3	442	568	501	89.1	7036	7242	7148
77.5	446	572	505	89.3	7043	7249	7156
77.7	450	575	508	89.5	7050	7256	7163
77.9	454	578	512	89.7	7057	7264	7170
78.1	457	582	515	89.9	7065	7271	7177
78.3	461	585	519	90.1	7072	7278	7184
78.5	465	588	522	90.3	7079	7285	7191
78.7	469	591	526	90.5	7086	7292	7198
78.9	474	594	529	90.7	7093	7299	7205
79.1	478	598	533	90.9	7100	7306	7212
79.3	482	601	536	91.1	7107	7313	7219
79.5	485	604	540	91.3	7114	7320	7226
79.7	489	608	543	91.5	7121	7327	7232
79.9	493	611	547	91.7	7128	7333	7239
80.1	497	615	551	91.9	7135	7340	7246
80.3	500	618	554	92.1	7142	7347	7253
80.5	504	622	558	92.3	7149	7354	7259
80.7	508	625	562	92.5	7156	7360	7266
80.9	512	629	565	92.7	7162	7367	7273
81.1	516	632	569	92.9	7169	7374	7279
81.3	520	636	573	93.1	7176	7380	7286
81.5	524	639	577	93.3	7183	7387	7292
81.7	528	643	580	93.5	7190	7393	7299
81.9	531	647	584	93.7	7196	7400	7305
82.1	535	650	588	93.9	7203	7406	7312
82.3	539	654	592	94.1	7209	7412	7318
82.5	543	657	596	94.3	7216	7419	7324
82.7	547	661	599	94.5	7223	7425	7331
82.9	551	664	603	94.7	7229	7431	7337
83.1	556	668	607	94.9	7235	7437	7343
83.3	560	672	611	95.1	7242	7444	7350
83.5	564	675	615	95.3	7248	7450	7356
83.7	568	679	619	95.5	7255	7456	7362
83.9	572	683	623	95.7	7261	7462	7368
84.1	576	687	626	95.9	7268	7469	7375
84.5	580	690	630	96.1	7274	7475	7381
84.7	584	694	634	96.3	7281	7481	7387
84.9	588	697	638	96.5	7287	7487	7393
85.1	592	701	642	96.7	7294	7493	7399
85.3	597	705	646	96.9	7300	7499	7405
85.5	601	709	650	97.1	7306	7505	7411
85.7	605	713	654	97.3	7313	7511	7417
85.9	609	717	658	97.5	7319	7517	7423
86.1	613	721	662	97.7	7325	7523	7429
86.3	617	725	666	97.9	7332	7529	7435
86.5	621	729	670	98.1	7338	7535	7441

86.7	625	732	675	98.3	7344	7540	7447
86.9	629	736	679	98.5	7351	7546	7453
104.1	633	740	683	98.7	7357	7552	7459
104.3	637	744	687	98.9	7363	7558	7465
104.5	642	748	691	99.1	7369	7564	7471
104.7	646	752	695	99.3	7375	7570	7477
104.9	650	756	699	99.5	7381	7575	7482
105.1	654	760	703	99.7	7388	7581	7488
105.3	658	763	707	99.9	7394	7587	7494
105.5	663	768	712	100.1	7400	7592	7500
105.7	667	771	716	100.3	7406	7598	7506
105.9	671	775	720	100.5	7412	7604	7511
106.1	675	779	724	100.7	7419	7609	7517
106.3	679	783	728	100.9	7425	7615	7523
106.5	684	787	733	101.1	7431	7621	7529
107.3	688	791	737	101.3	7437	7626	7534
107.5	693	795	741	101.5	7443	7632	7540
107.7	697	799	745	101.7	7449	7637	7546
107.9	702	803	750	101.9	7455	7643	7551
108.1	706	808	754	102.1	7461	7648	7557
108.3	710	812	758	102.3	7467	7654	7563
108.5	715	816	763	102.5	7473	7660	7569
108.7	719	820	767	102.7	7480	7665	7574
108.9	724	824	771	102.9	7486	7671	7580
109.1	728	828	776	103.1	7492	7676	7586
109.3	733	833	780	103.3	7498	7682	7591
109.5	737	837	784	103.5	7504	7687	7597
109.7	742	841	789	103.7	7510	7693	7602
109.9	746	845	793	103.9	7516	7698	7608
110.1	750	849	797	104.1	7522	7704	7614
110.3	755	854	802	104.3	7527	7709	7619
110.5	759	858	806	104.5	7534	7715	7625
110.7	764	862	810	104.7	7540	7720	7631
110.9	768	866	815	104.9	7546	7725	7636
111.1	773	870	819	105.1	7552	7731	7642
111.3	777	875	824	105.3	7558	7736	7648
111.5	782	879	828	105.5	7563	7742	7653
111.7	786	884	833	105.7	7569	7747	7659
111.9	791	888	837	105.9	7575	7753	7664
112.1	795	892	842	106.1	7581	7758	7670
112.3	800	897	846	106.3	7587	7764	7676
112.5	804	901	850	106.5	7593	7769	7681
112.7	809	905	855	106.7	7599	7775	7687
112.9	814	910	859	106.9	7605	7780	7693
113.1	818	914	864	107.1	7611	7786	7698
113.3	823	918	868	107.3	7617	7791	7704
113.5	827	922	873	107.5	7623	7797	7710
113.7	832	927	878	107.7	7629	7802	7715
113.9	836	931	882	107.9	7636	7808	7721
114.1	841	936	887	108.1	7642	7813	7727
114.3	846	940	891	108.3	7648	7819	7732
114.5	850	945	896	108.5	7654	7824	7738
114.7	855	950	900	108.7	7660	7830	7744
114.9	860	954	905	108.9	7666	7835	7749

115.1	864	958	909	109.1	7672	7841	7755
115.3	869	963	914	109.3	7679	7846	7761
115.5	874	967	919	109.5	7685	7852	7766
115.7	878	972	923	109.7	7691	7857	7772
115.9	883	976	928	109.9	7697	7863	7778
116.1	888	981	932	110.1	7703	7868	7784
116.3	892	985	937	110.3	7709	7874	7789
116.5	897	990	942	110.5	7715	7879	7795
116.7	902	994	946	110.7	7721	7885	7801
116.9	907	999	951	111.5	7728	7890	7807
117.1	911	1003	955	111.7	7734	7896	7813
117.3	916	1008	960	111.9	7740	7902	7818
117.5	921	1012	965	112.1	7746	7907	7824
117.7	926	1017	969	112.3	7753	7913	7830
117.9	930	1021	974	112.5	7759	7918	7836
118.1	935	1026	979	112.7	7765	7924	7842
118.3	940	1030	983	112.9	7771	7930	7848
118.5	945	1035	988	113.1	7778	7935	7854
118.7	949	1039	993	113.3	7784	7941	7860
118.9	954	1044	997	113.5	7790	7947	7866
119.1	959	1049	1002	113.7	7797	7953	7872
119.3	964	1053	1007	113.9	7803	7958	7878
119.5	969	1058	1011	114.1	7809	7964	7884
119.7	974	1062	1016	114.3	7816	7970	7890
119.9	978	1067	1021	114.5	7822	7976	7896
120.1	983	1072	1026	114.7	7829	7982	7902
120.3	988	1076	1030	114.9	7835	7988	7908
120.5	993	1081	1035	115.1	7841	7994	7914
120.7	998	1085	1040	115.3	7848	8000	7920
120.9	1002	1090	1044	115.5	7855	8006	7926
121.1	1007	1095	1049	115.7	7861	8012	7933
121.3	1012	1099	1054	115.9	7868	8018	7939
121.5	1016	1104	1059	116.1	7874	8025	7945
121.7	1021	1109	1063	116.3	7881	8031	7951
121.9	1026	1113	1068	116.5	7887	8037	7958
122.1	1031	1118	1073	116.7	7894	8043	7964
122.3	1036	1123	1078	116.9	7901	8049	7970
122.9	1041	1127	1082	117.1	7907	8056	7977
123.1	1045	1132	1087	117.3	7914	8062	7983
123.3	1050	1137	1092	117.5	7921	8068	7990
123.5	1055	1141	1097	117.7	7928	8075	7996
123.7	1060	1146	1101	117.9	7935	8081	8003
123.9	1065	1151	1106	118.1	7941	8088	8009
124.1	1070	1155	1111	118.3	7948	8095	8016
124.3	1075	1160	1116	118.5	7955	8102	8022
124.5	1080	1164	1120	118.7	7962	8108	8029
124.7	1085	1169	1125	118.9	7969	8115	8035
124.9	1089	1174	1130	119.1	7976	8122	8042
125.1	1094	1178	1135	119.3	7983	8128	8049
125.3	1099	1183	1140	119.5	7989	8135	8055
125.5	1104	1188	1144	119.7	7996	8142	8062
125.7	1109	1192	1149	119.9	8003	8149	8069
125.9	1114	1197	1154	120.1	8010	8156	8076
126.1	1119	1202	1159	120.3	8017	8163	8083

126.3	1124	1206	1163	120.5	8024	8170	8090
126.5	1129	1211	1168	120.7	8030	8177	8097
126.7	1133	1215	1173	120.9	8038	8184	8104
126.9	1138	1220	1178	121.1	8045	8191	8111
127.1	1143	1225	1183	121.3	8051	8199	8118
127.3	1148	1229	1187	121.5	8058	8206	8125
127.5	1153	1234	1192	121.7	8065	8214	8132
127.7	1158	1239	1197	121.9	8072	8221	8139
127.9	1163	1243	1202	122.1	8079	8229	8146
128.1	1168	1248	1207	122.3	8086	8236	8153
128.3	1173	1253	1211	122.5	8093	8243	8161
128.5	1178	1257	1216	122.7	8100	8251	8168
128.7	1183	1262	1221	122.9	8107	8258	8175
128.9	1188	1267	1226	123.1	8114	8266	8183
129.1	1192	1272	1231	123.3	8121	8273	8190
129.3	1197	1276	1235	123.5	8128	8280	8197
129.5	1202	1281	1240	123.7	8135	8288	8205
129.7	1207	1285	1245	123.9	8142	8296	8212
129.9	1212	1290	1250	124.1	8149	8304	8220
130.1	1217	1295	1254	124.3	8156	8311	8227
130.3	1222	1300	1259	124.5	8163	8319	8235
130.5	1227	1304	1264	124.7	8170	8327	8243
131.2	1232	1309	1269	124.9	8177	8335	8250
131.4	1237	1313	1274	125.1	8185	8343	8258
131.6	1242	1318	1278	125.3	8192	8351	8266
131.8	1247	1323	1283	125.5	8199	8359	8273
132.0	1252	1327	1288	125.7	8206	8367	8281
132.2	1257	1332	1293	125.9	8214	8375	8289
132.4	1261	1337	1298	126.1	8221	8383	8297
132.6	1266	1342	1302	126.3	8228	8392	8305
132.8	1271	1346	1307	126.5	8236	8400	8312
133.0	1276	1351	1312	126.7	8243	8408	8320
133.2	1281	1355	1317	126.9	8250	8416	8328
133.4	1285	1360	1321	127.1	8257	8424	8336
133.6	1290	1365	1326	127.3	8265	8433	8344
133.8	1295	1369	1331	127.5	8272	8441	8352
134.0	1300	1374	1336	127.7	8280	8449	8360
134.2	1305	1378	1341	127.9	8287	8458	8368
134.4	1310	1383	1345	128.1	8295	8466	8376
134.6	1315	1388	1350	128.3	8302	8475	8384
134.8	1320	1392	1355	128.5	8310	8483	8392
135.0	1324	1397	1360	128.7	8317	8491	8400
135.2	1329	1402	1364	128.9	8325	8500	8409
135.4	1334	1406	1369	129.1	8332	8508	8417
135.6	1338	1411	1374	129.3	8340	8517	8425
135.8	1343	1416	1379	129.5	8348	8526	8433
136.0	1348	1420	1383	129.7	8355	8534	8441
136.2	1353	1425	1388	129.9	8363	8543	8450
136.4	1358	1429	1393	130.1	8371	8551	8458
136.6	1363	1434	1398	130.3	8378	8560	8466
136.8	1367	1439	1402	130.5	8386	8569	8475
137.0	1372	1443	1407	130.7	8394	8578	8483
137.2	1377	1448	1412	130.9	8401	8587	8491
137.4	1382	1452	1416	131.1	8409	8596	8500

137.6	1387	1457	1421	131.3	8417	8604	8508
137.8	1391	1461	1426	131.5	8425	8613	8516
138.0	1396	1466	1431	131.7	8432	8622	8525
138.2	1401	1471	1435	131.9	8440	8630	8533
139.1	1406	1475	1440	132.1	8448	8639	8542
139.3	1411	1479	1445	132.3	8456	8648	8550
139.5	1416	1484	1449	132.5	8464	8657	8559
139.7	1420	1489	1454	132.7	8471	8666	8567
139.9	1425	1493	1459	132.9	8479	8675	8576
140.1	1429	1498	1463	133.1	8487	8685	8584
140.3	1434	1502	1468	133.3	8495	8693	8593
140.5	1439	1507	1473	133.5	8503	8702	8601
140.7	1443	1511	1477	133.7	8511	8711	8610
140.9	1448	1516	1482	133.9	8519	8720	8618
141.1	1452	1521	1487	134.1	8527	8730	8627
141.3	1457	1525	1491	134.3	8535	8739	8635
141.5	1462	1530	1496	134.5	8543	8748	8644
141.7	1467	1534	1501	134.7	8551	8757	8653
141.9	1471	1539	1505	134.9	8559	8766	8661
142.1	1476	1543	1510	135.1	8567	8775	8670
142.3	1481	1548	1514	135.3	8575	8785	8679
142.5	1485	1553	1519	136.2	8583	8794	8687
142.7	1490	1557	1524	136.4	8591	8803	8696
142.9	1494	1562	1528	136.6	8599	8812	8705
143.1	1499	1566	1533	136.8	8607	8821	8713
143.3	1503	1571	1537	137.0	8615	8830	8722
143.5	1508	1575	1542	137.2	8623	8839	8731
143.7	1513	1580	1547	137.4	8631	8848	8739
143.9	1517	1585	1551	137.6	8640	8857	8748
144.1	1521	1589	1556	137.8	8648	8866	8757
144.3	1526	1594	1560	138.0	8656	8876	8765
144.5	1530	1598	1565	138.2	8664	8885	8774
144.7	1535	1603	1569	138.4	8672	8893	8783
144.9	1540	1608	1574	138.6	8680	8902	8792
145.1	1544	1612	1578	138.8	8688	8911	8800
145.3	1549	1617	1583	139.0	8696	8920	8809
145.5	1553	1622	1587	139.2	8704	8930	8818
145.7	1558	1627	1592	139.4	8713	8940	8827
145.9	1562	1631	1596	139.6	8721	8949	8835
146.1	1567	1636	1601	139.8	8728	8958	8844
146.3	1571	1641	1605	140.0	8736	8967	8853
146.5	1575	1645	1610	140.2	8745	8976	8862
146.7	1580	1650	1614	140.4	8753	8985	8870
146.9	1584	1655	1619	140.6	8761	8994	8879
147.1	1588	1660	1623	140.8	8769	9003	8888
147.3	1593	1664	1628	141.0	8777	9012	8897
147.5	1597	1669	1632	141.2	8785	9022	8905
147.7	1601	1674	1637	141.4	8793	9031	8914
147.9	1606	1679	1641	141.6	8801	9040	8923
148.1	1610	1683	1645	141.8	8809	9050	8932
148.3	1614	1688	1650	142.0	8817	9059	8940
148.5	1619	1693	1654	142.2	8825	9068	8949
148.7	1623	1698	1659	142.4	8833	9078	8958
148.9	1627	1702	1663	142.6	8841	9086	8967

149.1	1631	1707	1667	142.8	8849	9096	8975
149.3	1636	1712	1672	143.0	8857	9105	8984
149.5	1640	1716	1676	143.2	8865	9115	8993
149.7	1644	1721	1681	143.4	8872	9124	9002
149.9	1648	1726	1685	143.6	8880	9133	9010
150.1	1652	1730	1689	143.8	8889	9142	9019
150.3	1656	1735	1694	144.0	8897	9152	9028
150.5	1661	1740	1698	144.2	8905	9161	9036
150.7	1665	1745	1702	144.4	8913	9170	9045
150.9	1669	1749	1707	144.6	8921	9179	9054
151.1	1673	1754	1711	144.8	8929	9188	9063
151.3	1677	1759	1716	145.0	8937	9197	9071
151.5	1681	1763	1720	145.2	8945	9206	9080
151.7	1685	1768	1724	145.4	8953	9215	9089
151.9	1689	1773	1729	145.6	8961	9225	9097
152.1	1693	1777	1733	145.8	8969	9234	9106
152.3	1698	1782	1737	146.0	8976	9244	9114
152.5	1702	1787	1742	146.2	8984	9253	9123
152.7	1706	1791	1746	146.4	8992	9262	9132
152.9	1710	1796	1750	146.6	9000	9271	9140
153.1	1714	1800	1755	146.8	9007	9280	9149
153.3	1718	1805	1759	147.0	9015	9289	9157
153.5	1722	1810	1763	147.2	9023	9297	9166
153.7	1726	1814	1767	147.4	9030	9306	9175
153.9	1730	1819	1772	147.6	9037	9316	9183
154.1	1734	1824	1776	147.8	9045	9325	9192
154.7	1738	1828	1780	148.0	9052	9334	9200
154.9	1742	1833	1785	148.2	9060	9343	9209
155.1	1746	1838	1789	148.4	9068	9351	9217
155.3	1751	1842	1793	148.6	9076	9360	9226
155.5	1755	1847	1797	148.8	9083	9370	9234
155.7	1759	1851	1802	149.0	9091	9379	9242
155.9	1763	1856	1806	149.2	9099	9388	9251
156.1	1767	1861	1810	149.4	9106	9397	9259
156.3	1771	1865	1815	149.6	9114	9406	9268
156.5	1776	1870	1819	149.8	9121	9416	9276
156.7	1780	1875	1823	150.0	9129	9425	9284
156.9	1784	1879	1827	150.2	9137	9433	9293
157.1	1788	1884	1832	150.4	9145	9442	9301
157.3	1792	1889	1836	150.6	9152	9451	9309
157.5	1796	1893	1840	150.8	9160	9459	9318
157.7	1800	1898	1844	151.0	9168	9468	9326
157.9	1804	1902	1849	151.2	9175	9477	9334
158.1	1808	1907	1853	151.4	9182	9486	9342
158.3	1812	1911	1857	151.6	9190	9495	9350
158.5	1815	1916	1861	151.8	9197	9504	9359
158.7	1819	1920	1866	152.0	9204	9513	9367
158.9	1823	1925	1870	152.2	9212	9521	9375
159.1	1827	1930	1874	152.4	9219	9530	9383
159.3	1831	1934	1878	152.6	9226	9539	9391
159.5	1835	1939	1883	152.8	9234	9548	9399
159.7	1839	1943	1887	153.0	9241	9557	9407
159.9	1843	1948	1891	153.2	9249	9566	9415
160.1	1847	1953	1895	153.4	9256	9575	9423

160.3	1851	1957	1899	153.6	9263	9582	9431
160.5	1855	1962	1904	153.8	9271	9590	9439
160.7	1859	1966	1908	154.0	9278	9599	9447
160.9	1863	1971	1912	154.2	9285	9607	9455
161.1	1867	1976	1916	154.4	9293	9616	9463
161.3	1871	1980	1921	154.6	9301	9624	9471
161.5	1875	1985	1925	154.8	9307	9633	9479
161.7	1879	1989	1929	155.0	9315	9642	9486
161.9	1883	1994	1933	155.2	9322	9651	9494
162.1	1887	1998	1937	155.4	9328	9659	9502
162.3	1891	2003	1942	155.6	9335	9667	9510
162.5	1895	2008	1946	155.8	9342	9676	9517
162.7	1899	2012	1950	156.0	9349	9684	9525
162.9	1903	2017	1954	156.2	9356	9692	9532
163.1	1907	2021	1959	156.4	9363	9701	9540
163.3	1911	2026	1963	156.6	9370	9708	9548
163.5	1915	2031	1967	156.8	9377	9717	9555
163.7	1919	2035	1971	157.0	9383	9724	9563
163.9	1922	2040	1975	157.2	9390	9733	9570
164.1	1926	2045	1980	157.4	9397	9741	9578
164.3	1930	2049	1984	157.6	9404	9749	9585
164.5	1934	2054	1988	157.8	9412	9757	9592
164.7	1938	2058	1992	158.0	9418	9765	9600
164.9	1942	2063	1996	158.2	9425	9773	9607
165.1	1946	2067	2001	158.4	9431	9780	9614
165.3	1950	2072	2005	158.6	9437	9788	9621
165.5	1954	2077	2009	158.8	9444	9796	9629
165.7	1958	2081	2013	159.0	9451	9803	9636
165.9	1962	2086	2017	159.2	9457	9810	9643
166.1	1966	2090	2022	159.4	9463	9818	9650
166.3	1970	2095	2026	159.6	9470	9825	9657
166.5	1974	2100	2030	159.8	9476	9833	9664
166.7	1978	2104	2034	160.0	9483	9841	9671
166.9	1982	2109	2039	160.2	9490	9849	9678
167.1	1985	2113	2043	160.4	9497	9856	9685
167.3	1989	2118	2047	160.6	9504	9864	9692
167.5	1993	2122	2051	160.8	9510	9871	9699
167.7	1997	2127	2055	161.0	9517	9879	9705
167.9	2001	2132	2060	161.2	9523	9885	9712
168.1	2005	2136	2064	161.4	9529	9893	9719
168.3	2009	2141	2068	161.6	9535	9899	9726
168.5	2013	2145	2072	161.8	9541	9906	9732
168.7	2017	2150	2077	162.0	9547	9913	9739
168.9	2021	2155	2081	162.2	9553	9920	9745
169.1	2025	2159	2085	162.4	9559	9927	9752
169.3	2029	2164	2089	162.6	9565	9933	9758
169.5	2033	2168	2094	162.8	9571	9940	9765
169.7	2036	2173	2098	163.0	9578	9946	9771
169.9	2040	2177	2102	163.2	9584	9953	9778
170.1	2044	2182	2106	163.4	9591	9959	9784
170.3	2048	2186	2110	163.6	9597	9967	9790
170.5	2052	2191	2115	163.8	9604	9973	9796
170.7	2056	2196	2119	164.0	9610	9980	9802
170.9	2060	2201	2123	164.2	9616	9986	9809

171.1	2064	2205	2127	164.4	9622	9991	9815
171.3	2068	2210	2132	164.6	9628	9997	9821
171.5	2072	2214	2136	164.8	9634	10003	9827
171.7	2076	2219	2140	165.0	9640	10008	9833
171.9	2080	2224	2145	165.2	9645	10013	9839
172.1	2084	2228	2149	165.4	9650	10018	9844
172.3	2088	2233	2153	165.6	9656	10024	9850
172.5	2092	2238	2157	165.8	9661	10030	9856
172.7	2096	2242	2162	166.0	9666	10036	9862
172.9	2100	2247	2166	166.2	9672	10042	9867
173.1	2104	2252	2170	166.4	9679	10047	9873
173.3	2108	2256	2174	166.6	9685	10053	9879
173.5	2112	2261	2179	166.8	9691	10058	9884
173.7	2116	2266	2183	167.0	9697	10063	9890
173.9	2120	2271	2187	167.2	9703	10069	9895
174.1	2124	2275	2192	167.4	9709	10074	9901
174.3	2128	2280	2196	167.6	9715	10079	9906
174.5	2132	2284	2200	167.8	9720	10084	9912
174.7	2136	2289	2204	168.0	9724	10090	9917
174.9	2141	2294	2209	168.2	9730	10096	9922
175.1	2145	2298	2213	168.4	9734	10101	9928
175.3	2149	2303	2217	168.6	9740	10106	9933
175.5	2153	2308	2222	168.8	9744	10111	9938
175.7	2157	2312	2226	169.0	9748	10117	9943
175.9	2161	2317	2230	169.2	9754	10123	9948
176.1	2165	2321	2235	169.4	9759	10129	9953
176.3	2169	2326	2239	169.6	9764	10134	9958
176.5	2173	2331	2243	169.8	9768	10139	9963
176.7	2177	2335	2248	170.0	9773	10145	9968
176.9	2181	2340	2252	170.2	9778	10150	9973
177.1	2185	2345	2256	170.4	9783	10156	9978
177.3	2189	2349	2261	170.6	9786	10161	9983
177.5	2193	2354	2265	170.8	9790	10167	9988
177.7	2198	2359	2270	171.0	9793	10172	9993
177.9	2202	2364	2274	171.2	9798	10176	9998
178.1	2206	2368	2278	171.4	9803	10181	10002
178.3	2210	2373	2283	171.6	9806	10186	10007
178.5	2214	2378	2287	171.8	9810	10192	10012
178.7	2219	2383	2291	172.0	9813	10198	10017
178.9	2223	2387	2296	172.2	9816	10203	10021
179.1	2227	2392	2300	172.4	9819	10209	10026
179.3	2231	2397	2305	172.6	9823	10213	10030
179.5	2235	2402	2309	172.8	9827	10218	10035
179.7	2239	2406	2313	173.0	9831	10223	10040
179.9	2243	2411	2318	173.2	9834	10227	10044
180.1	2248	2416	2322	173.4	9837	10232	10049
180.3	2252	2421	2327	173.6	9840	10237	10053
180.5	2256	2426	2331	173.8	9843	10243	10057
180.7	2260	2431	2336	174.0	9846	10248	10062
180.9	2264	2436	2340	174.2	9850	10253	10066
181.1	2269	2441	2345	174.4	9854	10258	10071
181.3	2273	2445	2349	174.6	9858	10263	10075
181.5	2277	2450	2353	174.8	9862	10267	10079
181.7	2281	2455	2358	175.0	9864	10272	10084

181.9	2286	2460	2362	175.2	9866	10277	10088
182.1	2290	2464	2367	175.4	9868	10282	10092
182.3	2294	2469	2371	175.6	9870	10287	10096
182.5	2298	2474	2376	175.8	9872	10291	10100
182.7	2303	2479	2380	176.0	9876	10296	10105
182.9	2307	2483	2385	176.2	9878	10301	10109
183.1	2311	2488	2389	176.4	9880	10305	10113
183.3	2315	2493	2394	176.6	9883	10309	10117
183.5	2320	2498	2398	176.8	9886	10314	10121
183.7	2324	2503	2403	177.0	9889	10318	10125
183.9	2328	2507	2408	177.2	9891	10322	10129
184.1	2333	2512	2412	177.4	9894	10326	10133
184.3	2337	2517	2417	177.6	9897	10330	10137
184.5	2341	2522	2421	177.8	9900	10335	10141
184.7	2346	2527	2426	178.0	9903	10339	10145
184.9	2350	2532	2430	178.2	9906	10344	10149
187.6	2355	2536	2435	178.4	9908	10348	10153
187.8	2359	2541	2440	178.6	9910	10353	10157
188.0	2363	2546	2444	178.8	9912	10358	10161
188.2	2368	2551	2449	179.0	9915	10362	10165
188.4	2372	2556	2453	179.2	9917	10367	10169
192.4	2376	2561	2458	179.4	9921	10372	10173
192.6	2381	2566	2463	179.6	9924	10376	10176
192.8	2385	2571	2467	179.8	9927	10380	10180
193.0	2390	2576	2472	180.0	9929	10385	10184
193.2	2394	2581	2477	180.2	9931	10390	10188
193.4	2399	2586	2481	180.4	9934	10395	10192
193.6	2403	2591	2486	180.6	9936	10400	10196
193.8	2408	2596	2491	180.8	9938	10405	10199
194.0	2412	2601	2495	181.0	9941	10410	10203
194.2	2417	2605	2500	181.2	9944	10415	10207
194.4	2421	2610	2505	181.4	9946	10420	10211
194.6	2426	2615	2509	181.6	9949	10425	10214
194.8	2430	2620	2514	181.8	9951	10430	10218
195.0	2435	2625	2519	182.0	9953	10434	10222
195.2	2440	2630	2524	182.2	9956	10439	10225
195.4	2444	2635	2528	182.4	9959	10443	10229
195.6	2449	2640	2533	182.6	9961	10447	10233
195.8	2453	2645	2538	182.8	9963	10451	10236
196.0	2458	2650	2543	183.0	9966	10456	10240
196.2	2463	2655	2547	183.2	9968	10459	10244
196.4	2467	2660	2552	183.4	9970	10464	10247
196.6	2472	2665	2557	183.6	9973	10469	10251
196.8	2477	2670	2562	183.8	9977	10473	10255
197.0	2481	2675	2567	184.0	9980	10478	10258
197.2	2486	2680	2571	184.2	9982	10482	10262
197.4	2491	2685	2576	184.4	9985	10485	10266
197.6	2495	2690	2581	184.6	9987	10490	10269
198.2	2500	2695	2586	184.8	9990	10494	10273
198.4	2505	2700	2591	185.0	9992	10498	10276
198.6	2510	2705	2596	185.2	9995	10503	10280
198.8	2515	2710	2601	185.4	9997	10507	10284
199.0	2520	2715	2605	185.6	10000	10512	10287
199.2	2524	2720	2610	185.8	10003	10516	10291

199.4	2529	2725	2615	186.0	10005	10520	10295
199.6	2534	2729	2620	186.2	10008	10524	10298
199.8	2539	2734	2625	186.4	10010	10527	10302
200.0	2544	2739	2630	186.6	10013	10532	10305
200.5	2549	2744	2635	186.8	10016	10536	10309
200.7	2553	2750	2640	187.0	10019	10539	10312
200.9	2558	2755	2645	187.2	10022	10543	10316
201.1	2563	2760	2650	187.4	10024	10548	10320
201.3	2568	2765	2655	187.6	10027	10552	10323
201.5	2573	2770	2660	187.8	10029	10556	10327
201.7	2578	2775	2665	188.0	10032	10560	10330
201.9	2583	2780	2670	188.2	10034	10564	10334
202.1	2588	2785	2675	188.4	10038	10569	10338
202.3	2593	2790	2680	188.6	10041	10572	10341
202.5	2598	2795	2685	188.8	10043	10576	10345
202.7	2603	2800	2690	189.0	10046	10580	10349
202.9	2608	2805	2695	189.2	10049	10584	10352
203.1	2613	2811	2700	189.4	10052	10589	10356
203.3	2618	2816	2705	189.6	10055	10592	10359
203.5	2623	2821	2710	189.8	10058	10597	10363
203.7	2628	2826	2716	190.0	10061	10601	10367
203.9	2633	2831	2721	190.2	10065	10605	10370
204.1	2638	2836	2726	190.4	10068	10609	10374
204.3	2643	2841	2731	190.6	10072	10613	10378
204.5	2648	2846	2736	190.8	10075	10617	10381
204.7	2654	2851	2741	191.0	10078	10621	10385
204.9	2659	2857	2746	191.2	10082	10625	10389
205.1	2664	2862	2752	191.4	10085	10629	10392
205.3	2669	2867	2757	191.6	10088	10633	10396
205.5	2674	2872	2762	191.8	10092	10636	10400
205.7	2680	2877	2767	192.0	10095	10640	10404
205.9	2685	2882	2772	192.2	10098	10644	10407
206.1	2690	2887	2778	192.4	10101	10648	10411
206.3	2695	2892	2783	192.6	10105	10652	10415
206.5	2701	2897	2788	192.8	10108	10656	10419
206.7	2706	2902	2793	193.0	10112	10660	10422
206.9	2711	2907	2799	193.2	10115	10664	10426
207.1	2716	2912	2804	193.4	10119	10667	10430
207.3	2721	2917	2809	193.6	10123	10672	10434
207.5	2727	2922	2814	193.8	10127	10675	10438
207.7	2732	2928	2820	194.0	10130	10679	10442
207.9	2738	2933	2825	194.2	10134	10683	10445
208.1	2743	2938	2830	194.4	10138	10687	10449
208.3	2748	2943	2836	194.6	10142	10691	10453
208.5	2754	2949	2841	194.8	10146	10694	10457
208.7	2759	2954	2846	195.0	10150	10698	10461
208.9	2765	2959	2851	195.2	10154	10702	10465
209.1	2770	2964	2857	195.4	10158	10706	10469
209.3	2775	2969	2862	195.6	10162	10710	10473
209.5	2781	2975	2868	195.8	10166	10714	10477
209.7	2786	2980	2873	196.0	10170	10718	10481
209.9	2792	2985	2878	196.2	10174	10722	10485
210.1	2797	2990	2884	196.4	10178	10726	10489
210.3	2802	2996	2889	196.6	10182	10730	10493

210.5	2808	3001	2894	196.8	10187	10733	10497
210.7	2813	3006	2900	197.0	10192	10737	10501
210.9	2819	3011	2905	197.2	10196	10741	10505
211.1	2824	3017	2911	197.4	10201	10745	10509
211.3	2829	3022	2916	197.6	10206	10749	10514
211.5	2835	3027	2922	197.8	10210	10753	10518
211.7	2840	3033	2927	198.0	10215	10757	10522
211.9	2846	3038	2933	198.2	10220	10761	10526
212.1	2851	3043	2938	198.4	10224	10764	10531
212.3	2857	3049	2943	198.6	10229	10769	10535
212.5	2862	3054	2949	198.8	10233	10773	10539
212.7	2868	3059	2954	199.0	10238	10777	10543
212.9	2873	3064	2960	199.2	10243	10781	10548
213.1	2879	3069	2965	199.4	10248	10785	10552
213.3	2884	3075	2971	199.6	10253	10789	10557
213.6	2890	3080	2976	199.8	10258	10793	10561
213.8	2896	3085	2982	200.0	10264	10797	10565
214.0	2901	3091	2987	200.2	10269	10801	10570
214.2	2907	3096	2993	200.4	10274	10804	10574
214.4	2913	3101	2999	200.6	10280	10808	10579
214.6	2918	3107	3004	200.8	10285	10812	10584
214.8	2924	3112	3010	201.0	10291	10816	10588
215.0	2929	3117	3015	201.2	10297	10820	10593
215.2	2935	3123	3021	201.4	10302	10824	10597
215.4	2941	3128	3026	201.6	10308	10828	10602
215.6	2946	3133	3032	201.8	10314	10832	10607
215.8	2952	3138	3038	202.0	10319	10836	10612
216.0	2957	3144	3043	202.2	10325	10840	10616
216.2	2963	3149	3049	202.4	10331	10844	10621
216.4	2969	3155	3054	202.6	10337	10848	10626
216.6	2974	3160	3060	202.8	10343	10852	10631
216.8	2980	3166	3066	203.0	10350	10856	10636
217.0	2986	3171	3071	203.2	10356	10859	10641
217.2	2992	3177	3077	203.4	10362	10864	10646
217.4	2998	3182	3083	203.6	10369	10868	10651
217.6	3003	3188	3088	203.8	10375	10872	10656
217.8	3009	3193	3094	204.0	10382	10876	10661
218.0	3015	3199	3100	204.2	10389	10880	10666
218.2	3021	3204	3105	204.4	10395	10884	10671
218.4	3027	3210	3111	204.6	10402	10888	10676
218.6	3032	3215	3117	204.8	10409	10892	10681
218.8	3038	3221	3122	205.0	10415	10896	10686
219.0	3044	3226	3128	205.2	10422	10900	10692
219.2	3050	3232	3134	205.4	10429	10904	10697
219.4	3055	3237	3139	205.6	10437	10908	10702
219.6	3061	3242	3145	205.8	10444	10912	10708
219.8	3067	3248	3151	206.0	10452	10916	10713
220.0	3073	3253	3157	206.2	10459	10920	10719
220.2	3078	3258	3162	206.4	10467	10924	10724
220.4	3084	3264	3168	206.6	10475	10928	10730
220.6	3089	3269	3174	206.8	10483	10932	10735
220.8	3095	3275	3180	207.0	10490	10936	10741
221.0	3101	3280	3185	207.2	10498	10940	10746
221.2	3107	3286	3191	207.4	10506	10944	10752

221.4	3113	3292	3197	207.6	10515	10948	10758
221.6	3119	3297	3203	207.8	10523	10952	10764
221.8	3124	3303	3208	208.0	10531	10957	10769
222.1	3130	3308	3214	208.2	10539	10961	10775
222.3	3136	3314	3220	208.4	10548	10965	10781
222.5	3142	3319	3226	208.6	10556	10969	10787
222.7	3148	3325	3232	208.8	10565	10973	10793
222.9	3154	3330	3237	209.0	10573	10977	10799
223.1	3160	3336	3243	209.2	10582	10982	10805
223.3	3166	3341	3249	209.4	10591	10986	10811
223.5	3171	3347	3255	209.6	10600	10990	10817
223.7	3178	3352	3261	209.8	10609	10994	10824
223.9	3183	3358	3267	210.0	10618	10998	10830
224.1	3189	3363	3272	210.2	10627	11002	10836
224.3	3195	3369	3278	210.4	10636	11007	10843
224.5	3201	3374	3284	210.6	10646	11011	10849
224.7	3207	3380	3290	210.8	10655	11015	10855
224.9	3212	3386	3296	211.0	10665	11020	10862
225.1	3218	3391	3302	211.2	10675	11024	10868
225.3	3225	3397	3308	211.4	10685	11028	10875
225.5	3231	3403	3313	211.6	10694	11033	10882
225.7	3237	3408	3319	211.8	10704	11038	10888
225.9	3243	3413	3325	212.0	10714	11042	10895
226.1	3249	3419	3331	212.2	10724	11047	10902
226.3	3255	3425	3337	212.4	10734	11051	10909
226.5	3261	3430	3343	212.6	10744	11056	10915
226.7	3267	3436	3349	212.8	10753	11060	10922
226.9	3273	3441	3355	213.0	10762	11065	10929
227.1	3279	3447	3361	213.2	10771	11070	10936
227.3	3285	3453	3367	213.4	10780	11074	10944
227.5	3291	3458	3372	213.6	10788	11079	10951
227.8	3297	3464	3378	213.8	10797	11084	10958
228.0	3303	3469	3384	214.0	10807	11088	10965
228.2	3309	3475	3390	214.2	10817	11093	10972
228.4	3315	3480	3396	214.4	10827	11098	10980
228.6	3321	3486	3402	214.6	10837	11102	10987
228.8	3327	3491	3408	214.8	10848	11107	10995
229.0	3332	3497	3414	215.0	10857	11112	11002
229.2	3338	3503	3420	215.2	10866	11117	11010
229.4	3344	3509	3426	215.4	10876	11121	11017
229.6	3350	3514	3432	215.6	10885	11126	11025
229.8	3356	3520	3438	215.8	10894	11131	11033
230.0	3361	3526	3444	216.0	10903	11136	11040
230.2	3367	3531	3450	216.2	10912	11141	11048
230.4	3373	3537	3456	216.4	10921	11146	11056
230.6	3379	3543	3462	216.6	10930	11151	11064
230.8	3385	3548	3468	216.8	10937	11156	11072
231.0	3391	3554	3474	217.0	10945	11161	11080
231.2	3397	3560	3480	217.2	10953	11165	11088
231.4	3403	3566	3486	217.4	10962	11170	11096
231.6	3409	3571	3492	217.6	10971	11175	11104
231.8	3415	3577	3498	217.8	10979	11180	11112
232.0	3420	3583	3504	218.0	10987	11186	11120
232.2	3426	3588	3510	218.2	10995	11191	11128

232.4	3432	3594	3516	218.4	11004	11196	11136
232.6	3437	3600	3522	218.6	11012	11201	11144
232.8	3443	3606	3528	218.8	11020	11206	11152
233.0	3449	3611	3534	219.0	11028	11211	11160
233.2	3454	3617	3540	219.2	11036	11217	11168
233.4	3460	3623	3546	219.4	11042	11222	11177
233.6	3466	3629	3552	219.6	11051	11228	11185
233.8	3472	3634	3558	219.8	11060	11233	11193
234.0	3477	3640	3564	220.0	11068	11239	11201
234.2	3483	3646	3570	220.2	11076	11245	11209
234.4	3489	3652	3576	220.4	11082	11251	11217
234.6	3495	3657	3582	220.6	11089	11258	11225
234.8	3501	3663	3588	220.8	11097	11268	11234
235.0	3507	3669	3594	221.0	11105	11280	11242
235.2	3513	3675	3601	221.2	11112	11293	11250
235.4	3519	3680	3607	221.4	11119	11306	11258
235.6	3524	3686	3613	221.6	11127	11320	11266
235.8	3530	3692	3619	221.8	11133	11333	11274
236.0	3536	3698	3625	222.0	11139	11346	11283
236.2	3542	3703	3631	222.2	11147	11359	11291
236.4	3548	3709	3637	222.4	11154	11372	11299
236.6	3554	3715	3643	222.6	11162	11386	11307
236.8	3560	3721	3649	222.8	11169	11399	11315
237.0	3565	3727	3655	223.0	11177	11412	11323
237.2	3571	3732	3661	223.2	11185	11425	11332
237.4	3577	3738	3667	223.4	11191	11439	11340
237.6	3583	3744	3673	223.6	11196	11452	11348
237.8	3589	3750	3680	223.8	11200	11465	11356
238.0	3595	3756	3686	224.0	11205	11478	11364
238.2	3601	3761	3692	224.2	11210	11492	11372
238.4	3606	3767	3698	224.4	11215	11505	11381
238.6	3612	3773	3704	224.6	11220	11518	11389
238.8	3618	3779	3710	224.8	11226	11531	11397
239.0	3624	3785	3716	225.0	11233	11545	11405
239.2	3630	3790	3722	225.2	11239	11558	11413
239.4	3636	3796	3728	225.4	11245	11572	11421
239.6	3642	3802	3735	225.6	11249	11585	11430
239.8	3648	3808	3741	225.8	11253	11598	11438
240.0	3654	3814	3747	226.0	11257	11611	11446
240.2	3660	3819	3753				
240.4	3666	3825	3759				
240.6	3672	3831	3765				
240.8	3677	3837	3771				
241.0	3683	3843	3777				
241.2	3688	3848	3784				
241.4	3694	3854	3790				
241.6	3700	3860	3796				
241.8	3706	3866	3802				
242.0	3711	3872	3808				
242.2	3717	3878	3814				
242.4	3723	3883	3820				
242.6	3729	3889	3827				
242.8	3735	3895	3833				
243.0	3741	3901	3839				

243.2	3747	3907	3845
243.4	3753	3913	3851
243.6	3759	3919	3857
243.8	3765	3924	3863
244.0	3770	3930	3870
244.2	3776	3936	3876
244.4	3782	3942	3882
244.6	3788	3948	3888
244.8	3794	3953	3894
245.0	3800	3959	3900
245.2	3806	3965	3906
245.4	3812	3971	3913
245.6	3818	3977	3919
245.8	3824	3983	3925
246.0	3829	3989	3931
246.2	3836	3994	3937
246.4	3842	4000	3943
246.8	3848	4006	3950
247.0	3854	4012	3956
247.2	3859	4018	3962
247.4	3865	4024	3968
247.6	3871	4030	3974
247.8	3877	4035	3980
248.0	3883	4041	3986
248.2	3889	4047	3993
248.4	3895	4053	3999
248.6	3901	4060	4005
248.8	3907	4066	4011
252.4	3913	4072	4017
252.6	3918	4078	4023
252.8	3925	4085	4030
253.0	3931	4091	4036
253.2	3937	4097	4042
253.4	3942	4103	4048
253.6	3948	4110	4054
253.8	3954	4116	4060
254.0	3959	4123	4067
254.2	3965	4129	4073
254.4	3971	4136	4079
254.6	3977	4143	4085
254.8	3983	4149	4091
255.0	3988	4156	4097
255.2	3994	4163	4104
255.4	4000	4169	4110
255.6	4006	4176	4116
255.8	4012	4183	4122
256.0	4018	4190	4128
256.2	4023	4196	4134
256.4	4028	4203	4141
256.6	4034	4210	4147
256.8	4040	4217	4153
257.0	4046	4223	4159
257.2	4052	4230	4165
257.4	4057	4237	4171

257.6	4063	4244	4177
257.8	4068	4251	4184
258.0	4073	4257	4190
258.2	4079	4264	4196
258.4	4084	4271	4202
258.6	4089	4278	4208
258.8	4095	4285	4214
259.0	4100	4291	4221
259.2	4106	4298	4227
259.4	4111	4305	4233
259.6	4116	4312	4239
259.8	4121	4319	4245
260.0	4127	4326	4251

Note: The min and max 95% columns represent the upper and lower limits of the 95% confidence interval produced by Clam 2.1 (Blaauw, 2010). All ages are calender years BP (relative to 1950).

APPENDIX E: EMERALD LAKE TEPHRA CORRELATION

Emerald Lake Core 3			Emerald Lake Core 2			Bear Lake			Paradox Lake			Tustumena Lake		
Age (cal yr BP)[a]	Depth blf (cm)[b]	Thickness (cm)	Age (cal yr BP)[a]	Depth blf (cm)[b]	Thickness (cm)	Age (cal yr BP)	Depth blf (cm)[b]	Thickness (cm)	Age (cal yr BP)	Depth blf (cm)[b]	Thickness (cm)	Age (cal yr BP)	Depth blf (cm)[b]	Thickness (cm)
-31 ± 4	3.2	0.2												
159 ± 87	23.5	1.5				150 ± 50	19.2	0.2	100 (-30-200)	17.2	0.8			
623 ± 56	84.2	0.2				590 ± 70	56.1	0.2						
679 ± 53	104.0	17.0	1022 ± 55.5	29.0	10.0	760 ± 80	75.0	5.2	710 (490-930)	66.2	0.5	780 (690-880)	22.0	-
741 ± 51	107.2	0.2												
1085 ± 44	123.0	0.5										950 (850-1040)	26.4	0.1
1264 ±39	131.0	0.5				1270 ± 90	114.4	0.4						
1440 ± 35	139.0	0.5				1450 ± 90	128.5	0.2						
1761 ± 45	154.5	0.5	1639 ± 63.0	34.0	0.5									
2364 ± 94	187.5	2.5				2390 ± 110	195.9	0.4	2420 (2210-2620)	153.2	3.8			
2585 ± 104	198.0	0.5				2600 ± 100	210.4	0.6	2460 (2260-	155.2	0.2			

									2660)					
2637 ± 105	200.5	0.5				2630 ± 100	212.8	0.6				2740 (2590 - 2880)	103.8	0.2
2971 ±101	213.6	0.1				3030 ± 90	238.4	1.8	2880 (2660-3090)	177.2	0.2			
3364 ± 85	227.6	0.1	3376 ± 118.0	44.0	1.0	3480 ± 90	270.6	1.2						
3944 ± 81	246.7	0.2				3930 ± 90	297.9	0.1						
4012 ± 82	252.5[c]	3.5	3501 ± 120.5	46[c]	1.5	4030 ± 90	310.5[c]	8.0	3740 (3520-3960)	230.8[c]	0.7	4120 (3870 - 4370)	201[c]	1.6
			6960 ± 100.5	84.2	0.2	7040 ± 110	473.3	0.7	6930 (6660-7200)	454.8	0.5	6930 (6740 - 7120)	340.6	-
			7801 ± 81.5	111.5	0.5	7640 ± 140	515.7	0.8				7790 (7540 - 8050)	360.2	0.9
			8666 ± 102.5	136.0	1.0	8660 ± 180	562.0	0.6	8650 (8380-8920)	621.4	0.7	8890 (8500 - 9270)	383.0	0.6

a Age estimates based on Clam age model models

b Depth to base of layer

c Hayes tephra bed

REFERENCES

Ager, T. A., 2001, Holocene vegetation history of the northern Kenai Mountains, south-central Alaska. In Gough, L.P. and Wilson, F.H., editors, Geological studies in Alaska by the U.S. Geological Survey, 1999. USGS Professional Paper, 1633, 91-107.

Anderson, R. S., Hallet, D. J., Berg, E., Jass, R. B., Toney, J. L., de Fontaine, C. S., and DeVolder, A., 2006, Holocene development of boreal forests and fire regimes on the Kenai Lowlands of Alaska, The Holocene, v. 6, p. 791-803.

Appleby, P. G. & Oldfield, F., 1978, The calculation of Lead-210 dates assuming a constant rate of supply of unsupported ^{210}Pb to the sediment, Catena, v. 5, p. 1-8.

Bakke, J., Nesje, A., and Dahl, S. O., 2005a, Utilizing physical sediment variability in glacier-fed lakes for continuous glacier reconstructions during the Holocene, northern Folgefonna, western Norway, The Holocene, v. 15, p. 161-176.

Bakke, J., Dahl, S. O., Paasche, O., Lovlie, R., and Nesje, A., 2005b, Glacier fluctuations, equilibrium-line altitudes and paleoclimate in Lyngen, northern Norway, during the Late glacial and Holocene, The Holocene, v. 15, p. 518-540.

Bakke, J. S., Dahl, O., Paasche, O., Simonsen, J. R., Kvisvik, B., Bakke, K., and Nesje, A., 2010, A complete record of Holocene glacier variability at Austre Okstindbreen, northern Norway: an integrated approach, Quaternary Science Review, v. 29, p. 1246-1262.

Barclay, D., Wiles, G., and Calkin, P., 2003, An 850 year record of climate and fluctuations of the iceberg-calving Nellie Juan Glacier, south central Alaska, U.S.A., Annals of Glaciology, v. 36, p. 51-56.

Barclay, D., Wiles, G., and Calkin, P., 2009a, Tree-ring crossdates for a First Millennium AD advance of Tebenkof Glacier, southern Alaska, Quaternary Research, v. 71, p. 22-26.

Barclay, D., Wiles, G., and Calkin, P., 2009b, Holocene glacier fluctuations in Alaska, Quaternary Science Reviews, v. 28, p. 2034-2048.

Beget, J. E., 1981, Early Holocene glacier advance in the North Cascade Range, Washington, Geology, v. 9, p. 409-413.

Beget, J. E., Stihler, S. D., Stone, D. B., 1994, A 500-year-long record of tephra falls from Redoubt Volcano and other volcanoes in upper Cook Inlet, Alaska, Journal of Volcanology and Geothermal Research, v. 62, p. 55-67.

Binford, M. W., 1990, Calculation and uncertainty analysis of 210Pb dates for PIRLA project lake sediment cores, Journal of Paleolimnology, v. 3, p. 253-267.

Bitz, C. M. and Battisti, D. S., 1999, Interannual to decadal variability in climate and the glacier mass balance in Washington, Western Canada, and Alaska, American Meteorological Society, v. 12, p. 3181-3196.

Blaauw, M., 2010, Methods and code for 'classical' age-modeling of radiocarbon sequences, Quaternary Geochronology, v. 5, p. 512-518.

Bradley D. C. and Kusky, T. M., 1990, Deformation history of the McHugh Complex, Seldovia Quadrangle, South-Central Alaska, Geologic Studies in Alaska by the U.S. Geological Survey, p. 17-32.

Briner, J. P. and Kaufman, D. S., 2008, Late Pleistocene mountain glaciation in Alaska: key chronologies, Journal of Quaternary Science, v. 23, p. 659- 670.

Briner, J. P., Stewart, H., Young, N., Philipps, W., and Losee, S., 2010, Using proglacial-threshold lakes to constrain fluctuations of Jokobshavn Isbrae ice margin, western Greenland, during the Holocene, Quaternary Science Reviews, v. 29, p. 3861-3874.

Calkin, P.E., 1988, Holocene glaciation of Alaska (and adjoining Yukon Territory, Canada), Quaternary Science Reviews, v. 8, p. 159-184.

Calkin, P. E., and Ellis, J. M., 1980, A lichenometric dating curve and its application to Holocene glacier studies in the central Brooks Range, Alaska. Arctic and Alpine Research, v. 12, p. 245-264.

Calkin, P. E., Wiles, G. C., and Barclay, D. J., 2001, Holocene coastal glaciation of Alaska, Quaternary Science Reviews, v. 20, p. 449-461.

Cashman, K. V., Sturtevant, B., Papale, P. and Navon, O., 2000, Magma Fragmentation. In Sigurdsson, H., (ed.) Encyclopedia of Volcanoes. Academic Press, 421-430 p.

Clegg, B. F., Kelly, R., Clarke, G. H., Walker, I. R. and Hu, F. S., 2011, Nonlinear response of summer temperature to Holocene isolation forcing in Alaska, Proceedings of the National Academy of Sciences of the United States of America, v. 108, p 19299-19304.

Cohen, A. S., 2003, Paleolimnology: The History and Evolution of Lake Systems: New York, Oxford University Press, 499 p.

Collinson, D. W., 1986. Methods in Rock Magnetism. London: Allen & unwin (publishers), v. 551.

Dahl, S. O., Bakke, J., Lie, Ø., and Nesje, A., 2003, Reconstruction of former glacier equilibrium-line altitudes based on proglacial sites: an evaluation of approaches and selection of sites, Quaternary Science Reviews, v. 22, p. 275-287.

Daigle, T., and Kaufman, D., 2009, Holocene climate inferred from glacier extent, lake sediment and tree rings at Goat Lake, Kenai Mountains, Alaska, USA, Journal of Quaternary Science, v. 24, p. 33-45.

Dall, W. H., 1896, 17th Annual report: Journal of the American Geography Society, v. 28, p. 1-20.

D'Arrigo, R. and Jacoby, G., 1999, Northern North American tree-ring evidence for regional temperature changes after major volcanic events, Climatic Change, v. 41, p. 1–15.

Davi, N. K., Jacoby, G. C., and Wiles, G. C., 2003, Boreal temperature variability inferred from maximum latewood density and tree-ring with data, Wrangell Mountain region, Alaska, Quaternary Research, v. 60, p. 252-262.

Davis, P. T., Menounos, B., and Osborn, G., 2009, Holocene and latest Pleistocene alpine glacier fluctuations: a global perspective, Quaternary Science Reviews, v. 28, p. 2021-2033.

de Fontaine, C. S., Kaufman, D. S., Anderson, R. S., Werner, A., Waythomas, C. F., and Brown, T. A, 2007, Late Quaternary distal tephra-fall deposits in lacustrine sediments, Kenai Peninsula, Alaska, Quaternary Research, v. 68, p. 64-78.

Doran, P. T., Berger, G. W., Lyons, W. B., Wharton, R. A., Davisson, M. L., Southon, J., and Dibb, J. E., 1999, Dating Quaternary lacustrine sediments in the McMurdo Dry Valleys, Antarctica, Paleogeography Paleoclimatology Paleoecology, v. 147, p. 223-239.

Evison, L. H., Calkin, L. H., and Ellis, J. M., 1996, Late-Holocene glaciation and twentieth-century retreat, northeastern Brooks Range, Alaska, Holocene, v. 6, p. 17- 24.

Finney, B. P., Bigelow, N. H., Barber, V. A., and Edwards, M. E., 2012, Holocene climate change and carbon cycling in a groundwater-fed, boreal forest lake: Dune Lake, Alaska, Paleolimnology, v. 48, p. 43-54.

Gilbert, G. K., 1903. Glaciers and glaciation, Harriman Alaska Expedition. Vol. III. New York, Doubleday and Page Company, pp. 231.

Hall, D., Giffin, B., and Chien, J., 2005, Changes in the Harding Icefield and the Grewingk-Yalik Glacier Complex, 62nd Eastern Snow Conference, Waterloo, ON, Canada, p. 29-30.

Heine, J. T., 1998, Extent, timing and climatic implications of glacier advances Mount Rainier, Washington, U.S.A., at the Pleistocene/ Holocene Transition, Quaternary Science Reviews, v. 17, p. 1139-1148.

Heiri, O., Lotter, A. F., and Lemcke, G., 2001, Loss on ignition as a method for estimating organic and carbonate content in sediments; reproducibility and comparability of results, Journal of Paleolimnology, v. 25, p. 101-110.

Hildreth, W. and Fierstein, J., 2012, The Novarupta-Katmai eruption of 1912 largest eruption of the twentieth century; centennial perspectives, U.S. Geological Survey Professional Paper 1791, 259 p. (Available at http://pubs.usgs.gov/pp/1791/.)

Hu, F. S., Nelson, D. M., Clarke, G. H., Ruhland, K. M., Huang, Y., Kaufman, D. S., and Smol, J. P., 2006, Abrupt climatic events during the last glacial-interglacial transition in Alaska, Geophysical Research Letters, v. 33, p. 1-5.

Jones, M. C., Peteet, D. M., Kurdyla, D., and Guilderson, T., 2009, Climate and vegetation history from a 14,000-year peatland record, Kenai Peninsula, Alaska, Quaternary Research, v. 72, p. 207-217.

Jones, M. C., Peteet, D. M., and Sambrotto, R., 2010, Late-glacial and Holocene $\delta^{15}N$ and $\delta^{13}C$ variations from a Kenai Peninsula, Alaska peatland, Palaeogeography, Palaeoclimatology, Palaeoecology, v. 293, p. 132-143.

Jones, M. C., Wooller, M., and Peteet, D. M., 2014, A deglacial and Holocene record of climate variability in south-central Alaska from stable oxygen isotopes and plant macrofossils in peat, Quaternary Science Revews, v. 87, p. 1-11.

Karlen, W., 1981, Lacustrine sediment studies, A technique to obtain a continuous record of Holocene glacier variation, Geografiska Annaler, v. 63, p. 273-281.

Karlstrom, T. N., 1964, Quaternary geology of the Kenai lowland and glacial history of the Cook Inlet region, Alaska, Geological Survey professional paper, United States Government printing office, Washington, p. 1-69.

Kaufman, D. S., Anderson, R. S., Hu, F. S., Berg, E., and Werner, A., 2010, Evidence for a variable and wet Younger Dryas in southern Alaska, Quaternary Science Reviews, v. 29, p. 1445-1452.

Kaufman, D. S., Axford, Y., Anderson, R. S., Lamoureux, S. F., Schindler, D. E., Walker, I. R., and Werner, A., 2012, A multi-proxy record of the Last Glacial Maximum and last 14,500 years of paleoenvironmental change at Lone Spruce Pond, southwestern Alaska, Journal of Paleolimnology, v. 48, p. 9-26.

Krinsley, Daniel B., “Southwest Kenai Peninsula, Alaska.” Pewe , T.L. and others, Multiple glaciation in Alaska: US Geological Survey Circulation 289. (1953): 5-6.

Leonard, E. M., 1985, Glaciological and climatic controls on lake sedimentation, Canadian Rocky Mountains, Zeitschrift fur Gletscherkunde und Glazialgeologie, v. 21, p. 35–42.

Leonard, E. M., 1997, The relationship between glacial activity and sediment production: evidence from a 4450-year varve record of neoglacial sedimentation in Hector Lake, Alberta, Canada, Journal of Paleolimnology, v. 17, p. 319-330.

Levy, L. B., Kaufman, D. S., and Werner, A., 2004, Holocene glacier fluctuations, Waskey Lake, northeastern Ahklun Mountains, southwestern Alaska, The Holocene, v. 14, p. 185–193.

Lowe, D., 2011, Tephrochronology and its application: a review, Quaternary Geochronology, v. 6, p. 107-153.

MacDonald, G. M. and Case, R. A., 2005, Variations in the Pacific Decadal Oscillation over the past millennium, Geophysical Research Letters, v. 32, p. 1-4.

Malcomb, N. L. and Wiles, G. C., 2013, Tree-ring-based reconstructions of North American glacier mass balance through the Little Ice Age- Contemporary warming transition, Quaternary Research, v. 79, p. 123-137.

Mantua, N. J., Hare, S. R., Zhang, Y., Wallace, J. M., and Francis, R. C., 1997, A Pacific interdecadal climate oscillation with impacts on salmon production, Bulletin of the American Meteorological Society, v. 78, p. 1069- 1079.

Maurer, M., Menounos, B., Luckman, B., Osborn, G., Clague, J., Beedle, M., Smith, R., and Atkinson, N., 2012, Late Holocene glacier expansion in the Cariboo and northern Rocky Mountains, British Columbia, Canada, Quaternary Science Reviews, v. 51, p. 71-80.

McKay, N. and Kaufman, D., 2009, Holocene climate and glacier variability at Hallet and Greyling Lakes, Chugach Mountains, south-central Alaska, Journal of Paleolimnology, v. 41, p. 143-159.

Meyers, P. A. and Lallier-Verges, E., 1999, Lacustrine sedimentary organic matter records of Late Quaternary paleoclimates, Journal of Paleolimnology, v. 21, p. 345-372.

Meyers, P., 2003, Applications of Organic Geochemistry to Paleolimnological Reconstructions: A Summary of Examples from the Laurentian Great Lakes, Organic Geochemistry, v. 34, p. 261-289.

Moberg, A., Sonechkin, D. M., Holmgren, K., Datsenko, N. M., and Karlen, W., 2005, Highly variable Northern Hemisphere temperatures reconstructed from low- and high-resolution proxy data, v. 3265, p. 1-5.

Nesje, A., Kvamme, M., Rye, N., and Løvlie, R., 1991, Holocene glacial and climate history of the Jostedalsbreen region, western Norway; evidence from lake sediments and terrestrial deposits, Quaternary Science Reviews, v. 10, p. 87-114.

Nesje, A., Matthews, J. A., Dahl, S. O., Berrisford, M. S., and Andersson, C., 2001, Holocene glacier fluctuations of Flatebreen and winter-precipitation changes in the Jostedalsbreen region, western Norvay, based on glaciolacustrine sediment records, The Holocene, v. 11, p. 267-280.

Osborn, G., Menounos, B., Koch, J., Clague, J. J., and Vallis, V., 2007, Multi-proxy record of Holocene glacial history of the Spearhead and Fitzsimmons ranges, southern Coast Mountains, British Columbia, Quaternary Science Review, v. 26, p. 479–493.

Osborn, G., Menounos, B., Ryane, C., Riedel, J., Clague, J., Koch, J., Clark, D., Scott, K., and Davis, P.T., 2012, Late Pleistocene and Holocene glacier fluctuations on Mount Baker, Washington, Quaternary Science Reviews, v. 49, p. 33-51.

Owen, L., Thackray, G., Anderson, R., Briner, J., Kaufman, D., Roe, G., Pfeffer, W., and Yi, C., 2009, Integrated research on mountain glaciers: Current status, priorities and future prospects, Geomorphology, v. 103, p. 158-171.

Reger, R. D., Sturmann, A. G., Berg, E. E., and Burns, P. A. C., 2008, A guide to the late Quaternary history of northern and western Kenai Peninsula, Alaska, State of Alaska Department of Natural Resources Division of geological & geophysical surveys, 112 p.

Rein, B. and Sirocko, F., 2002, In-situ reflectance spectroscopy-analysing techniques for high-resolution pigment logging in sediment cores, International Journal of Earth Sciences, v. 91, p. 950-954.

Riehle, J. R., Bowers, P. M., and Ager, T. A., 1990, The Hayes Tephra deposits, an Upper Holocene Marker Horizon in South-Central Alaska, Quaternary Research, v. 33, p. 276-290.

Rodionov, S. N., Bond, N. A., and Overland, J. E., 2007, The Aleutian Low, storm tracks, and winter climate variability in the Bering Sea, Deep-Sea Research Part II, Tropical Studies in Oceanography, v. 54, p. 2560-1577.

Schiff, C. J., Kaufman, D. S., Wallace, K. L., and Ketterer, M. E., 2010, An improved proximal tephrochronology for Redoubt Volcano, Alaska, Journal of Volcanology and Geothermal Research, v. 193, p. 203-214.

Schiff, C. J., Kaufman, D. S., Wallace, K. L., Werner, A., Ku, T., and Brown, T. A., 2008, Modeled tephra ages from lake sediments, base of Redoubt Volcano, Alaska, Quaternary Geochronology, v. 3, p. 56-67.

Schnurrenberger, D., James, R., and Kelts, K., 2003, Classification of lacustrine sediments based on sedimentary components, Journal of Paleolimnology, v. 29, p. 141-154.

Solomina, O., and Calkin, P. E., 2003, Lichenometry as applied to moraines in Alaska, U.S.A., and Kamchatka, Russia. Arctic, Antarctic, and Alpine Research, v. 35, p. 129-143.

Stuiver, M., and Reimer, P. J., 1993, Extended 14C database and revised CALIB radiocarbon calibration program, Radiocarbon, v. 35, p. 215-230.

Thompson, R., Battarbee, R. W., O`Sullivan, P. E., and Oldfield, F., 1975, Magnetic susceptibility of lake sediments, Limnology and Oceanography, v. 30, p. 687-698.

Trenberth, K.E. and Hurrell, J.W., 1994, Decadal atmospheric-ocean variations in the Pacific, Climate Dynamics, v. 9, p. 303–319.

Vaillencourt, D. A., 2013, Five-Thousand Years of Hydroclimate Variability on Adak Island, Alaska Inferred from δD of *n*-Alkanoic Acids, M.S. Thesis, Northern Arizona University, p. 92.

Viau, A. E., Gajewski, K., Sawada, M. C., and Bunbury, J., 2008, Low- and high-frequency climate variability in eastern Beringia during the past 25,000 years, Canadian Journal of Earth Sciences, v. 45, p. 1435-1453.

von Gunten, L., Grosjean, M., Kamenik, C., Fujak, M., and Urrutia, R., 2012, Calibrating biogeochemical and physical climate proxies from non-varved lake sediments with meteorological data: methods and case studies, Journal of Paleolimnology, v. 47, p. 583-600.

Waitt R. B. and Beget, J. E., 2009, Volcanic processes and geology of Augustine volcano, Alaska. U.S. Geological Survey Professional Paper, 1762: p 1-78.

Western Regional Climate Center, 2014, Seward and Homer meteorological stations (online). Alaska climate summaries section. Available from http://www.wrcc.dri.edu/summary/Climsmak.html (accessed 29 January 2014).

Wiles, G. C., Barclay, D. J., Calkin, P. E., and Lowell, T. V., 2008, Century to millennial-scale temperature variations for the last two thousand years indicated from glacial geologic records of Southern Alaska, Global and Planetary Change, v. 60, p. 115-125.

Wiles, G. C., Barclay, D. J., and Young, N. E., 2010, A review of lichenometric dating of glacial moraines in Alaska, Geografiska Annaler: Series A, Physical Geography, v. 92, p. 101-109.

Wiles, G. and Calkin, P., 1994, Late Holocene high-resolution glacial chronologies and climate, Kenai Mountains Alaska, Geological Society of America Bulletin, v. 106, p. 281-303.

Wiles, G. C., D`Arrigo, R. D., Barclay, D., Wilson, R. S., Jarvis, S. K., Vargo, L., and Frank, D., 2014, Surface air temperature variability reconstructed with tree rings for the Gulf of Alaska over the past 1200 years, The Holocene, v. 24, p. 198-208.

Wiles, G. C., D`Arrigo, R. D., and Jacoby, G. C., 1998, Gulf of Alaska atmosphere-ocean varability over recent centuries inferred from coastal tree-ring records, Climatic change, v. 38, p. 289-306.

Wiles, G. C., D`Arrigo, R. D., Villalba, R., Calkin, P. E., and Barclay, D. J., 2004, Century-scale solar variability and Alaskan temperature change over the past millennium, Geophysical Research Letters, v. 31, p. 1-4.

Wolfe, A. P., Vinebrooke, R. D., Michelutti, N., Rivard, B., and Das, B., 2006, Experimental Calibration of Lake-Sediment Spectral Reflectance to Chlorophyll a Concentrations: Methodology and Paleolimnological Validation, Journal of Paleolimnology, v. 36, p. 91- 100.

Yu, Z., Walker, K. N., Evenson, E. B., and Hajdas, I., 2008, Lateglacial and early Holocene climate oscillations in Matanuska Valley, south-central Alaska, Quaternary Science Reviews, v. 27, p. 148-161.

TABLES

TABLE 1. CORE LOCATION, LENGTH, AND WATER DEPTH, EMERALD LAKE

Core site	Length (cm)	Location		Water depth (m)
		Lon (°W)	Lat (°N)	
1A	252	-151.07419	59.62960	17.3
1B	64	-151.07419	59.62960	17.3
1C	81	-151.07419	59.62960	17.3
2A	304	-151.07399	59.62970	18.3
2B	46	-151.07399	59.62970	18.3
2C	68	-151.07399	59.62970	18.3
3A	260	-151.06469	59.62640	52.0
3B	55	-151.06469	59.62640	52.0
3C	79	-151.06469	59.62640	52.0

A and B cores are percussion cores and C cores are surface cores

TABLE 2: UNIT DESCRIPTIONS

	Dominant colors	Bedding	Sediment type
Core 3			
Unit 3-1	very dark grayish brown (2.5Y 3/2) to dark reddish brown (5YR 3/2)	massive	silty organic-rich mud
3-2	grayish brown (2.5Y 5/2)	laminated	clayey inorganic mud
3-3	very dark grayish brown (2.5Y 3/2) to dark reddish brown (5YR 3/2)	massive	silty organic-rich mud
Core 2			
Unit 2-1	gray (7.5YR 5/0)	weakly laminated	clayey inorganic mud with angular siltstone and lithic granules with rare pebbles <5 cm
2-2	dark brown (7.5YR 3/2) to very dark gray (7.5YR 3/0)	massive	silty organic-rich mud
2-3	gray (7.5YR 5/0)	weakly laminated	clayey inorganic mud with angular siltstone and lithic granules with rare pebbles <5 cm
2-4	very dark grayish brown (2.5Y 3/2)	massive	sandy organic-rich mud with 5-10 cm beds of black organic-rich detritus
2-5	grayish brown (2.5Y 5/2) to dark grayish brown (2.5Y 4/2)	laminated	clayey inorganic mud
2-6	very dark grayish brown (2.5Y 3/2)	massive	sandy organic-rich mud

TABLE 3: EMERALD LAKE TEPHRA DESCRIPTIONS

Age (cal yr BP)[a]	Depth blf (cm)[b]	Thickness (cm)	Description (visual)	Bulk grain size[c]	Crystal percentage	Mineralogy
Emerald Lake Core 3						
-31 ± 4	3.2	0.2	light brownish gray (2.5Y 6/2), diffuse upper and lower contacts, with fine (<0.03 mm) light brown ash with 0.33 mm crystals and rare angular frothy brown pumice	fine	40%	quartz and hornblende
159 ± 87	23.5	1.5	very dark grayish brown (2.5Y 3/2), diffuse upper and lower contacts, with fine (<0.03 mm) brown ash with 0.23 mm crystals and rare angular frothy brown pumice	medium	3%	quartz, feldspar, and hornblende
626 ± 55	84.3	0.2	light brownish gray (2.5Y 6/2), diffuse and wavy upper and lower contacts with fine (<0.03 mm) light brown ash	fine	0%	
679 ± 53	104.0	17.0	light gray (2.5Y 7/2) to dark grayish brown (2.5Y 4/2), fining upward, diffuse upper and lower contact with fine (<0.03 mm) brown ash with rare 0.03 mm crystals	fine	1%	quartz
733 ± 52	107.2	0.6	light gray (2.5Y 7/2), sharp upper and lower contacts with fine (<0.03 mm) white ash with few 0.05 mm crystals	medium	1%	quartz

1082 ± 43	122.9	0.4	light gray (2.5Y 7/2), sharp upper and lower contacts, fine (0.03 mm) white ash with 0.23 mm crystals and glass shards	medium	7%	quartz and magnetite
1269 ± 40	131.1	0.5	dark grayish brown (2.5Y 4/2), sharp upper and lower contacts, very fine (<0.03 mm) light brown ash	fine	0%	
1440 ± 35	139.0	0.7	dark grayish brown (2.5Y 4/2), sharp upper and lower contacts, very fine (<0.03 mm) light brown ash	fine	0%	
1780 ± 45	154.6	0.4	light brownish gray (2.5Y 6/2), diffuse upper and lower contacts, fine (0.03 mm) brown ash with 3.00 mm angular black chert clasts (local bedrock) and 0.30 mm crystals	medium	2%	feldspar
2430 ± 91	187.5	2.5	black (2.5Y 2/0) medium grained with diffuse upper and lower contacts, abundant organics, fine (0.03 mm) brown ash, 0.20 mm crystals, bubble wall shards and rare light brown, angular pumice	medium	5%	crystals, quartz, and hornblende
2453 ± 92	192.3	3.8	dark grayish brown (2.5Y 4/2) with diffuse upper and lower contacts with fine (<0.03 mm) light brown ash with few 0.18 mm crystals, and white angular frothy pumice	medium	5%	crystals, quartz, feldspar, and hornblende
2590 ± 104	198.2	0.4	light gray (2.5Y 7/2), diffuse upper and lower contacts, with fine (<0.03 mm) white ash with 0.30 mm crystals, light gray angular pumice clasts, rare bubble wall shards	coarse	30%	quartz, hornblende, feldspar, and magnetite

2635 ± 98	200.5	0.3	grayish brown (2.5Y 5/2) crystal-fall deposit, diffuse upper and lower contacts with abundant 0.25 mm crystals and fine (<0.03 mm) white ash	very coarse	95%	quartz, magnetite, and feldspar
2976 ± 95	213.6	0.1	light gray (2.5Y 7/2), diffuse upper and lower contacts, fine (0.03 mm) brown ash with rare 0.10 mm crystals	fine	2%	hornblende and quartz
3214 ± 89	222.1	0.1	grayish brown (2.5Y 5.2), diffuse upper and lower contacts, fine (0.03 mm) brown ash with 0.30 crystals	medium	30%	quartz, hornblende, feldspar, magnetite, and biotite
3372 ± 84	227.6	0.1	light brownish gray (2.5Y 6/2), diffuse upper and lower contacts, fine (<0.03 mm) brown ash with few 0.18 mm crystals	fine	2%	quartz
3950 ± 79	246.7	0.2	light gray (2.5Y 7/2), diffuse upper and lower contacts, fine (0.03 mm) light brown ash with few 0.10 mm crystals	medium	15%	quartz, feldspar, and hornblende
4017 ± 80	252.4	3.4	grayish brown (2.5Y 5/2) between layers of white (2.5Y 8/2) with sharp upper and lower contacts. Grades from fine (0.03 mm) white ash with with 0.08 mm biotite to fine (<0.03 mm) light brown ash with 0.10 mm quartz crystals, to fine (<0.03 mm) white ash with no crystals	fine	1%	biotite and quartz

Emerald Lake Core 2						
1079 ± 61	29.0	10.0	dark grayish brown (2.5Y 4/2) to very dark grayish brown (2.5Y 3/2) very thin bedded with diffuse upper and lower contacts, fine (0.03 mm) light gray ash with 0.08 crystals and light brown angular frothy pumice	fine	20%	quartz and magnetite
1724 ± 75	34.1	0.4	grayish brown (2.5Y 5/2) with diffuse upper and lower contacts, fine (0.03 mm) white ash with 0.28 mm crystals and rare bubble wall shards	medium	10%	quartz and hornblende
3426 ± 133	43.9	0.6	light brownish gray (2.5Y 6/2) with diffuse upper and lower contacts, fine (0.03 mm) ash with rare 0.08 mm crystals and bubble wall shards	medium	2%	biotite, hornblende, and quartz
3629 ± 140	46.0	1.3	light brownish gray (2.5Y 6/2), laminated with diffuse upper and lower contacts, fine (<0.03 mm) white ash with 0.08 mm crystals and bubble wall shards	medium	15%	biotite, quartz, and feldspar
4874 ± 175	52.7	0.3	light brownish gray (2.5Y 6/2) with diffuse upper and lower contacts, fine (0.03 mm) white ash with 0.10 mm crystals, rare elongated frothy pumice and bubble wall shards	fine	1%	quartz and magnetite

6539 ± 90	74.9	0.3	light brownish gray (2.5Y 6/2) with diffuse upper and lower contacts with fine (0.03 mm) white ash with rare 0.08 mm crystals and abundant tubular diatoms	medium	1%	hornblende
6962 ± 102	84.2	0.2	dark grayish brown (2.5Y 4/2) with diffuse upper and lower contacts, fine (<0.03 mm) white ash with 0.15 mm crystals and abundant diatoms	medium	2%	quartz and hornblende
7807 ± 81	111.5	0.6	crystal-fall deposit of with light brownish gray (2.5Y 6/2) with diffuse upper and lower contacts, fine (<0.03 mm) white ash with abundant 0.28 mm crystals, and rare angular frothy pumice and bubble wall shards	coarse	70%	hornblende and quartz
8687 ± 106	136.0	0.7	light brownish gray (2.5Y 6/2) with diffuse upper and lower contacts, fine (<0.03 mm) white ash with 0.20 mm crystals and bubble wall shards	fine	7%	quartz, hornblende, and magnetite

a Age estimates based on Clam age model models

b Depth to base of layer

c Sieve sizes are fine (<0.1 mm), medium (0.1 to 0.15 mm), coarse (0.15 to 0.25 mm), and very coarse (>0.25 mm)

TABLE 4. CORRELATION BETWEEN TEPHRAS IN EMERALD LAKE WITH GOAT LAKE AND HISTORICAL ERUPTIONS

Emerald Lake Core 3			Emerald Lake Core 2			Goat Lake			Goat Lake (CLAM)		AVO[d]	
Age (cal yr BP)[a]	Depth blf (cm)[b]	Thickness (cm)	Age (cal yr BP)[a]	Depth blf (cm)[b]	Thickness (cm)	Age (cal yr BP)	Depth blf (cm)[b]	Thickness[c] (cm)	Age (cal yr BP)	Depth blf (cm)[b]	Age (cal yr BP)	Volcano
-31 ± 4	3.2	0.2									-26	Augustine
											-36	Augustine
159 ± 87	23.5	1.5									138	Augustine
679 ± 53	104.0	17.0	1079 ± 61	29.0	10.0	715	56.0	10.0	537	56.0		
1780 ± 45	154.6	0.4	1724 ± 75	34.1	0.4	1663	95.2	0.1	1600	95.2		
2453 ± 92	192.3	3.8	3426 ± 133	43.9	0.6				2246	109.5		
4017 ± 80	252.4[e]	3.4	3629 ± 140	46[e]	1.3	3758	165.5[e]	0.2	3803[e]	165.5		
			4874 ± 175	52.7	0.3	4794	195.0	0.1	4614	195.0		
			6539 ± 90	74.9	0.3	6523	240.5	0.1	6474	240.5		
			6962 ± 102	84.2	0.2	7156	256.5	0.1	6951	256.5		
			7807 ± 81	111.5	0.6	7746	270.0	0.1	7768	270.0		
			8687 ± 106	136.0	0.7	8626	290.5	0.2				

a Age estimates based on Clam age model models
b Depth to base of layer
c Approximate maximum thickness estimated from Goat Lake magenetic susceptibility data
d Alaska Volcano Observatory, Alaska Volcano Observatory (2013)
e Hayes tephra bed

TABLE 5: LICHENOMETRIC AGES FROM THE LATERAL MORAINE ON THE TOPOGRAPHIC DIVIDE

Site	Number measured	Max long axis (cm)	Mean long (cm)	Stdev long	Mean short (cm)	Stdev short	Approximate age AD[a]	Location	
								Lon (°W)	Lat (°N)
1	17	52	40	5.2	35	4.9	1895	-151.057778	59.609722
2	9	42	36	3.3	33	2.1	1915	-151.057778	59.609720

a Ages based on a growth curve of $t = 43.950 \times 10^{(0.0081712 \times D)}$ from Solomina & Calkin (2003)

TABLE 6. ^{210}Pb AGES FROM EMERALD LAKE CORE 3C

Sample (EMD-3C)	Sample depth blf (cm)[a]	Total activity (DPM/g)[bc]	Age AD	Error	Dry bulk density (g/cm^3)
^{210}Pb					
12	0.5	47.50 ± 1.00	2000	1	0.312
14	2.5	22.40 ± 0.65	1984	1	0.351
17	5.5	8.95 ± 0.43	1968	4	0.473
20	8.5	10.89 ± 0.46	1904	18	0.449
24	12.5	1.64 ± 0.19	1872	39	0.516
^{226}Ra					
14	2.5	0.94 ± 0.10			0.351
34	22.5	0.89 ± 0.04			0.637

a Depth from midpoint of sample. Note: Analysis performed at Flett Research Lab

b ^{210}Po is the granddaughter isotope emitted by alpha decay of ^{210}Pb

c Disintegrations per minute per gram

TABLE 7. ^{14}C AGES, EMERALD LAKE

Laboratory ID (UCIAMS)[a]	Sample name	Depth blf (cm)[b]	Sample thickness (cm)	^{14}C age (yr BP)	±	Calibrated age (yr BP)[c]	± 1/2 of 1σ range	Material[d]
121211	3C 33	21.5	1.0	180	20	183	141	Leaves, stems, wood
121212	3A-1 76	72.5	1.0	320	15	387	57	Leaves, wood
128094	3A-1 82	82.0	2.0	590	110	592	65.5	Moss, insect, wood, leaf
121213	3A-1 147.5	144.0	1.0	1665	15	1559	28	Wood, stems
121215	3A-2 52.5	200	1.0	2515	15	2586	88	Large twig
121214	3A-2 105	252.5	1.0	3685	20	4037	50	Stems
131741	2C 40	32	1.0	1455	25	1342	24	Wood, leaves
128093	2A-1 55	56	1.0	4785	15	5511	50	Wood, leaves
128090	2A-1 85	86	1.0	6145	20	7062	88	Wood, leaves
128091	2A-1 120	121	1.0	7255	20	8083	70	Wood, twigs, leaves
128092	2A-1 150.5[e]	151.5	1.0	7160	35	7980	24	Leaves, wood, insect
128089	2A-2 11	164	2.0	8815	20	9841	65	Wood
128088	2A-2 61.5	214.5	1.0	9525	20	10850	166	Wood, insect
131740	2A-2 69.25	220	1.5	9835	30	11236	15	Wood and needle

a UCIAMS= Analysis performed at the University of California, Irvine by the W.M. Keck Carbon Cycle Accelerator Mass Spectromerty Laboratory

b Depth from midpoint of sample

c Median probablity. Note: calibrated using CALIB 7.0 (Stuiver and Reimer, 1993)

d Identification by R.S. Anderson (Northern Arizona University)

e Not used in age model

TABLE 8: EVENT CORRELATION WITH GOAT LAKE

Event	Emerald Lake	Goat Lake
LIA - lichen ages (AD)	1900	1900
LIA - end meltwater input (AD)	1770	~ 1900
LIA - minor retreat (AD)	1450- 1510	1660
LIA - start meltwater input (AD)	1350	just before 1660
Final deglacial (ka)	9.8	9.5
Readvance (ka)	10.7-9.8	NR
Initial deglacial (ka)	11.4	NR

NR = not represented in cores from Goat Lake

FIGURES

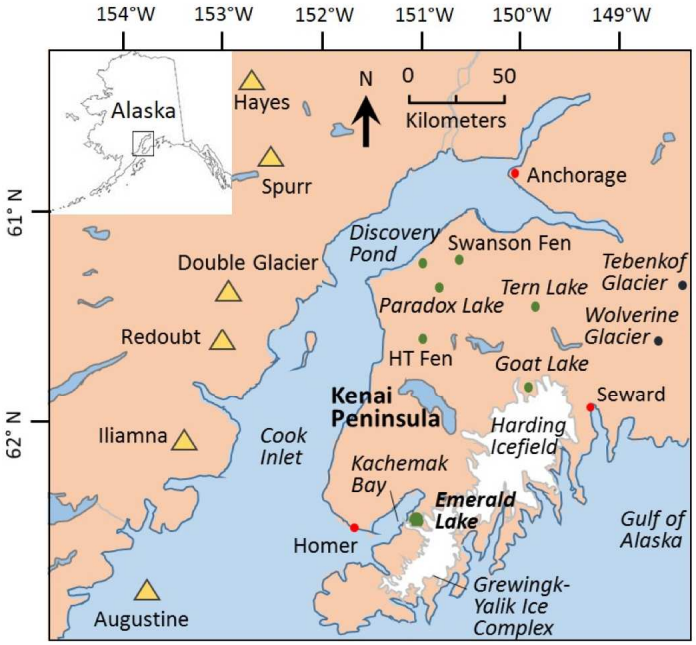

Figure 1: Cook Inlet with Emerald Lake and other locations discussed in text. Cook Inlet volcanoes are marked by yellow triangles, major cities with red circles, glaciers with blue circles, and lakes/fens with green circles.

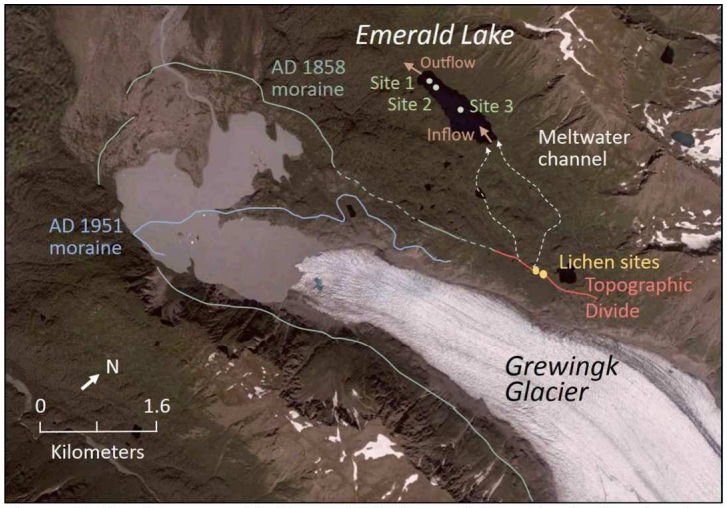

Figure 2: Study area with Emerald Lake and Grewingk Glacier showing current (2012) glacier position from aerial imagery and end moraines from Wiles & Calkin (1994). Grewingk Glacier is presently below the topographic divide of Emerald Lake and the meltwater does not flow into Emerald Lake. Lateral moraine age is estimated as AD 1900 in this study using lichenometry.

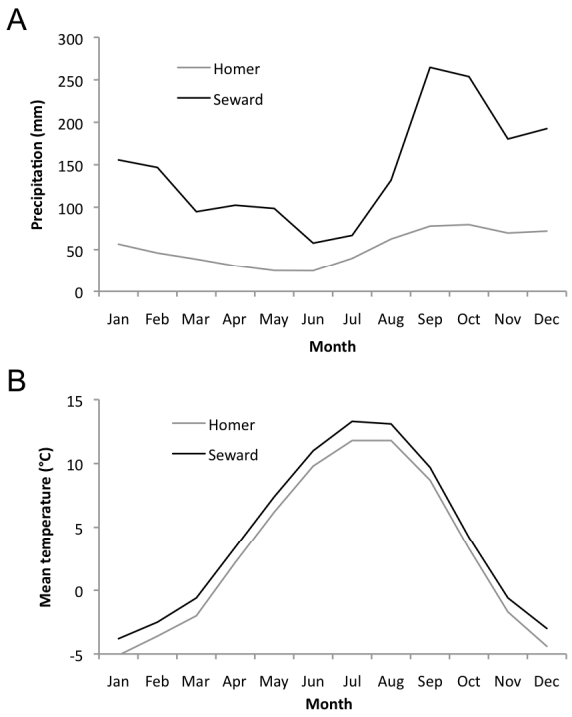

Figure 3: Average monthly A) precipitation and B) temperature in Homer and Seward, southern Kenai Peninsula. Data from Western Regional Climate Center (2014).

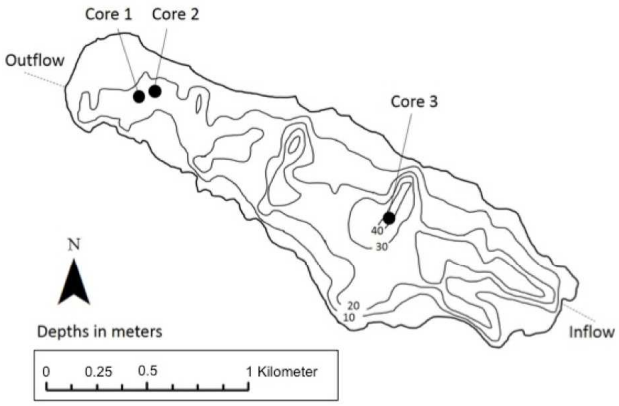

Figure 4: Bathymetric map of Emerald Lake with inflow to the east and outflow to the west.

A.

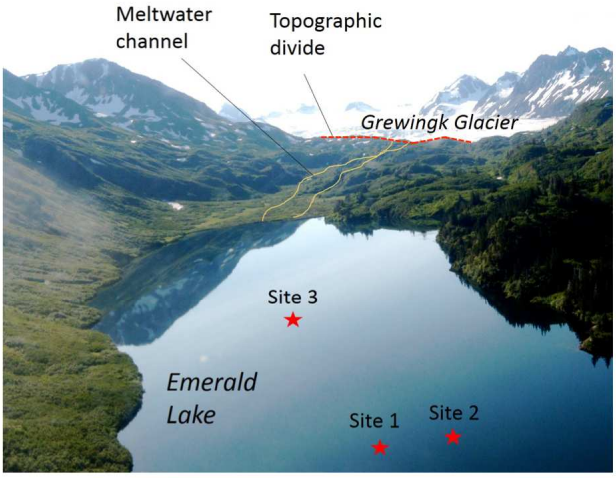

B.

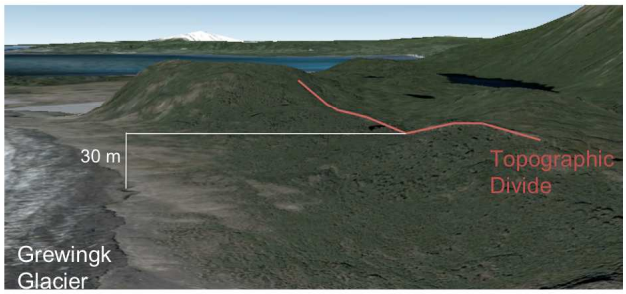

C.

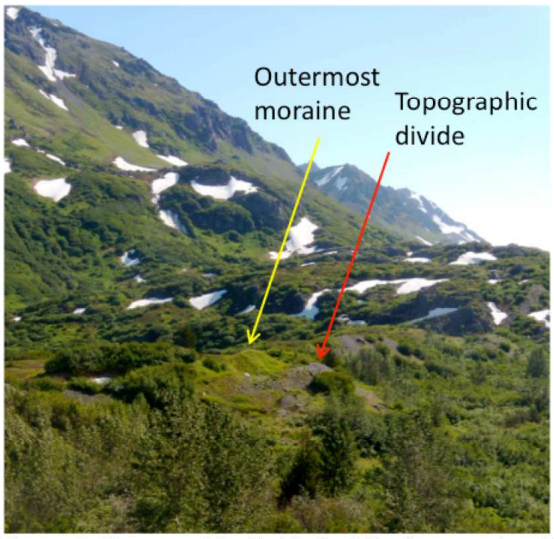

Figure 5: Topographic divide (red line) separating Grewingk Glacier from Emerald Lake as shown from A) view to the southeast towards the inflow with meltwater channel in yellow and core sites represented by red stars, B) view to the northwest with elevation of present glacial margin compared to the moraine on the topographic divide, and C) view to the east with the outermost moraine to the north of the topographic divide.

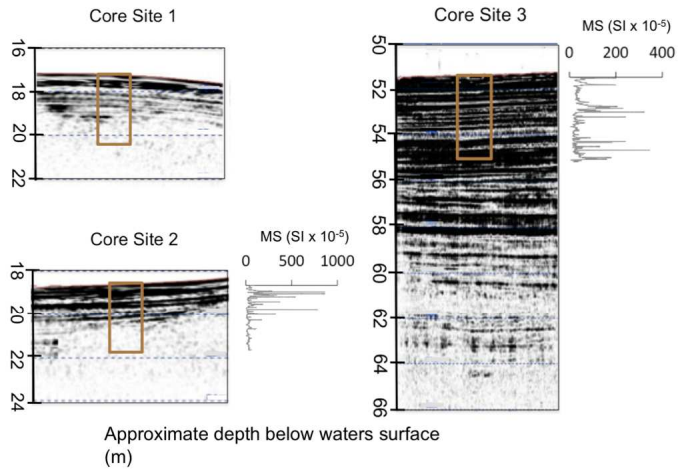

Figure 6: Sub-bottom acoustic profiles and downcore variation in magnetic susceptibility (MS) for cores 2 and 3. Cores penetrated depths indicated by brown rectangles. See Figures 2 and 4 for core site locations.

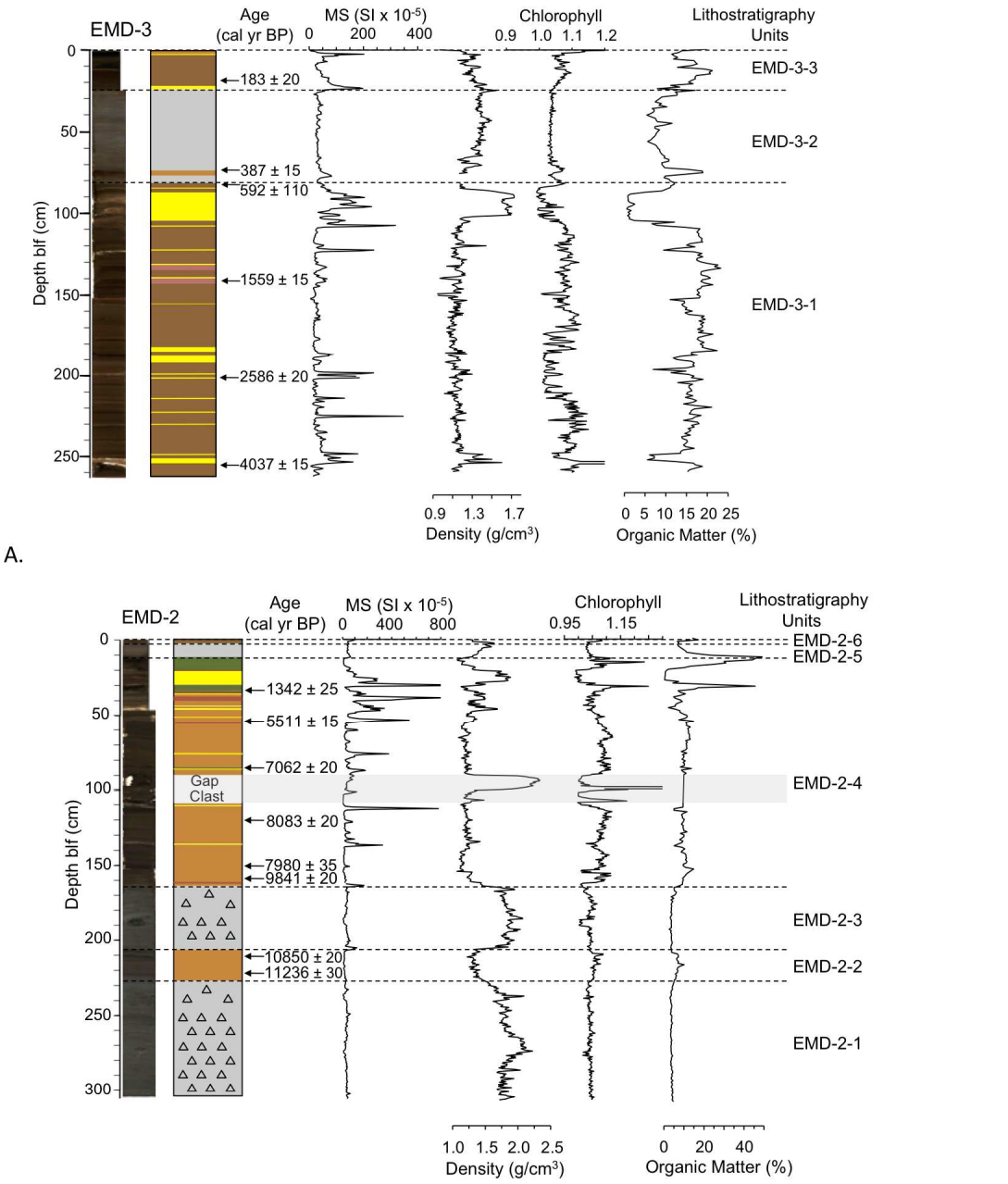

Figure 7: Lithology with linscan, radiocarbon ages, lithostratigraphic units, and sediment proxies (magnetic susceptibility (MS), bulk density, chlorophyll, and organic material) for A) core site 3 and B) core site 2. Grey bar in Core 2 highlights gap in sediment overlain by large clast. It's likely the large clast shifted between analyses. Core 2 is used for interpretations below the Hayes tephra (4012 cal yr BP) in core 3, and core 3 for interpretations above the Hayes tephra.

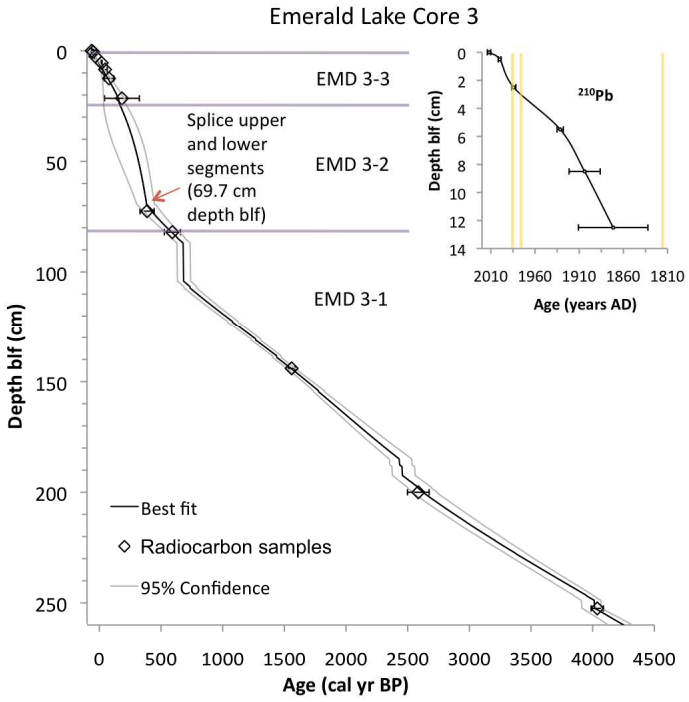

A.

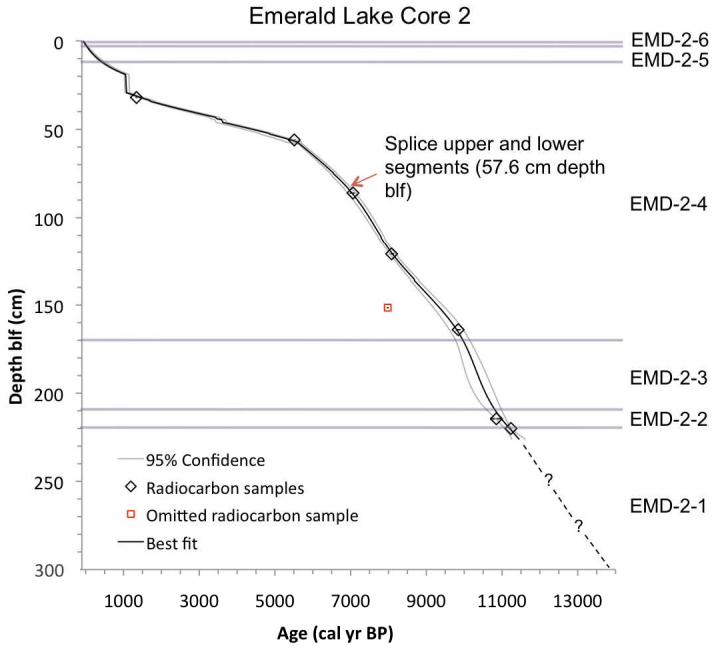

B.

Figure 8: Age models for A) core 3 and B) core 2. Inset to (A) shows ^{210}Pb ages, with tephras marked as yellow lines. Age models were generated using CLAM v2 (Blaauw, 2006). Lithostratigraphic units are marked as shown in Figure 7. ^{210}Pb ages are listed in Table 5 and ^{14}C ages are listed in Table 6. Error bars on ^{14}C ages are 1σ calibrated age range.

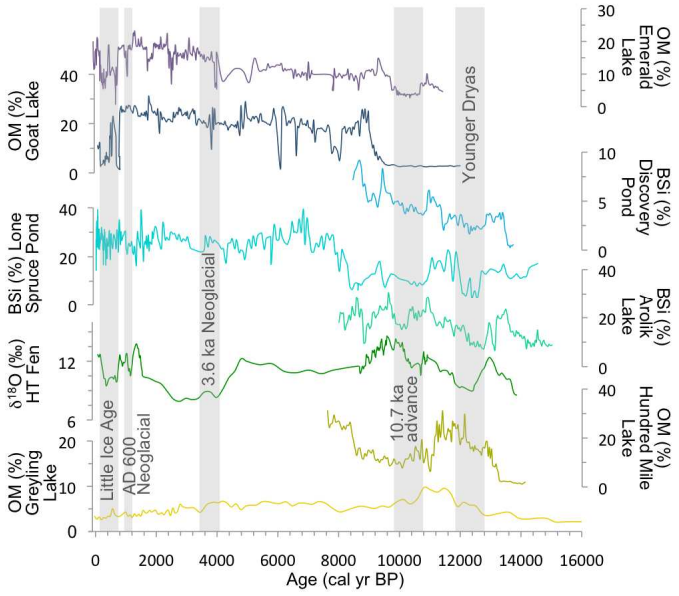

Figure 9: Emerald Lake organic-matter content (OM) compared with other recently published lacustrine proxy records in southern Alaska. Records, including from the top Emerald Lake (this study); Goat Lake (Daigle & Kaufman, 2009); Discovery Pond (Kaufman et al., 2010); Lone Spruce Pond (Kaufman et al., 2012); Arolik Lake (Hu et al., 2006); HT Fen (Jones et al., 2014); Hundred Mile Lake (Yu et al., 2008); and Greyling Lake (McKay & Kaufman, 2009). Grey bars highlight cold intervals discussed in the text. This study is the first documentation of the 10.7 ka re-advance. Higher values in all OM (%) and BSi records reflect increased productivity while higher $\delta^{18}O$ values reflect increased precipitation.

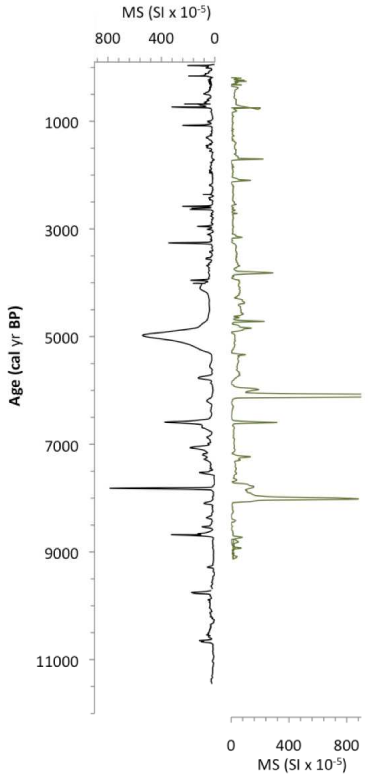

Figure 10: Comparison of magnetic susceptibility (MS) profiles between Emerald Lake (black) and Goat Lake (green) using linear age model from Daigle & Kaufman (2009).